

https://dspace.org/

The emergence of differentially culturable tubercle bacteria in clinical drug sensitive mycobacterium tuberculosis strains

Padarath, Kiyasha

2020
https://hdl.handle.net/10539/31975

Downloaded from a DSpace repository. https://dspace.org/

The emergence of differentially culturable tubercle bacteria in clinical drug sensitive *Mycobacterium tuberculosis* strains

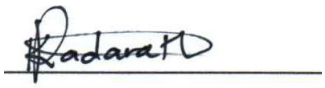
KIYASHA PADARATH (806617)



A dissertation submitted to the Faculty of Health Science, University of the Witwatersrand,
Johannesburg, in fulfillment of the requirements for the degree of Master of Science in Medicine.
2020

Declaration

I, Kiyasha Padarath (student number: 806617) declare that this dissertation is my own work. It is being submitted for the degree of Master of Science at the University of the Witwatersrand, Johannesburg. It has not been submitted before for any degree or examination at this any other University.



(Kiyasha Padarath)

22/07/2020

Date

Presentations arising from this dissertation

1. Conference: Molecular Biosciences Research Thrust, 2018

   Presentation: Oral

   Title: Hungry and sleepy TB bacteria: A robust *in vitro* model for the generation of non-replicating mycobacteria

   Venue: University of Witwatersrand

2. Conference: Pathology Research and Development Congress, 2019

   Presentation: Oral

   Title: Hungry and sleepy TB bacteria: A robust *in vitro* model for the generation of non-replicating mycobacteria

   Venue: Ekurhuleni International Conference Centre

3. Conference: 10th Cross Faculty Graduate Symposium, 2019

   Presentation: Oral

   Title: Hungry and sleepy TB bacteria: A robust *in vitro* model for the generation of non-replicating mycobacteria

   Venue: University of Witwatersrand

   Achievement: 2nd place in Faculty of Health Science

4. Conference: Molecular Biosciences Research Thrust, 2019

   Presentation: Poster

   Title: Hungry and sleepy TB bacteria: A robust *in vitro* model for the generation of non-replicating mycobacteria

   Venue: University of Witwatersrand

   Achievement: 1st place for best MSc poster

Acknowledgments

I would firstly like to thank my parents for their unwavering support. Nothing I say or do will compensate for all that you have done for me. Your time, love and guidance have allowed me to always be successful in life's many endeavours.

Secondly, I would like to thank my supervisors, Prof. Bavesh Kana and Dr Bhavna Gordhan – for the endless inspiration, support and guidance. Your scientific knowledge is unmeasurable and I will always appreciate the skills you have taught me.

I would like to thank all my funders, the National Research Foundation (NRF), the DST/NRF Centre of Excellence for Biomedical TB Research (CBTBR) and the Bill and Melinda Gates foundation, without whom this MSc would not have been possible.

To my colleagues at the CBTBR who became my family away from home. Thank you for your friendship, laughter and advice.

Table of Contents

Declaration ii
Presentations arising from this dissertation iii
Table of Contents v
List of Tables: ix
List of Figures: ix
List of symbols and abbreviations: xii
Abstract xv
1. Introduction 1
1.1 Background 1
1.1.1 Active Tuberculosis (TB) infection 1
1.1.2 Co-infection of Tuberculosis (TB) with Human immunodeficiency Virus (HIV) 3
1.1.3 Latent TB infection (LTBI) 4
1.1.4 The progression from LTBI to active disease 5
1.2 TB diagnosis 5
1.2.1 Mycobacterial culture 5
1.2.2 Smear microscopy 6
1.2.3 Molecular diagnostics 6
1.2.3.1 GeneXpert 6
1.2.3.2 Hain LPA 7
1.2.3.3 LAM Urine Assay 7
1.2.2 The gap in TB diagnostics 9
1.3 The spectrum of culturability 9
1.4 Antibiotic treatment and DCTB 11
1.5 *In vitro* models for DCTB 12
1.5.1 Starvation model 14
1.5.2 Biofilm model 15
1.5.3 Ion deficiency model 15
1.6 The relationship between *M. tuberculosis* genotype and DCTB 16
1.6.1 Evolution and strain lineage of clinical strains of *M. tuberculosis* 16

1.6.2 Strain diversity in South Africa 18
1.6.3 The impact of clinical strains on treatment outcomes 19
1.6.4 Adaptive mechanism of strains (Beijing and LAM) 20
1.7 Rational of the study 22
1.7.1 Aim 22
1.7.2 Objectives 22
2. Materials and Methods 23
2.1 Materials used 23
2.2 Strains and culturing conditions 23
2.2.1 Culturing conditions 24
°2.3 Genotyping of *M. tuberculosis* strains 24
2.3.1 Genomic DNA extraction 24
2.3.1.1 Large scale DNA extraction 24
2.3.1.2 Colony boil method 25
2.3.2 Spoligotyping 25
2.3.2.1 Polymerase chain reaction (PCR) 26
2.3.2.2 Hybridization and detection 27
2.4 *In vitro* stress models 29
2.4.1 Carbon starvation model 29
2.4.1.1 The Betts et.al, starvation model 29
2.4.1.2 Saito et.al, sequential stress DCTB model 29
2.4.2 Biofilm model 30
2.4.2.1 Removal of bacteria from biofilm 30
2.4.2.2 Treatment of biofilms with RIF 30
2.4.3 Potassium depletion model 31
2.4.3.1 Formation of biofilms in potassium depleted media 31
2.5 Assessment of differentially culturable bacteria 31
2.5.1 Most probable number (MPN) assay 31
2.5.2 Culture filtrate preparation 31
2.5.3 The set-up of the MPN assay in a 96 well plate 32
2.5.4 Resuscitation of DCTB 33
2.5.5 Incubation and plate reading using an MPN calculator 33
2.5.6 Colony forming units (CFU) Assay 33
2.5.7 Calculation of resuscitation index 34
2.6 Incorporation of metabolic probes 34
2.6.1 Labelling of *M. smegmatis* and *M. tuberculosis* cultures with TADA 35

2.7 Flow cytometry assessment of stained bacteria 35
2.7.1 Fluorescent channels 35
2.8 Cytological assessment of strained bacteria 36
2.8.1 Microscopy 36
2.8.2 Fluorescent staining patterns 36
2.8.3 Cell length measurements 37
2.9 Addition of CF from clinical strains to MGIT tubes 37
2.9.1 Addition of CF from different clinical strains to starved H°RV 37
2.9.2 Addition of CF from Beijing and LAM to starved Beijing and LAM 38
2.10 Data Analysis 38
3. Results 39
3.1. *In silico* analysis of the propensity of clinical *M. tuberculosis* strains to adopt the DC state 39
3.1.1. Selection criteria 39
3.1.2. Strain type distribution 41
3.1.3. Strain type affects the ability of bacteria to adopt the DC state 41
3.1.4. The effect strain type has on the quantity of DCTB induced 42
3.2. Optimization of *in vitro* models in *M. smegmatis* 44
3.2.1. Carbon starvation model 44
3.2.1.1. Metabolic activity of the bacteria produced by the carbon starvation model 47
3.2.1.2. Cytological profiling of the bacteria produced by the carbon starvation model 48
3.2.2. The Biofilm model 50
3.2.2.1. Metabolic activity of the bacteria produced by the biofilm model 53
3.2.2.2. Cytological profiling of the bacteria produced by the biofilm model 54
3.2.3. The Potassium depletion model 55
3.2.3.1. The importance of potassium ions in biofilm formation 57
3.2.3.2. Metabolic activity of the bacteria produced by the potassium depletion model 59
3.2.3.3. Cytology of the bacteria produced by the potassium depletion model 60
3.2.4. The role of CF in the detection of DCMS produced by *in vitro* models 62
3.2.4.1. Metabolic activity of the bacteria produced by various *in vitro* the models 64
3.2.4.2. Cytological profiling of the bacteria produced by the various *in vitro* models 66
3.3. Optimization of an *in vitro* carbon starvation model in *M. tuberculosis* 67
3.3.1. Metabolic activity of *M. tuberculosis* bacteria produced under the carbon starvation model 69
3.3.2. Cytological profiling of DCTB produced by the carbon starvation model 72
3.4. The propensity of clinical *M. tuberculosis* strains to adopt the differentially culturable (DC) state 76

3.4.1. Selection and confirmation of *M. tuberculosis* clinical strains 76
3.4.1.1. Growth kinetics of M. tuberculosis clinical strains 76
3.4.2. The propensity of starved clinical strains to adopt the DC state in carbon depleted media 78
3.4.3. Cytological profiling of the *M. tuberculosis* clinical bacteria produced by carbon starvation the model 82
3.4.4. The effect of clinical Beijing and LAM culture filtrate on the resuscitation of DCTB..... 88
3.4.5. The resuscitation capacity of clinical CF to change time to positivity in starved *M. tuberculosis* strains 92
4. Discussion 95
4.1 Optimization of nutrient depletion models 96
4.2 Clinical DCTB and disease progression 99
4.3 Using CF from clinical strains to improve current diagnosis test 101
4.4 Limitations and future studies 101
4.5 Concluding remarks 102
5. Appendices 103
5.1 Appendix A-Materials 103
5.2 Appendix B – Bioinformatics and software used for data analysis 105
5.3 Appendix C –Supplementary Figures 106
5.4 Appendix D- Ethic certificates 109
5.5 Appendix E- Turn-it-in report 111
6. References 113

List of Tables:

Table 1.1- Advantages and disadvantages of various TB diagnostic test

Table 1.2- Summary of the various *in vitro* stress models

Table 2.1- Laboratory *M. smegmatis* and *M. tuberculosis* strains used in this study

Table 2.2- PCR primers used for the conformation of clinical strains

List of Figures:

Figure 1.1. Granuloma formation in humans upon infection with *M. tuberculosis*

Figure 1.2. Spectrum of culturability indicating different culturable states based on metabolic activity of the bacterium

Figure 1.3. Evolution of *M. tuberculosis*

Figure 1.4. A world map indicating the distribution patterns of strain types

Figure 1.5. The transmissibility of clinical strains

Figure 2.1. Spoligotyping procedure

Figure 2.2. Spoligotyping blot orientation

Figure 2.3. The set-up of the MPN and CFU protocol.

Figure 2.4. Incorporation of the metabolic probe into the cell wall of the bacterium.

Figure 2.5. Gating strategy to determine metabolic activity

Figure 2.6. Addition of clinical CF to MGIT tubes

Figure 3.1. Selection criteria flow chart

Figure 3.2. Strain type distribution in the BMG phase 1 and MGIT plus cohorts

Figure 3.3. Propensity of clinical strains to adopt the DC state

Figure 3.4. Effect of CF on resuscitation of DCTB

Figure 3.5. RIF negatively affects the generation of differentially culturable (DC) bacteria in starved cells

Figure 3.6. DCMS produced by the two sequential stress model displays reduced metabolic activity

Figure 3.7. Starved DCMS produced by the two sequential stress model have reduced cell length

Figure 3.8. RIF negatively affects the generation of differentially culturable bacteria in biofilm cells

Figure 3.9. Biofilm cells contain a heterogeneous population of replicating and non-replication bacteria

Figure 3.10. DCMS produced by the biofilm model have increased cell length

Figure 3.11. Bacteria cultured in potassium depleted for up to 168 hrs, increases the generation of DCMS

Figure 3.12. The removal of potassium ion from Sautons media prevents the formation of biofilms

Figure 3.13. Bacteria cultured in potassium depleted media contain a larger population of non-replicating bacteria, compared to an axenic culture

Figure 3.14. DCMS produced under the potassium depletion model have decreased cell length

Figure 3.15. The effect of CF in the resuscitation of DCTB in the various models tested

Figure 3.16. Carbon starvation and growth in potassium depleted media both induce non-replicating bacteria

Figure 3.17. Microscopy analysis of probe incorporation in DCMS bacteria from the various models

Figure 3.18. Carbon starvation and Potassium-depleted models, produce shorter *M. smegmatis* cells

Figure 3.19. The effect of CF in the resuscitation of DCTB in the carbon starvation model

Figure 3.20. Carbon starvation induces non-replicating bacteria

Figure 3.21. Resuscitation of starved bacteria in CF restored the non-replicating bacteria to their active state after 7 days.

Figure 3.22. Bacterium starved in PBS for 2 weeks, produce shorter DCTB cells

Figure 3.23. Resuscitated bacteria have increase metabolic activity

Figure 3.24. Genetic conformation and growth kinetics of Beijing strains

Figure 3.25. Genetic conformation and growth kinetics of LAM strains

Figure 3.26. Beijing strains have an increased propensity to produce DCTB compared to LAM strains

Figure 3.27. Metabolic activity of Beijing analysed by flow cytometry and microscopy

Figure 3.28. Metabolic activity of LAM analysed by flow cytometry and microscopy

Figure 3.29. Cytological profiling of Beijing strain analysed by fluorescent microscopy

Figure 3.30 The incorporation of the metabolic probe along the cells wall in Beijing cells

Figure 3.31 Cytological profiling of LAM strain analysed by fluorescent microscopy

Figure 3.32 The incorporation of the metabolic probe along the cells wall in LAM cells

Figure 3.33 Addition of clinical CF increases time to positivity in starved H37Rv bacteria

Figure 3.34- Beijing-CF enhances the resuscitation of DCTB from Beijing strains

Figure 3.35 Addition of Beijing-CF increases time to positivity in starved Beijing bacteria

List of symbols and abbreviations:

µg	Microgram
µL	Microlitre
µm	Micrometre
AIDS	Acquired Immune Deficiency Syndrome
AMK	Amikacin
BCG	Bacillus Calmette-Guérin
BTZ	1,3-benzothiazin-4-ones
CAP	Capreomycin
CBTBR	Centre of Excellence for Biomedical TB Research
CF	Culture filtrate
CFU	Colony Forming Unit
CLS	Clinical Laboratory Services
DC	Differentially culturable
DCMS	Differentially culturable *M. smegmatis*
DCTB	Differentially Culturable Tubercle Bacilli
DNA	Deoxyribonucleic acid
DR	Direct Repeat
DST	Drug Susceptibility Testing
ECL	Enhanced chemiluminescence
EDTA	Ethylenediaminetraacetic acid
EMB	Ethambutol
FQ	Fluoroquinolone
HIV	Human Immunodeficiency Virus
INH	Isoniazid
KAN	Kanamycin
L	Litre

LAM	Lipoarabinomannan
LAM	Latin American Mediterranean
LJ	Lowenstein-Jensen
LPA	Line probe Assay
LTBI	Latent tuberculosis infection
MDR	Multi drug resistant
MGIT	Mycobacterial Growth Indicator Tube
mL	Millilitre
MPN	Most Probable Number
MTBC	Mycobacterium tuberculosis complex
NaOH	Sodium hydroxide
NHLS	National Health Laboratory Service
NOS	Nitrogen Intermediate Species
OADC	Oleic acid, Albumin, Dextrose, Catalase
OFX	Ofloxacin
PANTA	Polymyxin B, Amphotericin B, Nalidixic acid, Trimethoprim and Azlocillin
PBS	Phosphate Buffer Solution
PCR	Polymerase Chain Reaction
PG	Peptidoglycan
PHRU	Perinatal HIV Research Unit
PZA	Pyrazinamide
RI	Resuscitation Index
RIF	Rifampicin
RNI	Reactive Nitrogen Intermediates
ROS	Reactive Oxygen Species
Rpf	Resuscitation-Promoting Factor

SDS	Sodium Dodecyl Sulphate
SMRC	Small resting cell
SNPs	Single nucleotide polymorphism
SOP	Standard Operating Procedure
TAE	Tris, Acetic acid, EDTA
TB	Tuberculosis
TE	Tris-EDTA buffer
TNF-α	Tumour Necrosis Factor Alpha
TST	Tuberculin Skin Test
TTP	Time to positivity
UV	Ultra-violet
VBNC	Viable But Non-Culturable
VNTR	Variable Number of Tandem Repeats
WHO	World Health Organization
XDR	Extremely drug-resistant

Abstract

Mycobacterium tuberculosis (*M. tuberculosis*) is the causative agent of tuberculosis (TB) infection and disease. Since its discovery, various diagnostic tools have been developed to detect bacteria in sputum samples from TB-infected patients including bacterial culture, auramine staining and nucleic acid amplification tests (NAATs). Recent studies have revealed a distinct population of bacteria in sputum samples from patients with drug susceptible TB that are undetected by standard culturing techniques. These bacteria, defined as differentially culturable tubercle bacteria (DCTB), exist in a non-replicating state that is reactivated only in liquid media, supplemented with growth factors, and not on solid media. Laboratory models that induce this differentially culturable state are important for studying the physiology and metabolism of these bacteria to ultimately develop new diagnostic tests for TB. In this study we tested and optimised *in vitro* stress models in laboratory media using the laboratory strain H37Rv, to determine the conditions that robustly generate DCTB. The quantity of DCTB was assessed using the most probable number assay and colony forming units. In addition, the phenotype of these cells was analysed using microscopy and flow cytometry, with metabolic probes that target remodelling of the peptidoglycan (PG) component of the bacterial cell wall. Our results indicated that application of the carbon starvation model to clinical *M. tuberculosis* strains (Beijing and LAM), produced robust levels of DCTB as illustrated by limited growth on agar plates and enhanced growth in liquid media supplemented with culture filtrate from an axenic culture of *M. tuberculosis*. These DCTB cells were non-replicating and significantly shorter compared to cells grown in normal media. Using probes that report on PG biosynthesis representing metabolically active cells, confirmed a lack of *de novo* biosynthesis in DCTB, providing evidence for the establishment of a non-replicating state. Microscopy revealed a lack of metabolic probe uptake in a large proportion of the DCTB population, which was restored when the bacteria were resuscitated. We also demonstrated that Beijing strains have greater propensity to produce DCTB compared to LAM strains. Collectively, our observations allow for the improvement of experimental systems that enable further investigation of DCTB and how these bacteria contribute to treatment response. In addition, these efforts will further allow for the development of a shorter TB regimen, with reduced daily pill burden and limited side effects.

1. Introduction

1.1 Background

Tuberculosis (TB), caused by *Mycobacterium tuberculosis* (*M. tuberculosis*), is currently the leading cause of death by an infectious disease in South Africa (WHO, 2019). Globally TB infects a quarter of the world's population resulting in 9 million new cases and 1.5 million deaths annually (WHO, 2019). *M. tuberculosis* is transmitted to humans through inhalation of aerosolized droplets or particles containing the bacterium (Chengalroyen et al., 2016; Rosser, Stover, Pareek, & Mukamolova, 2017). *M. tuberculosis* infection can present as a range of disease in the human host, spanning from asymptomatic infection, active granuloma disease to latent infection.

1.1.1 Active Tuberculosis (TB) infection

M. tuberculosis bacteria which evade clearance by the host immune system, may replicate and cause active TB disease. The development of active disease is present in less than 10% of exposed cases (Chao & Rubin, 2010; WHO, 2019). In the remaining 90-95% of individuals, infection does not progress to disease existing as a clinically latent state (Bhatt & Salgame, 2007; Chao & Rubin, 2010). One of the hallmarks of an active TB infection is the presence of a granuloma that creates an immune microenvironment to control the infection (Schluger, Condos, Lewis, & Rom, 1994). Granulomas are composed of a variety of cell types with alveolar macrophages being the primary cellular component responsible for its formation (Schuger & Rom, 1997). For *M. tuberculosis* to effectively cause infection, it has to survive by modulating the immune response induced by alveolar macrophages (Glickman & Jacobs, 2001). The bacterium strikes a balance between the pro-inflammatory and anti-inflammatory cytokines, both of which are produced as part of the immune response to reduce or control bacterial proliferation (Sasindran & Torrelles, 2011). Chemokines released by infected alveolar macrophage attract the first wave of inflammatory cells including neutrophils, monocyte derived macrophages, natural killer NK cells, and T cells, which collectively promote inflammation and tissue remodelling (Actor, Hunter, & Jagannath, 2008). Once initial inflammatory cells are located to the site of infection, T-cells are primed to differentiate into activated T-cells (Lockhart, Green, & Flynn, 2006). These primed pathogen-specific T-cells are responsible for activating macrophages and hindering mycobacterial growth within developing granulomas (North & Jung, 2004) (Figure 1.1). The presence of activated T-cells

initiate the organisation of the granuloma, where macrophages infected with *M. tuberculosis* are drawn to the centre and are surrounded by lymphocytes (North & Jung, 2004). Within the granuloma there is a constant battle between pathogen and the immune system, which causes cell death and recruitment of new immune cells, together with vascular and tissue remodelling (Actor et al., 2008). Caseous granulomas are formed when macrophages surrounding a cellular region, become necrotic and die creating a caesium (North & Jung, 2004; Okada & Shirakawa, 2005). Bacteria within the caesium are released into the lung when a cavity is formed and these bacteria are then spread into the air by coughing. (Keane, Remold, & Kornfeld, 2000; North & Jung, 2004).

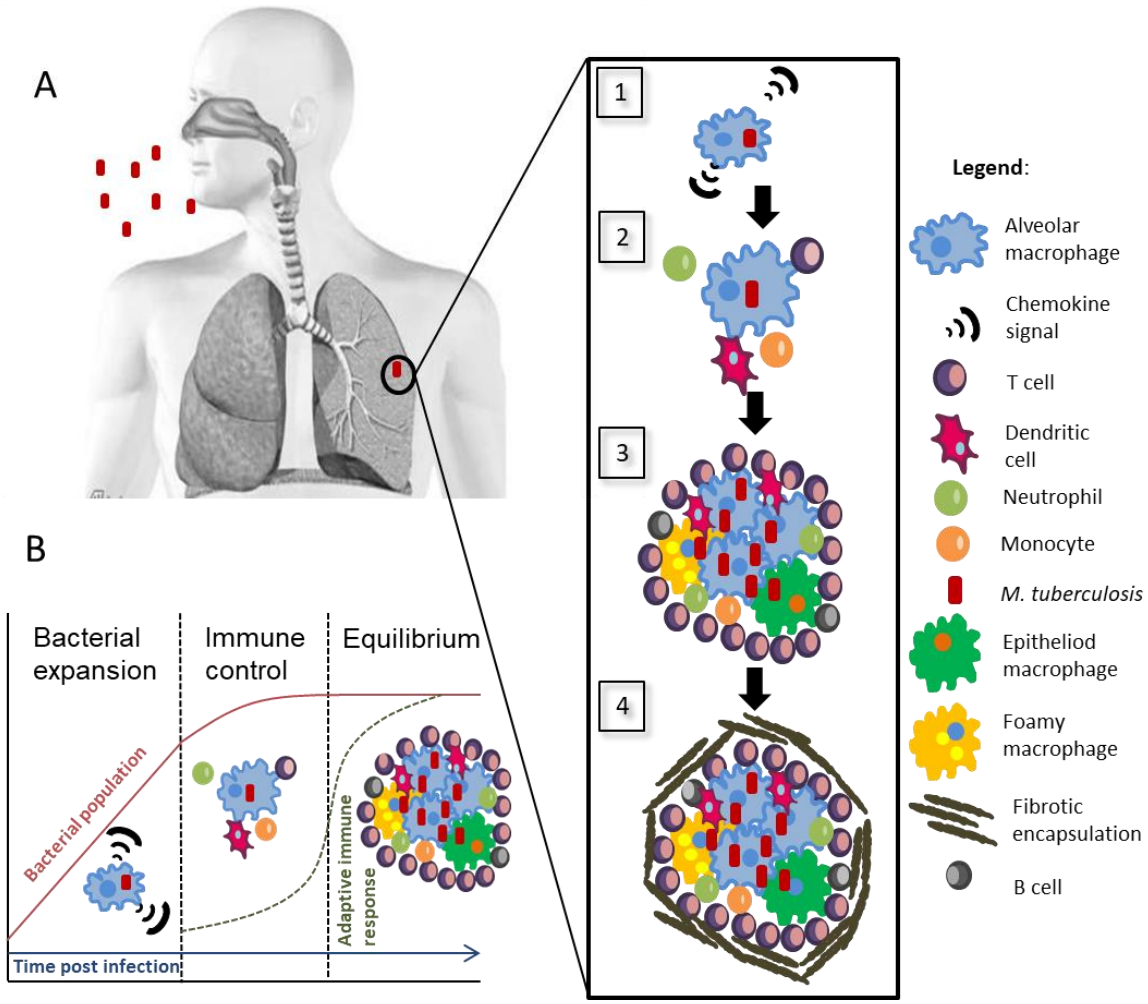


Figure 1.1 Granuloma formation in humans upon infection with *M. tuberculosis*: A) Visual representation of the steps involved in granuloma formation; (1) *M. tuberculosis* bacteria are engulfed by alveolar macrophages, which induced chemokine signalling. (2) Arrival of immune cells from the chemokines signals released. 3) Formation of a granuloma, through the recruitment of pro-inflammatory cells such as neutrophils, monocytes and natural killer cells 4) Maturation of the granuloma, containment of infection can be characterized by fibrotic encapsulation B) Graphs showing bacterial growth kinetics during granuloma formation The graph represents the change in bacterial load (y-axis) over a period of time post infection (x-axis). This image was adapted from (Harris, Hope, & Lavelle, 2009).

TB is a curable disease however, effective diagnosis and compliance to treatment is essential to achieve positive outcomes (Castelnuovo, 2010), as non-adherent therapy can facilitate emergence of resistant bacteria (Nuwaha, 1998). Resistance occurs when the bacterial genome acquires mutations in the drug target gene that increase survival in the presence of the drug (Castelnuovo, 2010; Muture et al., 2011; Nuwaha, 1998). There are two ways in which drug resistant TB can arise in patients: acquired or transmitted. Acquired resistance is when a TB infected patient develops resistance during treatment and transmitted resistance is when a person gets infected with a *M. tuberculosis* strain harbouring pre-existing drug resistance conferring mutations (Dartois, 2014; Nuwaha, 1998). South Africa is among the 10 highest burdened countries with drug-resistant TB, placed fourth after China, India and Russia, with an estimated 6900 cases of multidrug resistant TB per annum (MDR-TB) (WHO, 2017). Active drug-susceptible TB disease is treated by a daily dose of combination chemotherapy including the first-line drugs: Rifampicin (RIF), Isoniazid (INH), Pyrazinamide (PZA) and Ethambutol (EMB) for six months. Resistance to INH and RIF is considered to be MDR-TB and is found in 3.3% of new TB cases and 20% of previously treated cases (WHO, 2017). In 2016, there were 967 cases of extensively drug-resistant TB (XDR-TB) in South Africa, defined as resistance to INH, RIF and additional resistance to a fluoroquinolone or one of the three injectable second line drugs: Amikacin (AMIK), Kanamycin (KAN) or Capreomycin (CAP) (WHO, 2017).

1.1.2 Co-infection of Tuberculosis (TB) with Human immunodeficiency Virus (HIV)

TB infection is more prevalent in South Africa due to the co-infection with Human immunodeficiency Virus (HIV). The sub-Saharan African countries have the highest TB and HIV co-incidence rates and mortality (WHO, 2017). In South Africa, more than 60% of new TB cases are diagnosed in patients with HIV (Mayosi et al., 2009). In patients who are co-infected, the immune system is a major component that contributes to the complexity of the disease (Abdool, Churchyard, Karim, & Lawn, 2009). In these patients, the *M. tuberculosis* infection is not confined to the lungs, and maybe disseminated to other organs, such as the spleen, lymph nodes, liver and kidney (Abdool et al., 2009; Wood, 2007). The lower level of the CD4 T-cell counts in these patients limits the formation of granulomas that confine bacteria to the lung (Bloom et al., 2017; Gandhi et al., 2006; North & Jung, 2004). In addition to this, poor socio-economic conditions, reduced patient-compliance to treatment and a high

proportion of undiagnosed infection all aid in driving the TB-HIV pandemic in South Africa (Ahmad, 2010; Gomez & McKinney, 2004).

1.1.3 Latent TB infection (LTBI)

Latent TB infection (LTBI) is defined as the absence of clinical symptoms despite being infected with *M. tuberculosis* (Bhatt & Salgame, 2007; Bloom et al., 2017; Gomez & McKinney, 2004). LTBI is diagnosed by a positive tubercle skin test (TST), which measures a delayed hypersensitivity response to *M. tuberculosis* proteins or antigens injected intra-dermally (Munoz, Stagg, & Abubakar, 2015; WHO, 2017). In South Africa, one third of the population carry latent TB, which is probably an underestimation as individuals with LTBI are asymptotic, and may remain undetected (Leung, Lange, & Zhang, 2013; WHO, 2017). With regards to bacterial turnover, there are two hypotheses associated with LTBI. The first hypothesis states that LTBI is characterised by a population of both growing and dying organisms, the balance of which is maintained by an efficient immune system (Leung et al., 2013). Initially fibrotic granulomas were thought to be well structured with activated macrophages able to control proliferation of bacteria resulting in LTBI (Barry et al., 2009; Scanga et al., 1999). A study by Hobby and colleagues in 1973 revealed that viable tubercle bacteria were able to be cultured from 78% of closed necrotic or healed lesions in patients who had received TB treatment. The authors concluded that surviving *M. tuberculosis* cells appear to be in a suppressed metabolic state and when the immune pressure was removed, the bacteria were able to proliferate (Hobby, Holman, Iseman, & Jones, 1973).

The second hypothesis states that during LTBI, bacteria are present in a dormant-like state and the transition to active disease is the result of reactivation of these dormant organisms (Leung et al., 2013). In the literature, the terms latency and dormancy are used interchangeably, however for the purposes of this dissertation, dormancy is a term used to describe the bacteria that are quiescent or metabolically inactive and latency is a term used to describe the state of infection when no symptoms are displayed (Dartois, 2014; Lin & Flynn, 2010). Bacteria enter a low metabolic state when faced with stressful conditions and this state can be reversed by resumption of growth when conditions become favourable (Scanga et al., 1999). Strains from the genus *Bacillus* (defined as gram-positive, rod-shaped bacilli) adopt a dormant state under stressful conditions that is phenotypically different from actively growing cells. The dormant phenotypes include the formation of spores and elementary bodies which protect genetic material by nucleoid condensation (Higgins & Dworkin, 2012; Meneghini, 2015). However,

unlike *Bacillus* species, mycobacteria are non-sporulating and lack the genes necessary for entry into spore-like states (Higgins & Dworkin, 2012). *In vitro* studies with *Mycobacterium smegmatis* (*M. smegmatis*) a non-pathogenic, faster growing model organism for *M. tuberculosis* has shown that mycobacteria are able to adopt an ovoid morphology in nitrogen-limited media with low metabolic activity. These cells display increased resistance to heat and antibiotics as well as the inability to be cultured on solid media, resembling a dormant phenotype (Anuchin et al., 2009). Although *M. tuberculosis* can adopt a dormant-like state *in vitro*, an association with LTBI is yet to be determined.

1.1.4 The progression from LTBI to active disease

Individuals with LTBI carry a risk of progression to active TB disease. This risk is minimised in individuals with a competent immune system that is capable of limiting bacterial replication (Actor et al., 2008; Bloom et al., 2017; Chee, Sester, Zhang, & Lange, 2013). However, in immune compromised individuals such as individuals with HIV co-infection, those undergoing tumour necrosis factor (TNF-α) therapy, being treated for inflammatory diseases, transplant patients and patients with autoimmune diseases, there is a higher risk for progression to active TB (Ahmad, 2010; Barry et al., 2009; R. Kumar et al., 2019). In South Africa, the risk of reactivation disease is significantly increased due to the high prevalence of co-infection with HIV (Abdool et al., 2009; WHO, 2017). Once reactivation has occurred, TB disease presentation is heterogeneous in pathology spanning from active TB disease in the lungs (pulmonary TB) to TB disease outside the lungs (extra pulmonary TB) (North & Jung, 2004). Factors that contribute to the broad spectrum of disease presentation include bacterial replication, bacterial load, host resistance, immune activation and inflammation (Muture et al., 2011; Nuwaha, 1998; Okada & Shirakawa, 2005). As a result, TB diagnosis is complex and remains a major issue in TB-endemic areas.

1.2 TB diagnosis

1.2.1 Mycobacterial culture

Since the discovery of *M. tuberculosis* by Robert Koch in 1882, the standard method for detecting tubercle bacilli is the culturing of the bacterium from sputum samples (Kyu et al., 2018; WHO, 2017). The initial method of culturing involved the growth of *M. tuberculosis*, as colonies on Lowenstein-Jensen (LJ) media (Rubin, 2018; Sulis et al., 2016). *M. tuberculosis* is a slow growing organism with a replicative cycle of 18 hours; thus, it can take between 4-6 weeks to confirm TB diagnosis. Following the use of the LJ method of culturing, other

improved culturing methods have been developed in order to decrease the turnaround time to confirm a TB diagnosis, such as the BACTEC mycobacterial growth indicator tubes (MGIT) (Gupta & Kakkar, 2018; Nguyen, Anton-Le Berre, Bañuls, & Nguyen, 2019). MGIT is a liquid culture based system, that contains a fluorescent compound embedded in silicone at the bottom of the tube (Yu et al., 2011). The fluorescent compound is sensitive to the consumption of oxygen, thus actively respiring organisms consume the oxygen and allow for the fluorescence signal to be observed using UV light. However, a positive MGIT test result still needs confirmation for *M. tuberculosis* as other actively respiring organisms from sputum, can lead to false positives (Ahmad, 2010; Yu et al., 2011). Advantages and disadvantages of the various diagnosis tests are described in table 1.1.

1.2.2 Smear microscopy

Smear microscopy is the current gold standard for TB diagnosis. This technique is rapid and reliable for patients with pulmonary TB with bacterial loads of more than 5000 bacilli/ml of sputum (WHO, 2017). However, smear microscopy is insensitive, and more difficult, for patients with low bacterial loads and LTBI (Desikan, 2013). Initially bacteria were stained using the Ziehl-Neelsen method which stains acid fast bacteria, but later the auramine stain was used to detect bacteria in sputum as it is more sensitive and cheaper (Desikan, 2013; Van Rie et al., 2008). One of the major downfalls of auramine staining is that it is non-specific and is able to detect non-tuberculous mycobacteria in addition to *M. tuberculosis* and therefore can result in misdiagnosis. The reliability of smear microscopy depends on the quality of sputum as well as the accuracy of the preparation and interpretation of slides (Van Rie et al., 2008). Thus, this diagnostic test requires skilled, trained laboratory technicians with regular quality control checks to produce reliable results (Van Rie et al., 2008; WHO, 2017). Due to the poor sensitivity with low bacterial loads, many TB endemic countries are shifting away from the use of smear, with greater reliance on molecular diagnostics.

1.2.3 Molecular diagnostics

1.2.3.1 GeneXpert

There is a constant need to develop better and faster diagnostic tools, and the one recent advancement has been the development of Nucleic Acid Amplification Tests (NAATs). NAATs use polymerase chain reaction (PCR) to amplify DNA extracted from bacteria in sputum (Rubin, 2018; Sulis et al., 2016). Currently, the most widely used NAAT system for

TB diagnosis is the GeneXpert (Cephaid). This system is able to simultaneously detect the presence of *M. tuberculosis* and resistance to RIF in sputum (Nguyen et al., 2019; Rubin, 2018; WHO, 2019). More recently the GeneXpert technology was improved with the development of a GeneXpert Ultra cartridge that can detect as low as 10 organisms/ml of sputum (Bloom et al., 2017; Rufai et al., 2014) and making it useful for diagnosing patients with low bacterial loads. These current molecular-based diagnostic tools have already improved, treatment outcomes and transmission of TB (Nguyen et al., 2019; Rufai et al., 2014).

1.2.3.2 Hain LPA

The Hain Line probe assay is a different NAAT which is comprised of a strip-based DNA test that can identify bacterial strains from the *Mycobacterium tuberculosis* complex (MTBC) and drug resistance profile through binding patterns of DNA amplicons to probes, which target common speciation and resistance markers (Nathavitharana et al., 2017). Although the WHO has approved Hain LPA for the rapid detection of resistance to first and second line TB drugs, some mutations that lead to resistance can fall outside the range covered by the assay (WHO, 2019). Therefore, a complete resistance profile may not be determined and in some cases a phenotypic drug sensitivity test (DST) is necessary. Comparison of LPA to GeneXpert results for patients with mono-resistant RIF, showed that the LPA (sensitivity 90.0% and specificity 99.1%) had a better performance compared to GeneXpert (sensitivity 62.50%, specificity 96.50%) (Rufai et al., 2014).

1.2.3.3 LAM Urine Assay

Lipoarabinomannan (LAM) is a lipopolysaccharide substrate, typically found in the cell wall of *M. tuberculosis* and can be detected in an infected individual's urine (Gupta & Kakkar, 2018). Based on this, a laboratory urine-based ELISA was developed as a diagnostic test at point of care facilities (Iskandar, Nursiloningrum, Arthamin, Olivianto, & Chandrakusuma, 2017). The LAM assay is a rapid, disposable assay that can diagnose TB in 20 minutes. However, several studies have demonstrated that whilst the LAM assay has adequate diagnostic specificity, it has poor sensitivity thus, it is used in combination with smear microscopy to increase sensitivity (Mathabire Rucker et al., 2019). The intensity of LAM band produced in the assay also gives an indication of the bacterial load; the thicker the band, the higher the bacterial load (Gupta & Kakkar, 2018).

Table 1.1 Advantages and disadvantages of various TB diagnostic tests

Diagnostic test	Advantages	Disadvantages
MGIT	• Important diagnostic tool in patients with paucibacillary tuberculosis • Allows for phenotypic drug sensitive testing • Gold standard	• Expensive • Slow diagnostic technique • Requires additional identification once culture tube flags positive
Auramine smear	• High specificity • Short turnaround time	• Low sensitivity in people with a low bacillary load • Does not distinguish between live and dead bacilli
Hain LPA	• Detects *M. tuberculosis* and resistance to RIF and INH at the same time from one specimen • Reduces time to diagnosis of MDR-TB to 7 days • Specific for *M. tuberculosis* complex (MTBC)	• Does not distinguish between live and dead bacilli • Labor intensive and is prone to contamination and human error • Requires 3 separate rooms for the different steps of the procedure
LAM	• Point of care diagnosis • Reduces time to diagnosis to 20 minutes	• Low sensitivity in people with a low bacillary load
GeneXpert	• Detects *M. tuberculosis* and RIF resistance from one specimen at the same time • Processing time is approx. 2 hours • Specific for MTBC • Can also be used on cerebral spinal fluid (CSF), aspirates and tissue • Test carried out in a closed system - reduced risk of cross-contamination and human error	• Does not distinguish between live and dead bacilli • A small proportion of RIF resistance detected may not correlate with physiological resistance • Is not cost effective

1.2.2 The gap in TB diagnostics

Despite the fact that the use of NAATs has become routine and has the potential to shorten diagnostic procedures, the major limitation is that these tools cannot distinguish between live and dead bacteria. As a result, culture is still the gold standard for TB diagnosis and drug susceptibility testing (Gupta & Kakkar, 2018). However, culture may also be limited if bacteria are unable to emerge under standard culture conditions. In 2010, Mukamolova et al., described that 80 to 99.9% of viable *M. tuberculosis* in the sputum of TB patients prior to treatment initiation, were undetectable by the standard colony forming units (CFU) assay, which quantifies the growth of colonies on agar plates (Mukamolova, Turapov, Malkin, Woltmann, & Barer, 2010). Instead, these sputum samples contained a hidden population of bacteria termed "Differently Culturable Tubercle Bacteria (DCTB)". These bacteria could not be cultured on solid media but could be stimulated to grow in liquid media, when supplemented with mycobacterial culture filtrate (CF), which presumably contains growth stimulatory molecules (Chengalroyen et al., 2016; Kato, Haruta, Cui, Ishii, & Igarashi, 2008; Rosser et al., 2017; Sasindran & Torrelles, 2011). These observations were recently corroborated by another study that described several distinct DCTB populations prior to treatment initiation (Chengalroyen et al., 2016). Based on these results, current TB diagnostic tools are most likely failing to detect a large proportion of bacteria present in sputum.

1.3 The spectrum of culturability

Exponential growth of bacteria outside a laboratory setting is rare as laboratory grown bacteria are supplemented with growth enhancers in media (Chao & Rubin, 2010; Chee et al., 2013). The natural environment for *M. tuberculosis* is constantly limiting and fluctuating and as a result, the bacterium encounters nutrient deprivation (Ayrapetyan, Williams, Baxter, & Oliver, 2015; Gibson, Harrison, & Cox, 2018). At present, little is known about the metabolism of DCTB however, it is hypothesized that the complex microenvironment within the granuloma exposes bacteria to hostile conditions such as acidification, hypoxia, starvation and reactive oxygen and nitrogen species (Bamford et al., 2017; Keane et al., 2000; Samanich et al., 2000). To adapt to these environmental stresses, mycobacteria enter non-replicating states, and

become differentially culturable (Anuchin et al., 2009). It has been proposed that during this period most bacilli persist in a dormant state, with a few bacteria in an active replicating state which are known as 'scout cells' (Buerger et al., 2012; Herranz et al., 2018). These scout cells are an evolutionary survival mechanism to facilitate microbial wakening. The scout cell model proposed by S. Buerger and colleagues in 2012 states that *"if a scout cells forms under growth-permissive conditions, it will establish a new population, thus achieving the main objective: the multiplication of the population genome. Once the environmental conditions become adversarial again the revived population returns to dormancy, initiating a new round of the cycle. The model thus proposes that a generalised microbial population achieves survival under hostile conditions, and growth favourable ones by cycling between dormancy and activity* (Buerger et al., 2012)*"*. The regulatory mechanism to form scout cells as yet to be identified, but it is proposed that at any given time there are bacteria that are 'scouting' the environment for signals to restart growth, and can scout for several decades before extinction (Gibson et al., 2018). The presence of scout cells and environmental stresses affect the bacterial population growth rate leading to heterogeneous populations with a spectrum of culturability, spanning from metabolically active cells which are able to grow on solid media, to DCTB that are non-platable (Chengalroyen et al., 2016; Kana et al., 2008). The latter includes bacteria that require a combination of growth factors to recover, including resuscitation promoting factors (Rpfs). Rpfs are growth stimulatory molecules, identified in CF, which enhance the recovery of DCTB (Chengalroyen et al., 2016; Kana et al., 2008; G. Kumar et al., 2017; Mukamolova et al., 2010). Different DCTB populations have been identified in sputum, including CF-independent DCTB, Rpf –independent DCTB and CF-dependant DCTB, explained in figure 1.2 (Chengalroyen et al., 2016).

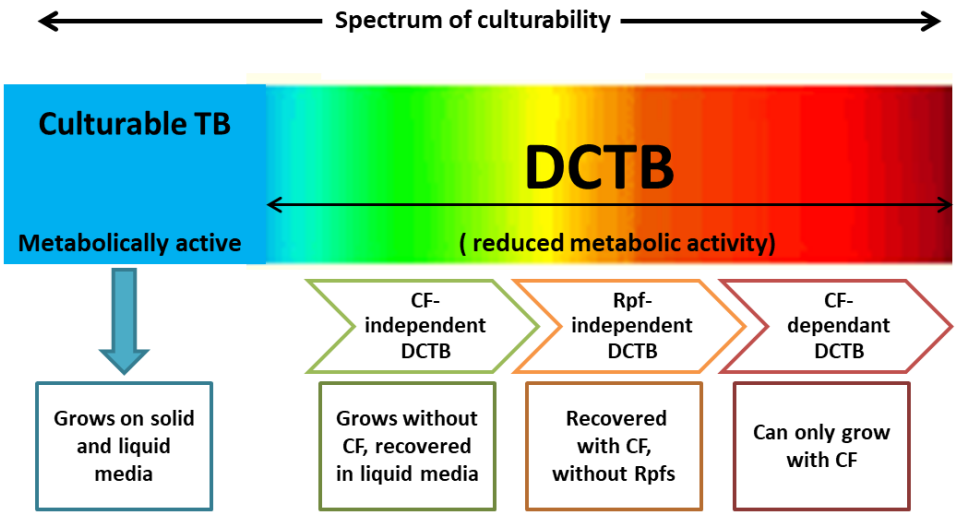


Figure 1.2 Spectrum of culturability indicating different culturable states based on metabolic activity of the bacterium. The left side of the spectrum shows the metabolically active bacteria that can grow on solid and liquid media (blue) while the right side shows a spectrum of non-replicating bacteria representing the DCTB population that are unable to grow on solid media and require various factors to recover (green to red) in liquid media (Chengalroyen et al., 2016).

1.4 Antibiotic treatment and DCTB

Antibiotics generally target actively growing bacteria and as a result, the DCTB state may be associated with an increased drug tolerance (Bamford et al., 2017; Kim, Chowdhury, Yamasaki, & Wood, 2018). Antimicrobial therapies are designed to target the entire bacterial population and assume that all cells will be equally sensitive (Anuchin et al., 2009; Ayrapetyan et al., 2015; Kim et al., 2018). Within genetically identical bacterial populations, there are sub-populations with differential drug susceptibility. These bacterial subpopulations display phenotypic heterogeneity (Ayrapetyan, Williams, & Oliver, 2018; Chao & Rubin, 2010; Fonseca et al., 2009). Phenotypic heterogeneity is an evolutionary selectable trait which plays an essential role in the fitness of the bacterium (Ayrapetyan et al., 2018; Fonseca et al., 2009; Lin & Flynn, 2010). The term 'phenotypic antibiotic tolerance' is used to describe the reduced efficacy of antibiotics against non-replicating bacteria in the absence of known genotypic resistance (Honeyborne et al., 2016; Jones, 2000). For a pathogen to be successful it must be able to persist in the host tissue hence, the presence of non-replicating, phenotypically antibiotic tolerant bacteria such as DCTB might aid *M. tuberculosis* to persist and could contribute to the need for prolonged drug therapy during active TB disease (Gomez & McKinney, 2004; Nguyen et al., 2019; Stewart, Robertson, & Young, 2003).

1.5 *In vitro* models for DCTB

Metabolic activity is quantified by the synthesis of nucleotides, proteins and metabolites, to allow growth and replication (Alnimr, 2015; Ayrapetyan et al., 2018). The production of ATP as energy is essential in maintaining metabolic activity and disruption in energy processes results in metabolic quiescence (Alnimr, 2015; Higgins & Dworkin, 2012). Exposure to environmental stress, such as nutrient starvation, hypoxia, pH imbalances and temperature fluctuations, cause disruption in energy processes and force the bacterium to conserve energy (Alnimr, 2015; Anuchin et al., 2009; Meneghini, 2015). Mycobacterial species conserves energy by selectively expressing essential genes and transcripts to enable survival under these conditions (Buerger et al., 2012). It is unclear if the reduction in metabolism that is expected to occur during the DCTB state is due to the absence of required metabolic precursors such as carbon, nitrogen and phosphorus or if the bacterium is strategically using less to minimize its nutritional needs (Buerger et al., 2012; Glickman & Jacobs, 2001). There are several *in vitro* stress models that attempt to recapitulate the DCTB or dormant state, these are summarized in table 1.2.

Table 1.2-Summary of the various *in vitro* stress models

DCTB model	Description	State of the bacteria	Authors
1. Wayne model	Gradual depletion of oxygen, as abrupt depletion of oxygen leads to cell death. The depletion is done in two stages. The 1st stage, often referred to as the microaerophilic stage, as oxygen levels are reduced to 1%. The 2nd stage is close to the anaerobic stage, as oxygen levels are reduced to 0.06 %.	The bacteria in the 1st stage have reduced replication, however there is still ATP production and some active mechanisms of DNA repair. The anaerobic environment induces the DosR regulator, which is essential for survival under hypoxic conditions and bacteria. In the second stage, bacteria transition into an NRP*.	Wayne et al, 1996
2. Starvation model	The culturing of *M. tuberculosis* in nutrient rich media, before transferring the culture into PBS with no carbon source.	When the bacteria are cultured in PBS respiration levels slowly decrease as the bacteria transition into a non-replicative state that is reversible.	Loebel et al, 1933 and Betts et al, 2002
3. Chemostat culture system	Chemostat is used to tightly control conditions such as temperature, oxygen and pH. A culture of *M. tuberculosis* is grown with oxygen levels reduced to 50%. This culture is then maintained until all nutrients have been depleted from the media.	Prolonged stationary phase results in gradual nutrient depletion in cultures. The bacteria have a population of unculturable cells on solid media that can be grown in liquid. However, after 80 days the bacteria are able to restart growth as a result of adaption to the new environment.	Shleeva et al, 2002
4. Biofilm model	Biofilms are complex structures which, are formed at the air -media interface when *M. tuberculosis* is cultured in Sautons minimal media.	The formation of the biofilm creates a heterogonous microenvironment consisting of both hypoxia and nutrient starvation.	Kukla et al, 2012
5. Potassium depletion model	*M. tuberculosis* is cultured in Sautons minimal media, before transferring the culture in potassium depleted Sautons media.	Potassium is crucial for maintaining an electrochemical gradient, regulating intracellular osmotic pressure and pH in bacteria. When potassium ions are depleted from the media, the bacteria are able to switch to alternative metabolism	Salina et al, 2014
6. Nitric Oxide model	*M. tuberculosis* is exposed to low levels of Nitric Oxide (NO) to mimic immune response in activated macrophages.	When the bacteria are exposed to NO, it acts as an inhibitor of aerobic respiration and creates a hypoxic environment. The bacteria enter an anaerobic state, with reduced replication and respiration.	Voskuil et al, 2003

*NRP- non-replicating persister

1.5.1 Starvation model

One of the first *in vitro* models of non-replicating persister bacteria (NRP) was discovered in 1933 when Loebel and colleagues transferred a *M. tuberculosis* culture grown in nutrient rich media into phosphate-buffered saline (PBS) and found that respiration levels slowly decreased whilst the culture remained in an early stationary phase (Loebel, Shorr, & Richardson, 1933). Loebel and colleges concluded that "*it was possible for M. tuberculosis to survive for extended periods of time in PBS and that this virulence factor could be attributed to the bacteria's ability to depress its oxygen consumption and live off previously stored food stuff* (Loebel et al., 1933)." Conditions within the granuloma, differ greatly from those encountered *in vitro*. Despite this difference, *in vitro* carbon starved *M. tuberculosis* has a similar morphology to the phenotype of bacteria from the granuloma, suggesting that carbon starvation is an essential environmental stress that the bacteria encounter within the granuloma (Wu, Gengenbacher, & Dick, 2016). Betts and colleagues developed a model based on Loebel's observations wherein an *M. tuberculosis* culture was sub-cultured in PBS for 7 days, in a sealed container to generate a carbon starved environment (Betts, Lukey, Robb, McAdam, & Duncan, 2002). During this period, the transcriptional profile of the *M. tuberculosis* showed decreased transcription in processes involving energy metabolism, lipid biosynthesis and cell division in order to maintain long-term survival. These observations were in concurrence with previous observations made by Loebel and colleagues (Betts et al., 2002). However, when the starved bacteria in sealed container were monitored for oxygen consumption, there was no indication of hypoxia therefore, indicating that instead of consuming oxygen, the bacteria slowed down their respiration rate and entered a NRP state (Betts et al., 2002; Lipworth et al., 2016).

Recently, an *in vitro* model was described to produce DCTB that requires two sequential stresses: starvation with phosphate buffered saline (PBS) and drug exposure to RIF (Saito et al., 2017). The authors concluded that the generation of DCTB is specific to RIF exposure, as inhibitors of bacterial macromolecular synthesis can exert differential effects on individual genes or gene products, rather than halt transcription (Saito et al., 2017). Saito et .al speculated that treatment of starved bacteria with RIF rather than halting transcription altogether, selectively affect the transcription of different genes in a way that allows the bacterium to enter a DC state (Saito et al., 2017).

1.5.2 Biofilm model

Another model that could be used to generate DCTB is the biofilm model. Biofilms are formed when bacteria undergo stress in minimal media (Kulka, Hatfull and Ojha, 2012). Nutrients, ions, and carbon sources influence bacterial behaviour and have a regulatory role in biofilm formation (Esteban and García-coca, 2018). Biofilm formation is initiated by the adherence of a single microorganism to a surface. However, some mycobacteria can also develop these structures at the air-media interfaces of stationary cultures due to the high lipid content of the mycobacterial cell wall (Ojha et al., 2008). Biofilms consist of heterogeneous conditions, with a constant balance between consumption and diffusion of nutrients (Brennan, 2017; Kulka, Hatfull, & Ojha, 2012). A study done on mixed species heterotrophic biofilms revealed that oxygen concentrations at the biofilm-fluid interface was reduced to 40% compared to planktonic culture and continued to decrease with increasing depth of the biofilm. Furthermore, any nutrient that is consumed in the biofilm will also decrease with increasing depth into the biofilm and distance from the nutrient source (Esteban & García-Coca, 2018). In a mature biofilm, three distinctive physiological states can be found. The first stage consists of cells that are located near the biofilm-air interface, which grow by aerobic metabolism as oxygen will be available (Kulka et al., 2012; Solokhina, Brückner, Bonkat, & Braissant, 2017). In the next state, which is located in the middle of the biofilm between the air-biofilm interface and the biofilm-fluid interface, the cells grow by fermentation, as oxygen is sparingly soluble and is the usually the first metabolite to be depleted (Solokhina et al., 2017). The third stage in located deeper in the biofilm at the biofilm–fluid interface, and consist of a region where oxygen and substrate have been depleted and cells become inactive or begin to die (Solokhina et al., 2017). Adaption to these varying stages of environmental stress most likely contributes to phenotypic heterogeneity. Recent studies have demonstrated that genetic variants in the population have arisen in biofilms due to mutations in scholastic gene expression following biofilm growth in a stressful environment (Esteban & García-Coca, 2018; Kulka et al., 2012; Solokhina et al., 2017). The presence of varying stresses and genetic variation in sub-populations, could aid in the generation of DCTB.

1.5.3 Ion deficiency model

Another nutrient depletion condition that bacteria need to adapt to in the host, is the changes in ion concentrations. Mycobacteria engulfed by macrophages are subjected to potassium (K^+) depletion in the phago-lysosome caused by K^+ efflux pumps (Actor et al., 2008). K^+ ions are essential for many cellular functions, including the maintenance of intracellular pH and

membrane osmolarity (Rodriguez, Ocampo, Salazar, & Patarroyo, 2018). Potassium concentrations within bacterial cells range from 0.1 to 1 M, compared to 140 mM found in eukaryotic cells (Treuner-Lange, Kuhn, & Dürre, 1997). Mycobacteria are dependent on K+ ions to maintain pH in mildly acid conditions, thus *M. tuberculosis* has several tightly regulated pathways to regulate disruptions in potassium ions (Cholo, van Rensburg, & Anderson, 2008; Salina et al., 2019). One of the major pathways involved in potassium regulation is the inducible KDP potassium ion transport system, which is encoded by the *kdpA-E* genes (Cholo et al., 2008; X. Liu et al., 2020). The potassium ion is important for the function of Na^+K^+ transporting ATPases in mycobacteria. In the early stages of potassium limitation, the membrane becomes hyperpolarized and disrupts ion transport activity by induction of the high-affinity ATP KDP transport system (Cholo et al., 2008; X. Liu et al., 2020).

In 2015, Salina and colleagues revealed that generation of non-culturable bacteria occurred in media deficient of potassium, when cultured for minimum of 28 days in minimal media (Salina et al., 2014). *M. tuberculosis* cells grown under potassium limitation, displayed changes in cell morphology. The cells appeared coccoid with intact membranes and a condensed cytoplasm that closely resembled forms associated with dormant phenotypes. These bacteria were not sensitive to INH and 1,3-benzothiazin-4-ones (BTZ) antibiotics that target cell wall biosynthesis pathways, but were sensitive to RIF, suggesting that transcription was still occurring.

1.6 The relationship between *M. tuberculosis* genotype and DCTB

1.6.1 Evolution and strain lineage of clinical strains of *M. tuberculosis*

The MTBC has evolved into six lineages based on their geographical location. These include, East Asian, Euro-American, West Africa 1 and 2, Indo-Oceanic and East African-Indian (Figure 1.3) (Gagneux & Small, 2007; Shabbeer et al., 2012). In addition to geographical location, the six lineages of MTBC are classified by the variations in large sequence polymorphisms (LSPs) and single nucleotide polymorphisms (SNPs) (Van der Spoel van Dijk, Makhoahle, Rigouts, & Baba, 2016). These strains can be further subdivided into two categories, ancient or modern, based on the deletion of the TbD1 region. The Indo-oceanic lineage, West Africa 1 and West Africa 2 are strains that contain the TbD1 region and are classified as ancient strains, whilst East Asian, Euro-American and East-African-Indian are classified as modern strains (Shabbeer et al., 2012). In each lineage, strains are typed based on

the variability found in the direct repeat (DR) locus, which contains a variable number of short direct repeats. The presence or absence of these repeats at 43 spaces on the DR locus determines the spoligotype family, which are sub-lineages within the main lineage (Gagneux & Small, 2007; Glickman & Jacobs, 2001). These strain types include: Beijing, (Latin American-Mediterranean (LAM), T-strains, S-family, X-strains, Central Asian strain (CAS), East African-Indian (EAI), Haarlem and *Mycobacterium africanum* subtype 1 (AFRI), as shown in figure 1.3.

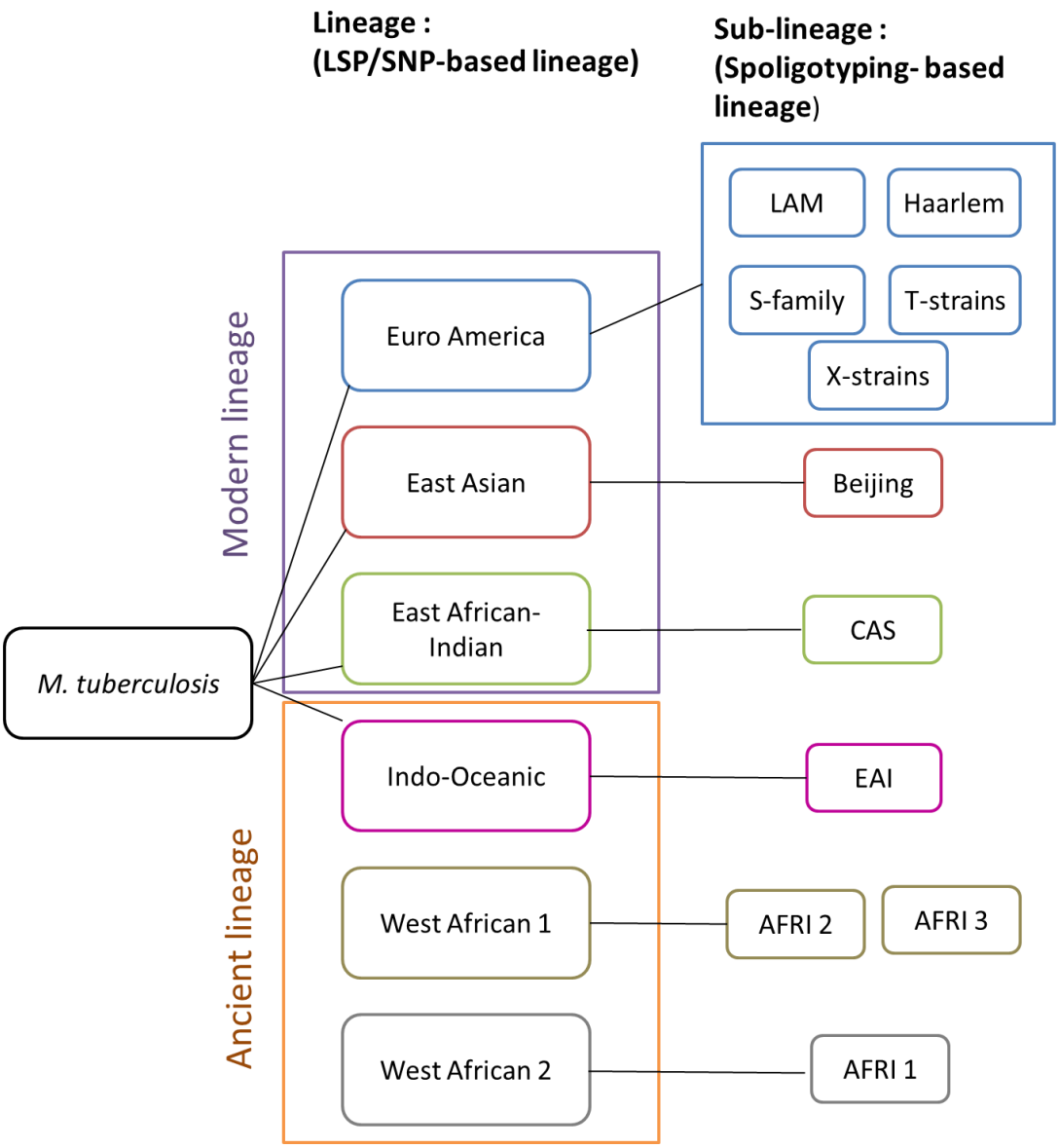


Figure 1.3 Evolution of *M. tuberculosis* Phylogeny of *M. tuberculosis* clinical strains and their classification. Adapted from (Gagneux & Small, 2007).

1.6.2 Strain diversity in South Africa

In South Africa, several *M. tuberculosis* strain types, including Beijing, LAM, CAS, S-family, X and T1 strains, which have evolved from the six lineage strains are well distributed (Figure 1.4) (Chihota et al., 2018; Gagneux, 2013; Hanekom et al., 2010). This diverse distribution is a result of the founder effect where certain *M. tuberculosis* strains were initially introduced into the country as a result of colonization and sea trade and later were distributed around the country through the movement of individuals (Chihota et al., 2018; Hanekom et al., 2011). The TB epidemic in South Africa is dominated by four strain types: LAM, Beijing, T-strains and X-strains (Chihota et al., 2018). Beijing and LAM strains have been the subject of intensive studies directed to unravelling the mechanistic basis for their increased penetration in the human population (Chihota et al., 2018; Hanekom et al., 2011).

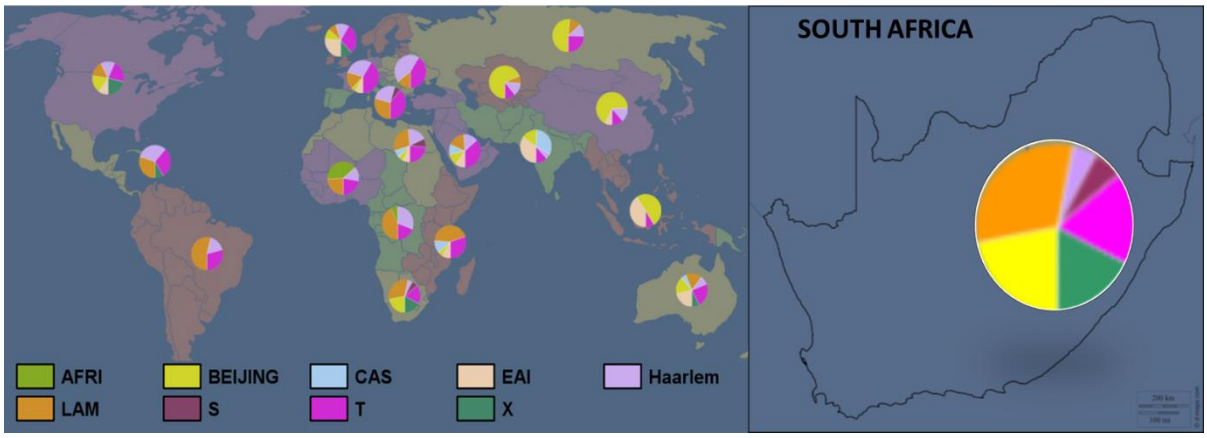


Figure 1.4 A world map indicating the distribution patterns of strain types derived from (online SITVIT database: www.pasteur-guadeloupe.fr:8081/SITVIT_ONLINE). On the right is a map of South Africa showing that the LAM, X, Beijing and T strains are the dominate strain type infecting the population.

The Beijing strain, first identified in 1995, has evolved into a successful strain due to its increased virulence and transmission properties relative to other clinical strains (Glynn, Whiteley, Bifani, Kremer, & van Soolingen, 2002; Y. Liu et al., 2017). Since its origin in East Asia, the strain has spread globally and was introduced to South Africa (currently infecting 20% of diagnosed patients) through trade routes (Chihota et al., 2018; Hanekom et al., 2010). This increase in prevalence of the Beijing lineage in South Africa, is speculated to be due to the HIV epidemic (Parwati, van Crevel, & van Soolingen, 2010). The sub-lineage strain LAM, is thought to have been introduced to Southern Africa through expeditions and trade from Portugal. A LAM derivative: F15/LAM4/KZN strain has been associated with MDR-TB, and was responsible for the first case of XDR-TB in South Africa (Ashiru, Pillay, & Sturm, 2010; Gandhi et al., 2006). Furthermore, a LAM3/F11 derivative strain, has been shown to be as

successful as Beijing, in contributing to the TB epidemic in the Western Cape (Chihota et al., 2018). Part of the success of LAM and Beijing in dominating the TB epidemic, is due to the increased transmissibility associated with these strains. A recent study based on the collection of clinical isolates in the Western Cape showed that Beijing strains had a high to very high transmission rate, whilst the LAM strains had a moderate to high transmission rate in a guinea pig infection model (Hanekom et al., 2011) (Figure 1.5).

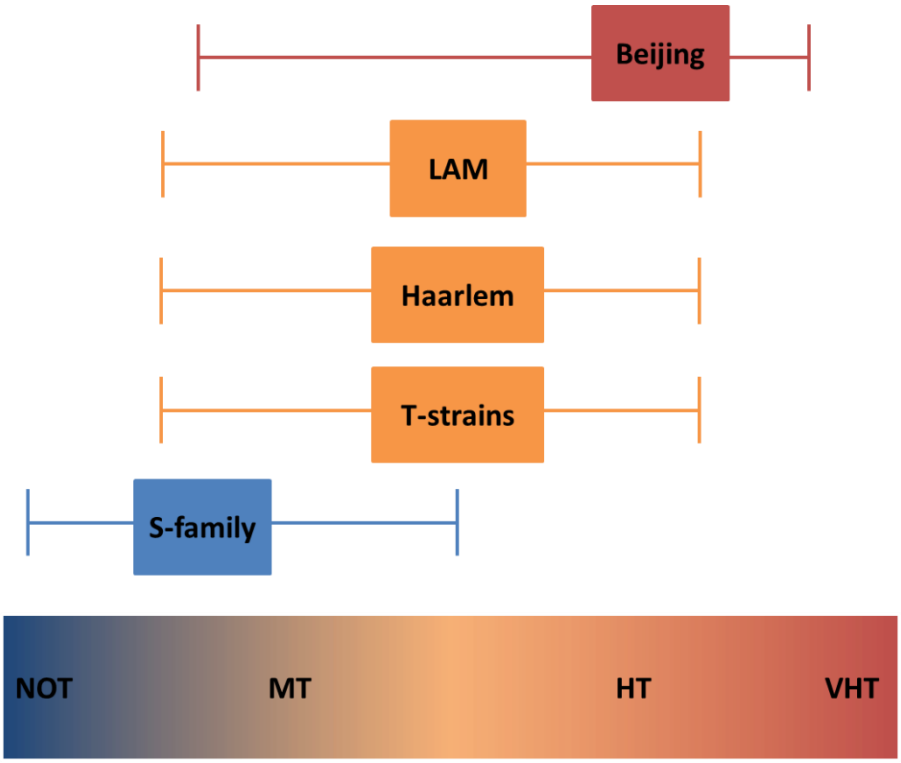


Figure 1.5 The transmissibility of clinical strains. The spectrum shows the range of strain transmission and was derived from the work done by (Shanley et al., 2018). The authors selected the dominant strain types from the Western Cape, South Africa (LAM, Beijing, Haarlem, S-family and T-strains) that had undergone epidemiological genetic typing to determine the transmissibility of the strains. Transmissibility was calculated in four categories: not transmissible (NOT), moderate transmissibility (MT), high transmissibility (HT) and very high transmissibility (VHT)

1.6.3 The impact of clinical strains on treatment outcomes

M. tuberculosis clinical strains were considered to be genetically monomorphic with high levels of genome sequence similarity (99.95%). Hence, it was assumed that because of this high level of similarity, the treatment outcomes between patients infected with different clinical strains would be insignificant (Coscolla & Gagneux, 2014; Gagneux & Small, 2007). However,

advances in whole genome sequencing have shown that there is 10-20 functional differences due to unique SNPs between the various *M. tuberculosis* clinical isolates (Gagneux, 2013; Murase, 2011) indicating that the genetic diversity of *M. tuberculosis* has been greatly underestimated. Recent studies in animal models and human epidemiology have demonstrated that the variability amongst clinical isolates include adaptions for stress survival, transmission and pathology. These various adaptions amongst clinical strains have consequences for treatment outcomes and can result in treatment failure (Coscolla & Gagneux, 2014).

1.6.4 Adaptive mechanism of strains (Beijing and LAM)

Numerous studies have shown that Beijing and LAM strains possess a unique genotype and phenotype compared to other clinical strains. The Beijing and LAM associated phenotype includes characteristics such as alternative host modulation, pathological features and drug resistance (Glynn et al., 2002; Keane et al., 2000; G. Kumar et al., 2017; Y. Liu et al., 2017).

A study by Pheiffer *et al*. demonstrated that the Beijing strain had decreased levels of cell wall mannoprotein Pst1 compared to the H37Rv laboratory strain (Pheiffer, Betts, Flynn, Lukey, & van Helden, 2005). Pst1 is a phospho-binding lipoprotein that stimulates host activation of B and T cells, thus reduced levels of this protein in the Beijing strain allows for evasion of the host immune response (Hanekom et al., 2011; Parwati et al., 2010).

In addition, the Beijing strains have increased expression of the dormancy regulon genes, *dosR*, *Rv3130c*, *hspX*, *fdxA* and *narX* (Reed, Gagneux, Deriemer, Small, & Barry, 2007). These genes are involved in the adaptive response under hypoxic and nitrosative stress conditions (Anuchin et al., 2009). The basal transcription levels of the DosR regulon was 50-fold higher in the Beijing strain compared to LAM and other clinical strains (Reed et al., 2007). This increased expression of the regulon in the Beijing strain is speculated to allow bacteria to alter its metabolism in order to survive under host derived stress conditions.

LAM and Beijing strains have evolved an alternative mechanism to evade detection by the host immune system, through immunomodulation of phenolic glycolipid (PGL) (Gagneux, 2013). Most *M. tuberculosis* clinical isolates, and the laboratory strains H37Rv do not produce PGL due to a frameshift mutation in the polyketide synthase gene *pks15/1*(Gagneux & Small, 2007; Lipworth et al., 2016). PGL is a component of the mycobacteria membrane and whilst the composition of the membrane is highly conserved amongst mycobacteria, the individual lipid constituents can differ in clinical strain isolates (Erie et al., 2017; Parwati et al., 2010). LAM

and Beijing strains have an intact *pks15/1* and are known producers of PGL, allowing these bacteria to survive the host immune response by immunomodulation of the Th1-type cytokines, which are responsible for the pro-inflammatory response (Hanekom et al., 2010; Rindi, Lari, Cuccu, & Garzelli, 2009).

In the clinical setting, Beijing strains have commonly been associated with drug resistance and have the highest MDR prevalence of 17.5% compared to non-Beijing strains (Y. Liu et al., 2017). This increased association with drug resistance suggested that the Beijing sub-type was either more transmissible or had an increased inherent propensity to evolve drug resistance. Kong et al., concluded that the Beijing strain favours transmission rather than acquisition of resistance, as MDR-TB cases appeared to result from patient-to-patient transmission and not from the *de novo* acquisition of resistance during treatment (Kong et al., 2007; Sebastian et al., 2017). In addition to the Beijing lineage, there is emerging evidence suggesting that molecular features of other strain types may influence the ability to evolve drug resistance. As an example, LAM and Haarlem strains have a predisposition to developing RIF resistance due to an evolution of compensatory mutations, such as single nucleotide polymorphisms in the *rpoC* gene (Herranz et al., 2018).

In summary, the above-mentioned adaptations of Beijing and LAM strains provide the bacteria with an advantage to survive and persist within the host for decades before reactivation. These observations suggest that the genetic variation of clinical *M. tuberculosis* isolates is important for pathogenesis, virulence, transmission and treatment outcomes, but little is known about their ability to enter a DC state, as the discovery of DCTB is recent. Thus, the focus of this study was to determine the propensity of clinical strains to induce the DCTB state by modelling environmental conditions such as nutrient depletion encountered by *M. tuberculosis* during host infection.

1.7 Rational of the study

1.7.1 Aim

To develop and optimize *in vitro* models to generate DCTB, as well as to determine the propensity of various clinical *M. tuberculosis* strain types to adopt a DC state.

1.7.2 Objectives

- To determine the propensity of clinical strains to adopt the DC state using DCTB data from two cohort studies using a bioinformatics approach.
- To optimize and test the effectiveness of various models in generating DCTB, using the most probable number (MPN) vs the colony forming units (CFU) assays and flow cytometry.
- To test the propensity of clinical strains to adopt the DC state using the carbon starvation model.
- To test the efficacy of CF from clinical strains, on improving resuscitation of clinical strains.

2. Materials and Methods

2.1 Materials used

A detailed list of materials used in this study can be found in Appendix A

2.2 Strains and culturing conditions

Table 2.1- Laboratory *M. smegmatis* and *M. tuberculosis* strains used in this study

Strain	Description	Origin
M. smegmatis mc^2155	Mutant of mc^2 6 that displays a highly efficient plasmid transformation phenotype. *M. smegmatis* is used in this study as it is a non-pathogenic, model strain for *M. tuberculosis.* In this study, *M. smegmatis* is used to optimize *in vitro* models for generation of differentially culturable *M. smegmatis* (DCMS).	(Snapper, Melton, Mustafa, Kieser, & WR Jr, 1990).
M. tuberculosis H37Rv	H37Rv was initially derived from a clinical isolate, H37 obtained from a patient with TB in 1905. This strain has undergone serial passages to become a laboratory strain, used to study the bacteria. In this study H37RV Johannesburg strain was used (ACCT: 25618). In this study, *M. tuberculosis* is used to optimise a carbon starvation model for generation of DCTB.	(Ioerger et al., 2010)
Beijing strains	Five Beijing strains (Beijing 1, Beijing 2, Beijing 3, Beijing 4, Beijing 5) were isolated from TB infected patients (57165, 59129, 57134, 57154, 59014) in the two clinical studies (BMG and MGIT plus) conducted at the Centre of Excellence for Biomedical TB Research (CBTBR). In both clinical studies, the patient's sputum was collected and tested for the presence of DCTB, using the MPN and CFU assay. After analysis patient samples were stored for future use in this study. The Beijing strains have undergone serial passages to become laboratory strains. In this study, Beijing strains are used to observe the generation of DCTB using a carbon starvation model.	BMG and MGIT plus (Julian Peters et al Manuscript in progress 2020)
LAM strains	Five LAM strains (LAM 1, LAM 2, LAM 3, LAM 4, LAM 5) were isolated from TB infected patients (57165, 59129, 57134, 57154, 59014) in the two clinical studies (BMG and MGIT plus) conducted at the CBTBR. In both clinical studies, the patient's sputum was collected and tested for the presence of DCTB, using the MPN and CFU assay. After analysis patient samples were stored for future use in this study. The LAM strains have undergone serial passaged to become laboratory strains. In this study, LAM strains are used to observe the generation of DCTB using a carbon starvation model.	BMG and MGIT plus (Julian Peters et al, Manuscript in progress 2020)

2.2.1 Culturing conditions

The *M. smegmatis* laboratory strain mc^2155 used in this study was grown in Middlebrook 7H9 liquid media supplemented with 10X glucose salt and 0.05 % Tween®80. *M. smegmatis* was also grown on solid Middlebrook 7H10 media supplemented with 10X glucose salt.

The *M. tuberculosis* laboratory strain H37Rv and clinical strains (Beijing and LAM) from table 2.1, used in this study were grown in liquid Middlebrook 7H9 media supplemented with 0.2 % glycerol, Middlebrook oleic acid-albumin-dextrose-catalase (OADC), and 0.05% Tween®80, unless otherwise stated. *M. tuberculosis* was also grown on solid BBL ™ Middlebrook 7H11 media supplemented with OADC.

2.2.2 Clinical strains used in *in vitro* analysis

In this study, five Beijing clinical strains and five LAM clinical strains (Table 2.1) that produced DCTB (sputum specimens had a resuscitation index greater than 1) were selected at random for *in vitro* analysis. These samples were thawed and streaked out on BBL ™ Middlebrook 7H11 media, and incubated for 3 weeks at 37°C. Single colonies were selected and subcultured twice for 7 days at 37 °C in 5 ml of Middlebrook 7H9 media supplemented with OADC and Polymyxin B, Amphotericin B, Nalidixic acid, Trimethoprim and Azlocillin (PANTA). During the first round of subculturing, double the recommended dose of PANTA was added to ensure that majority of the contaminating bacteria were killed while the second exposure to PANTA was to ensure the sample contained only *M. tuberculosis*. To confirm this, the culture was streaked out on BBL™ Middlebrook 7H11 plates and incubated for 3 weeks at 37 °C, after which single colonies were selected and spoligotyped (Section 2.3.2), to reconfirm the strain type.

2.3 Genotyping of *M. tuberculosis* strains

2.3.1 Genomic DNA extraction

2.3.1.1 Large scale DNA extraction

The *M. tuberculosis* laboratory strain (H37Rv) and the clinical strains Beijing and LAM were grown on 7H11 Middlebrook BBL plates from which two to four loops of the culture were re-suspended in 500 µl of TE buffer until a homogenous mixture was formed. The cells were then killed by heating the suspension at 65 °C for 20 minutes before 70 µl of lysozyme (10 mg/ml) was added and incubated at 37 °C for 1 hour. Following lysozyme treatment, 6 µl of proteinase K and 70 µl of 10% SDS were added to the suspension and incubated for two hours at 65ºC,

after which, 100 µl of NaCl (5M) and 80 µl of pre-warmed CTAB/NaCl was added and the mixed suspension incubated at 65°C for 10 minutes. Thereafter, an equal volume of chloroform:isoamyl alcohol (24:1 v/v) was added and the suspension mixed vigorously before centrifugation at 1240 ×g for 5 minutes. The top aqueous layer containing the DNA was decanted into a fresh Eppendorf tube without disturbing the protein interphase. The DNA was precipitated with 450 µl isopropanol by centrifugation at 1240 ×g for 20 minutes at 4 °C. The DNA pellet was washed with 70% ethanol by centrifugation for one minute. The DNA pellet was dried in a speedvac and re-suspended in 100 µl of sdH2O.

2.3.1.2 Colony boil method

M. tuberculosis laboratory strain (H37Rv) and the of LAM and Beijing clinical strains were grown on 7H11 Middlebrook plates supplemented with OADC and a loopful of the bacteria was re-suspended in 50 µl of TE buffer. The samples were placed in a heating block for 15 minutes at 90°C, to kill the bacteria. After heat killing, the samples were centrifuged at 1240 ×g for 10 minutes. The top aqueous layer containing the DNA was removed to a fresh Eppendorf tube and used for spoligotyping

2.3.2 Spoligotyping

Spoligotyping is a method used to classify the lineage of *M. tuberculosis* clinical strains. In each lineage, strains are typed based on the variability found in the direct repeat (DR) locus, which contains a variable number of short direct repeats. The presence or absence of these repeats at 43 spaces in the DR locus determines the spoligotype family. Figure 2.1 shows the various steps for spoligotyping, which are further described in detail in the following text.

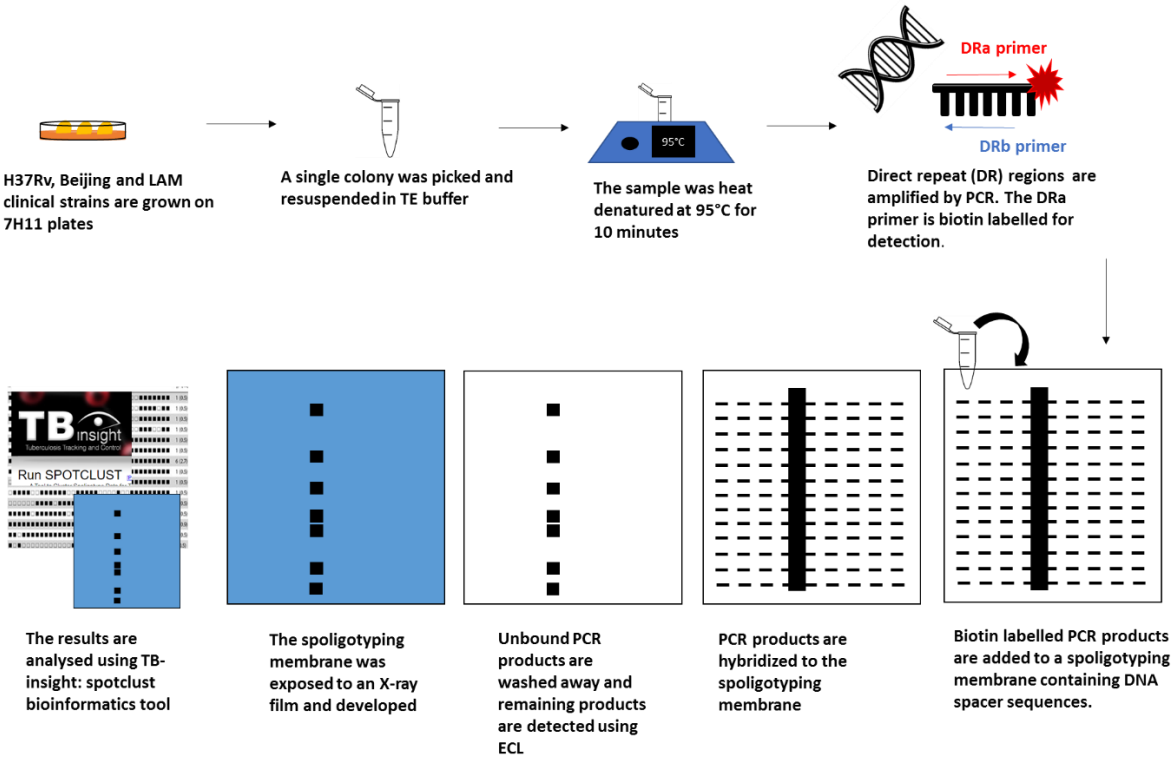


Figure 2.1 Spoligotyping procedure. A flow diagram showing the various steps involved in the spoligotyping procedure. DNA is extracted from bacteria, and the DR region is amplified using PCR. The amplified DNA products are hybridised to a spoligotyping membrane, which contains bound oligo spacer sequences. The bound products are detected using enhanced chemiluminescence (ECL).

2.3.2.1 Polymerase chain reaction (PCR)

The first step in spoligotyping procedure requires the DR regions in DNA of the clinical *M. tuberculosis* strains to be amplified by polymerase chain reaction. The DRa and DRb primers (Table 2.2) supplied in the spoligotyping kit were used to amplify the DR regions from genomic DNA extracted from the H37Rv, Beijing and LAM strains. The DRa primer contains non-radioactive biotin molecule, which integrates into the amplified DR regions, and can later be detected by a chemical reaction using streptavidin. The DRa and DRb primers were received as a 100 µM stock and were reconstituted in 1 ml of nuclease free water.

Table 2.2- PCR primers used for the conformation of clinical strains.

Primer	***Primer oligonucleotide sequence (5'-3')***	***Annealing (T_m) of primer***	***Storage temp***
DRa (5' biotin)	GGTTTTGGGTCTGACGAC	55°C	4 °C
DRb	CCGAGAGGGGACGGAAAC		-20 °C

The ReadyMix™ Taq PCR reaction mix supplied with the kit (Sigma-Aldrich) contained 12.5 µl of ReadyMix, 6.5 µl of dH_2O, 2 µl of DRa primer, 2 µl of DRb primer, to which 2 µl of template DNA was added to make up a 25 µl reaction. The PCR reaction was briefly spun down for 1-5 seconds to ensure that all components were mixed before placing the tubes into the Bio-Rad thermocycler machine. The following cycling conditions were used: an initial denaturation step at 95 °C for 3 minutes followed by 35 cycles of sample denaturation at 95°C for 30 seconds, annealing at 55 °C for 1 minute and elongation at 72 °C for 30 seconds. The PCR was completed with a final elongation step at 72 °C for 10 minutes. Once the PCR was completed, the reaction was stored at 4°C for not longer than a week if it was not used immediately for spoligotyping.

2.3.2.2 Hybridization and detection

The next step of spoligotyping involves the hybridization of the biotin labelled PCR products to a spoligotyping membrane that contains immobilized membrane-bound spacer oligo nucleotides of the DR region. The extracted DNA is hybridised on the spoligotyping membrane and the bound PCR products are detected with streptavidin-peroxidase, together with an enhanced chemiluminescence (ECL) reagent on an X-ray film. The bound DNA is detected by presence of spacer sequences represented by a black square. The absence or presence of a black square reveals a pattern that is used to determine the strain type. A detailed description of the process is noted below.

To the 25 µl PCR reaction, 150 µl of 2X SSPE/ 0.1% sodium dodecyl sulphate (2XSSPE/0.1% SDS) was added and the tube transferred to the Bio-Rad thermocycler for 10 minutes at 99 ºC to heat denature the PCR product. The tubes were immediately placed on ice until they were ready to be loaded onto the membrane to prevent the DNA from reannealing.

The spoligotyping membrane was washed twice in 2X SSPE/0.1% SDS and placed in the oven at 60 °C for five minutes after every wash. The washed membrane was placed on a cushion in the mini-blotter in the correct orientation, with all the marked sides lined up and the slot of the mini-blotter running parallel to the line pattern on the membrane (Figure 2.2). Any excess fluid was wiped with a paper towel, before the mini-blotter was tightly sealed using plastic screws. Any residual fluid was removed from the slots of the mini-blotter by aspiration using a syringe and a vacuum pump (Figure 2.2).

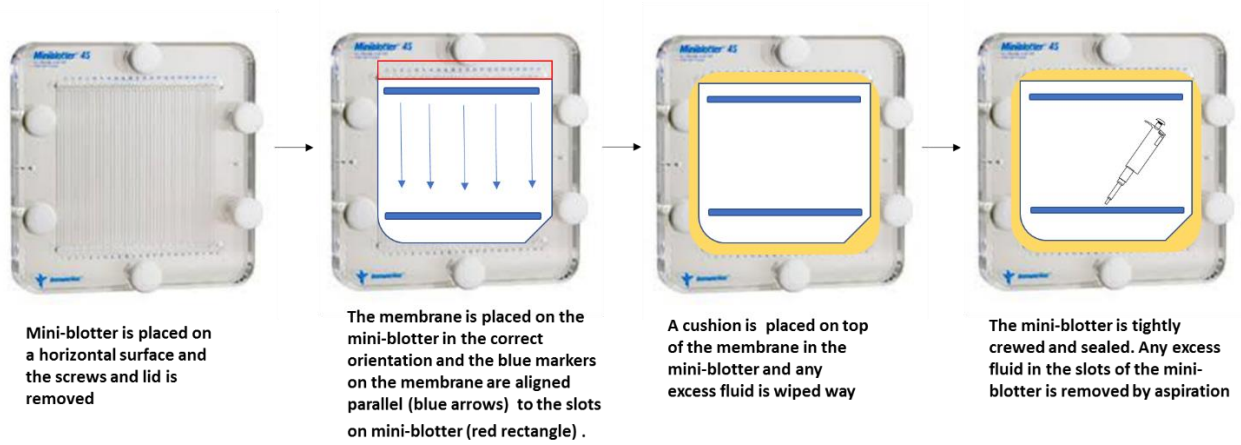


Figure 2.2 Spoligotyping blot orientation. A flow diagram showing the steps involved in placing the membrane in the correct orientation on the mini-blotter. The mini-blotter is opened and the membrane is placed in the corrected orientation marked by the cut edge and positioned running parallel to the open slots marked by the red rectangle. Excess fluid is wiped away and aspirated using a pipette.

The sealed mini-blotter was placed on a horizontal surface and 160 µl of the DNA mixture was loaded into the slots of the mini-blotter. The first and the last wells of the 45 well membrane were filled with 2X SSPE/0.1% SDS. The PCR reaction using DNA from H37Rv and BCG (supplied in the kit) together with a no DNA template reaction were included as controls for each run. The mini-blotter was then transferred to the hybridization oven and incubated on a horizontal surface at 60 °C for one hour. After hybridization, any remaining sample was removed from the mini-blotter by aspiration before removing the membrane from the mini-blotter. The membrane was washed twice in 2X SSPE/0.5% SDS for five minutes at 60 °C.

Next the hybridized biotin-labelled PCR products, bound to spacer-oligos on the membrane, were detected using chemiluminescent detection. The membrane was placed in a roller bottle, containing a mixture of 40 ml of 2X SPPE/0.5% SDS and 10 µl Streptavidin-peroxidase conjugate (500U/mL) and incubated at 42 °C for one hour. The membrane was washed twice with 2XSSPE0.5% SDS and incubated at 42 °C for 5 minutes. An ECL detection kit (GE Healthcare) was used, and 10 ml of detection solution 1 and solution 2 was added to a glass bowl containing the membrane. Both solutions were swirled in the glass container for 90 s, after which the solution was discarded. The membrane was then placed in a clear plastic sleeve and exposed to three light sensitive X-ray film sheets for 20 minutes. The X-ray films were developed manually in the dark room. The spoligotyping membrane was stripped by incubation in 10% SDS at 80 °C for an hour and stored in 20 µM EDTA at 4 °C for reuse.

The spoligotype pattern was displayed by the presence or absence of black squares on the membrane representing the spacer sequences. The black squares were allocated a binary value of 1 whilst the blank space was allocated a binary value of 0. The 43 character binary value was entered into the spotclust spoligotyping website to determine the strain type (http://tbinsight.cs.rpi.edu/run_spotclust.html, (Vitol et al., 2006).

2.4 *In vitro* stress models

2.4.1 Carbon starvation model

2.4.1.1 The Betts et.al, starvation model

M. tuberculosis (laboratory and clinical strains) and *M. smegmatis* were grown in triplicate to log phase in 20 ml of 7H9 Middlebrook media, to an optical density (OD_{600nm}) between 0.5 and 0.8, which corresponds to a CFU/ml between 10^5 to 10^9. The cultures were centrifuged 4000 ×g for 10 minutes, and washed twice in phosphate buffer saline, with 0.05% tyloxapol (1X PBS-Tx), After the second wash, the cell suspension in 1X PBS-Tx was centrifuged at 123 ×g for 8 minutes with no deceleration to generate a single cell suspension. The single cell suspension was diluted to OD_{600nm} = 0.1 in a 25 ml culture and the colony forming units/ml (CFU) was determined by plating serial dilutions in duplicate on 7H10 Middlebrook media for *M. smegmatis* and 7H11 Middlebrook media for *M. tuberculosis*. The remaining culture was incubated without shaking at 37 °C, 20% O_2, and 5% CO_2, for 1 week (*M. smegmatis*) or 2 weeks (*M. tuberculosis*). After 1 or 2 weeks, three 1 ml aliquots of the starved cultured was removed for (1) MPN and CFU analysis as described in section 2.5, (2) flow cytometry as described in section 2.7 and (3) microscopy as described in section 2.8

2.4.1.2 Saito et.al, sequential stress DCTB model

The bacteria were initially starved following the protocol described in Method 2.4.1.1. After starvation for 1 week in PBS at 37 °C, the cultures were swirled gently to remove any excess bacteria on the side of the flask. The culture was split into five equal volumes in a new flask (each flask containing 5 ml culture), four of the flasks were treated with Rifampicin (RIF) (25 µM, 50 µM 75 µM and 100 µM) whilst the other flask was treated with DMSO as a control. All flasks were placed in a dark plastic container , as RIF is sensitive to light and incubated at 37 °C, 20% O_2, and 5% CO_2, without shaking or agitation for 1 week. After 1 week, three 1 ml aliquots of the starved cultured treated with RIF was removed for (1) MPN and CFU analysis as described in section 2.5, (2) flow cytometry as described in section 2.7 and (3) microscopy as described in section 2.8.

2.4.2 Biofilm model

Sautons minimal media was prepared by adding 0.5 g of KH_2PO_4, 0.5 g of $MgSO_4$, 4 g of L-Asparagine, 2 g of Citric acid, 0.05 g of Ferric Ammonium Citrate and 60 ml of glycerol in 900 ml of water. The pH of the media was adjusted to 7.0 with NaOH. The media was then autoclaved, cooled and sterile $ZnSO_4$ was added to a final concentration of 0.1% w/v just before using the media. *M. smegmatis* was grown to an OD_{600nm} = 0.8-1 in 10 ml of 7H9 Middlebrook media and resuspended in a 1:100 dilution in Sautons minimal media. One ml of the mixture was removed for plating on 7H10 Middlebrook media to determine the CFU/ml of the inoculum, using the procedure described in section 2.5.2. Two millilitre aliquots of the remaining cells were dispensed into each well of a 24 well plate. The closed plate was sealed with biohazard tape and incubated undisturbed for 7 days at 37 °C. Plates containing the biofilm were viewed after 7 days, using a dissecting microscope.

2.4.2.1 Removal of bacteria from biofilm

Once the biofilm was fully formed, the bacteria were removed and assessed for DCMS by the MPN and CFU assay, following the protocol described in section 2.5. Bacteria were removed by scraping the top layer with an inoculation loop and placing it in a 5 ml conical tube. The bottom aqueous layer was then removed using a pipette and placed in the same tube. To the 5 ml tube, containing both the top and bottom layer of the biofilm, 0.5% Tween®80 and 3 mm glass beads were added. The mixture was then rocked gently overnight to create a homogenous mixture. The mixture was extremely viscous and diluted to a 1:10 ratio with Sautons minimal media in three 1 ml aliquots for the assessment of DCMS by (1) MPN and CFU assay as described in section 2.5, (2) flow cytometry as described in section 2.7 and (3) microscopy as described in section 2.8

2.4.2.2 Treatment of biofilms with RIF

After the biofilm was fully formed, it was treated with varying concentration of RIF: 100 µM, 150 µM, 200 µM and 300 µM, in order to enhance the production of DCMS. RIF was applied to the biofilm as drops to the centre of the biofilm and after a few minutes, the plates were resealed to allow the RIF to diffuse throughout the structure. The plates were placed back in the incubator for 3, 5, or 7 days. After treatment with RIF, the bacteria from the biofilms were removed following the protocol described in section 2.4.2.1.

2.4.3 Potassium depletion model

Sautons minimal media, without potassium ions was prepared following the recipe described in section 2.4.2, and the 0.5g of KH_2PO_4 was substituted by adding 0.5 g of Na_2PO_4. *M. smegmatis* was grown to an OD_{600nm} = 0.6-0.8, in 10 ml of 7H9 media. The culture was spun down and washed twice with Sautons minimal media depleted of potassium ions, before being sub-cultured to an OD_{600nm} = 0.1 in potassium depleted media. The culture was incubated over a period of 24 hrs, 72 hrs, 120 hrs, 168 hrs and 336 hrs at 37 °C, with shaking. Three 1 ml aliquots of culture were removed at each time point for the assessment of DCMS by (1) MPN and CFU assay described in section 2.5, (2) flow cytometry described in section 2.7 and (3) microscopy described in section 2.8

2.4.3.1 Formation of biofilms in potassium depleted media

Sautons minimal media with and without potassium ions was prepared as described in section 2.3.2.1 and 2.3.3. The inoculum was prepared by growing *M. smegmatis* to an OD_{600nm} = 0.8-1. The inoculum was diluted to a 1:100 ratio in a Falcon tube containing Sautons minimal media with and without potassium ions and 1ml of the mixture was removed to be plated on 7H10 Middlebrook media plates to determine the inoculum CFU/ml. The remaining mixture was gently swirled, before adding 2 ml into a well on a 24 well plate. The plate was covered with a lid, sealed with biohazard tape and incubated undisturbed for 7 days at 37 °C. Plates were viewed after 7 days for biofilm formation.

2.5 Assessment of differentially culturable bacteria

2.5.1 Most probable number (MPN) assay

The MPN assay, determines an approximate number of bacteria in liquid media using a limiting serial dilution and a Poisson distribution calculation. The limit of detection in the MPN assay is dependent on the dilution factor, number of dilutions set up and number of replicates.

2.5.2 Culture filtrate preparation

Culture filtrate (CF), contains a collection of growth stimulatory molecules that the bacteria release into the media, during growth. In this study, CF is used to supplement liquid media and aid in the resuscitation of DCTB.

Axenic cultures of *M. tuberculosis* (laboratory and clinical strains) and *M. smegmatis* were prepared by inoculating a 1 ml freezer stock to 8 ml of 7H9 Middlebrook media and grown for

to an OD_{600nm} = 0.5. The pre-culture was added to 42 ml of 7H9 Middlebrook media and grown to an OD_{600nm}= 0.6-0.8. The culture was centrifuged at 3000 ×g for 10 minutes. The supernatant was filter-sterilized using a 0.2-µm filter and diluted in a 1:1 ratio with 7H9 Middlebrook media, before use.

Samples of the CF were tested for mycobacterial contamination by spreading 500µl of the sample onto a 7H11 Middlebrook plate and 1 ml aliquots of CF were incubated at 37 °C. The aliquots were checked weekly for contamination, while the 7H11 Middlebrook plates were checked after 3 weeks.

2.5.3 The set-up of the MPN assay in a 96 well plate

In a 96 well microtiter plate, 180 µl of 7H9 Middlebrook media or CF was added to each well across the plate (Figure 2.3). To column 2B-2F, 20 µl of the sample was added, after the sample was vortexed 3 times for 10 seconds (Figure 2.3). The wells containing the sample were mixed by pipetting the 100 µl volume using a multichannel pipette. A 10-fold serial dilution was performed across the plate, by transferring 20 µl of 2B-2F into 3B-3F and mixing. This process was repeated until column 11B-11F (Figure 2.3), and the last set of 20 µl was discarded. The MPN plates were sealed using biohazard tape and placed in resealable bag. The MPN plates were incubated at 37 °C for 5 weeks. All experiments were conducted with three biological replicates, and six internal replicates to increase the accuracy of the MPN calculator.

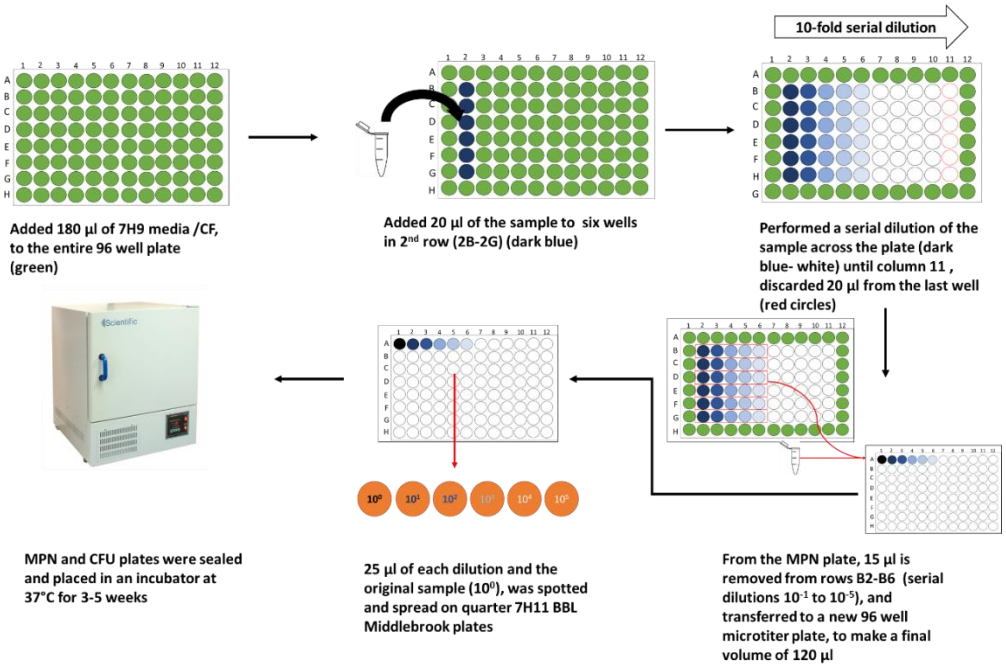


Figure 2.3. The set-up of the MPN and CFU protocol. A Visual representation on how the MPN assay is performed. MPN assay calculates the number of bacteria in a liquid culture using a limiting serial dilution of the sample represented in blue, across a 96 well plate. In this study a 10-fold serial dilution was performed across

the 96 well plate. A sample was extracted from the MPN plate and placed in a separate plate for the CFU count, to ensure that there were no discrepancies in experimental set up between the liquid and solid assay. Both MPN and CFU plates were sealed and incubated for 3-5 weeks at 37 °C

2.5.4 Resuscitation of DCTB

In addition to a 96 well plate, 200µl of the starved cultures from section 2.4.1 was added to a 24 well plate to monitor the resuscitation of the DCTB. The experiment was up scaled to ensure the sample volume would be sufficient for further analysis. In a 24-well microtiter plate, 1.8 ml of media was added to 12 wells of the plates while 1.8 ml of CF was diluted with media in a 1:1 ratio before it was added to the remainder of the wells in the microtiter plate. To the entire plate, 200 µl of culture was added to each well. The 24 well microtiter plates were sealed and incubated at 37 °C for 7 days. All experiments were conducted with three biological replicates.

2.5.5 Incubation and plate reading using an MPN calculator

The MPN plates were incubated at 37 °C and scored for growth after 5 weeks using an inverted mirror. Wells which contained growth were recorded as positive in the MPN calculator program. The total number of bacteria recovered from the MPN assay was estimated using software (available at http://www.wiwiss.fuberlin.de/fachbereich/vwl/iso/ehemalige/wilrich/index.html).

2.5.6 Colony forming units (CFU) Assay

CFU analysis was carried out using the protocol described by Saito et al., (2017). The serial dilutions were taken from the MPN plate, containing media. From the MPN plate, 15 µl was removed from rows B2-B6 (serial dilutions 10^{-1} to 10^{-5}) as depicted in figure 2.3 and transferred to a new 96 well microtiter plate. This process was repeated for rows G2-G6 in Figure 2.3, and each row was transferred into the same coordinate row in the new 96 well microtiter plate. There was a total of 120 µl for each dilution (10^{-1} to 10^{-5}) in each well. Thereafter, 25 µl of each dilution and the original sample (10^{0}), was spotted and spread on quarter BBL ™ Middlebrook 7H11 plates. Experiments were conducted with three biological replicates. The CFU was done in duplicate for each replicate of cultures and the plates were incubated at 37 °C for 3-5 weeks.

After 5 weeks the 7H11 Middlebrook plates were analysed for growth, by counting the number of colonies for each dilution. The CFU/ml was determined using the following formula:

$$CFU/ml = \frac{The\ number\ of\ colonies\ x\ Dilution\ factor}{volume\ spread\ on\ the\ plate}$$

2.5.7 Calculation of resuscitation index

The resuscitation index was calculated by comparing growth on liquid media (MPN value) to solid media (CFU/ml) using the following the formula:

$$DCTB = \frac{MPN\ value\ (\ calculated\ using\ an\ MPN\ calculator)}{CFU}$$

2.6 Incorporation of metabolic probes

The metabolic activity of DCTB induced by the carbon starvation model was determined, using a fluorescent TAMRA (5-(and-6)-carboxytetramethylrhodamine, succinimidyl ester) molecule attached to a D-alanine (abbreviated as TADA) probe which incorporates into the peptidoglycan (PG) layer of the cell wall. The terminal D- alanine is the last molecule to be incorporated into the PG side chain during PG subunit synthesis. Mycobacterial replication requires the production of new cell wall, therefore the TADA probe will incorporate into actively replicating cells only and not into non-replicating cells (Figure 2.4) (Kuru et al., 2012).

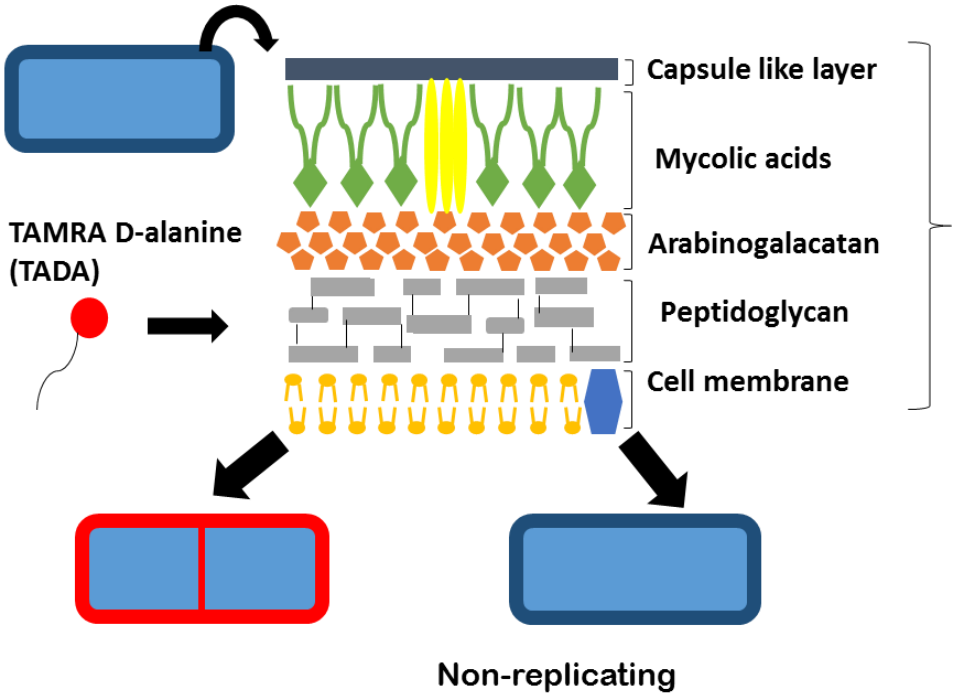


Figure 2.4 Incorporation of the metabolic probe into the cell wall of the bacterium. A visual representation of the incorporation of the tamra D-alanine (TADA) probe into the peptidoglycan layer of

replicating mycobacteria, represented by the red cell wall. The TADA probe does not get incorporated into non-replicated bacteria represented by the dark blue cell wall.

2.6.1 Labelling of *M. smegmatis* and *M. tuberculosis* cultures with TADA

Samples were stained with 2 µl of TADA and incubated for 24 hours at 37 °C. Cells were harvested by centrifugation (3000 ×g for 10 minutes) and washed twice with an equal volume of 1X PBS. After washing, the cells were fixed in an equal volume of 2.5% glutaraldehyde for 3 hours (*M. smegmatis*) and 24 hours (*M. tuberculosis*). Metabolic fixed and labelled cells were harvested by centrifugation (3000 ×g for 10 minutes), and then washed twice with 1X PBS, before being resuspended in 300 µl of 1X PBS. All experiments were conducted with three biological replicates.

2.7 Flow cytometry assessment of stained bacteria

2.7.1 Fluorescent channels

After labelling and fixation of the various cells with TADA, 200 µl of the sample was analysed using the Beckman Coulter CytoFLEX (B9662) and compared to a control unlabelled population of *M. tuberculosis* grown in 7H9 media. The CytoFLEX has 4 different lasers, and the 488-nm blue laser for the PE channel (585/42 BP), was used to detect the TADA probe. Fluorescence data was obtained for 100,000 cells per sample and processed using the CytExpert software (version 1.2). Experiments were conducted with three biological replicates.

Using the CytExpert software, the samples were grouped into to three categories. Bacterial populations were analysed using fluorescent counts, to display differences in mean fluorescent intensity. The 1st category represented replicating bacteria based on a mean fluorescent intensity signal that appeared with the range of a labelled exponentially grown control (Figure 2.5-red graph). The 2nd category was the non-replicating bacteria based on a mean fluorescent signal that appeared within the range of the unlabelled control (Figure 2.5-grey graph). The 3rd category was the bacteria with reduced replication based on a mean fluorescent intensity signal that appeared between category 1 and category 2 (Figure 4.5 -green double side arrow).

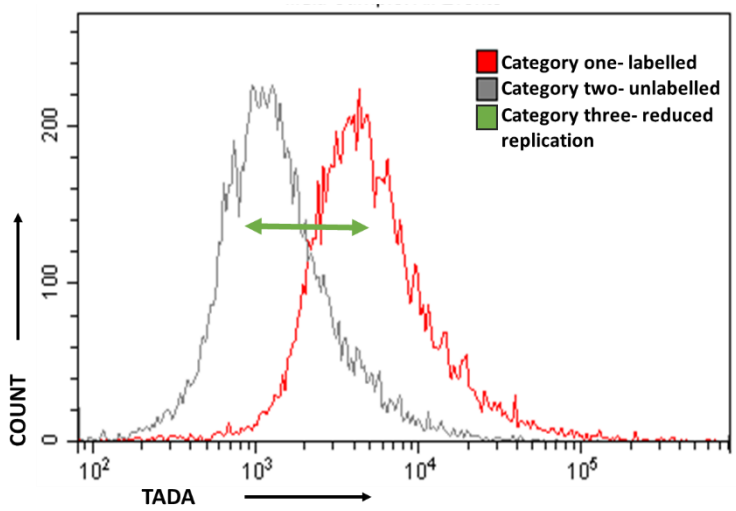


Figure 2.5 Gating strategy to determine metabolic activity. A visual representation of various categories. Category one is a measure of labelled replicating bacteria (red graph). Category two represents unlabelled bacteria (non-replicating) (grey graph) and category three measures mycobacteria with reduced replication (green double-sided arrow).

2.8 Cytological assessment of strained bacteria

2.8.1 Microscopy

After labelling and fixation, cells were harvested by centrifugation (3000 ×g for 10 minutes), and then washed twice with 1X PBS, before being resuspended in 10 µl of 1X PBS. Five µl of cell suspension was spotted onto slides, covered with coverslips, and sealed with adhesive. Microscopy was performed on a Nikon A1R fluorescent microscope equipped with a Plan Fluor 100X oil immersion 1.30– numerical aperture objective. This instrument is equipped with NIS-Elements AR software (Nikon Inc.), which was used to process images. All image acquisition and processing were executed under identical conditions for control and test samples.

2.8.2 Fluorescent staining patterns

One hundred cells per replicate (experiment done in triplicate) were visualized for the incorporation of the metabolic probe into the PG layer of the cell wall, using a Zeiss Elyra super resolution confocal microscope. The slides were prepared following the protocol described in section 2.8.1, and viewed with the Zeiss Elyra equipped with a Plan-apochromat 100X 1.46 Oil aperture. The brightfield images were captured under the PLAM storm application whilst the fluorescent images were captured under the structural illumination super-

resolution application. The captured images were process using the structural illumination software from the Zen black. Each cell was analysed for the presence of a fluorescent signal, thereafter, in cells where a fluorescent signal was seen, the staining patterns were recorded. There were 6 categories for staining pattern: uniform staining, polar staining, side wall staining, Polar and septal staining and strong and weak pole and uneven staining.

2.8.3 Cell length measurements

One hundred cells per replicate (experiment done in triplicate) were visualized for cell length. Cell length was measured and recorded in the Nikon software (NIS –Elements AR). Cell length was recorded for all 100 cells and the mean, median and interquartile ranges were determined for each data set using Graphpad prism 6.

2.9 Addition of CF from clinical strains to MGIT tubes

2.9.1 Addition of CF from different clinical strains to starved H37RV

Thirty mycobacterial growth indicator tubes (MGITs) were prepared to test if CF from the five Beijing and five LAM strains would improve time to detection in starved *M. tuberculosis* (H37Rv) samples. The 30 MGIT tubes were divided into 3 groups: CF from H37Rv, CF from Beijing strains and CF from the LAM strains with 1 MGIT tube serving as a control. Using a pipette, 3.5 ml of media was removed from the MGIT tubes except for the control tube and replaced with 3.5 ml of H37RV CF or clinical CF produced as described in methods section 2.4.1.1 and graphically depicted in figure 2.4. In this experiment, the CF was diluted in a 1:1 ratio in media before it was added to the MGIT tube. All MGIT tubes were inoculated with 800 µL of Polymyxin B, Amphotericin B, Nalidixic acid, Trimethoprim and Azlocillin (PANTA) reconstituted in OADC. H37Rv was starved following the protocol described in methods section 2.3.1, and 500 µl of the starved cells were added to the MGIT tubes. Each tube was incubated in the BACTEC MGIT 960 instrument, and the time to positivity was recorded. All experiments were done in triplicate.

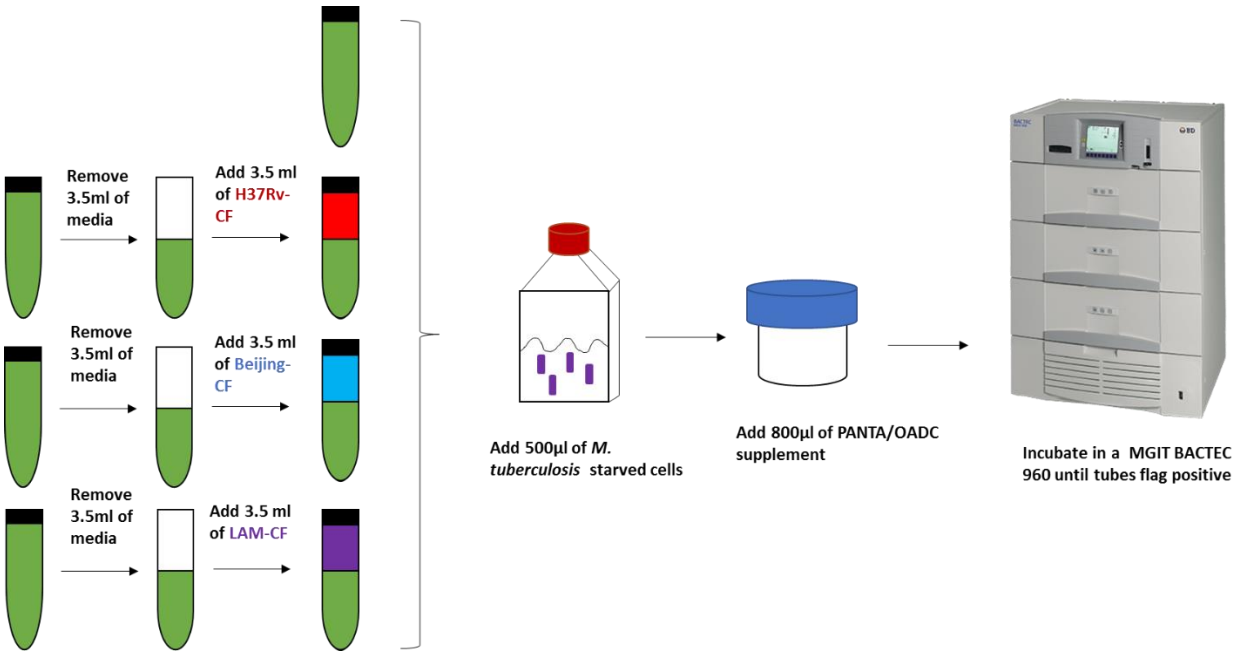


Figure 2.14 Addition of clinical CF to MGIT tubes. Flow diagram showing the steps involved in removing the media and adding CF from clinical strains to MGIT tubes. Media is shown in green; H37Rv-CF is shown in red; Beijing-CF is shown in blue and LAM CF is shown in purple. DCTB cells added to the MGIT tubes were produced using the carbon starvation model.

2.9.2 Addition of CF from Beijing and LAM to starved Beijing and LAM

MGIT tubes were set-up following the protocol described in section 2.9.1. In addition, for this experiment starved H37Rv, Beijing and LAM strains were produced following the protocol described in Method 2.3.1. CF from the Beijing strain was only added to tubes containing starved Beijing samples, and CF from the LAM strain was only added to tubes containing starved LAM strains. Both Beijing and LAM CF was added to tube containing 500 µl of starved H37Rv. Each tube was incubated in the BACTEC MGIT 960 instrument, and the time to positivity was recorded. All experiments were done in triplicate

2.10 Data Analysis

GraphPad prism 6 is a data management and analysis software and was used to construct graphs and figures for data analysed from this study. Additionally, it was used for statistical analysis to compare statistically significant differences between data groups.

A detailed list of bioinformatics and software used can be found in Appendix B

3. Results

3.1. *In silico* analysis of the propensity of clinical *M. tuberculosis* strains to adopt the DC state

The objective of this component of the study was to test the propensity of *M. tuberculosis* clinical strains to adopt the DCTB state by compiling a meta-analysis of data generated in two previous clinical studies completed at the CBTBR. The studies in question were (1) Mycobacterial biomarkers of TB response and success in adult patients: A prospective cohort (BMG phase 1- Peters J, et al,. In preparation, 2020) and (2) Operational assessment of a novel acid-fast bacilli detection process and procurement of sputum specimens for resuscitation promoting factors study (MGIT plus – McIvor A et al,. In preparation, 2020). Ethics clearance for both clinical studies, and this study was obtained from Human Research Ethics Committee of the University of Witwatersrand (Wits HREC) (Refer to Appendix D for ethics certificates)

3.1.1. Selection criteria

Study participants were selected through the Perinatal HIV Research Unit (PHRU), University of the Witwatersrand's TB diagnostic clinics based in Soweto and Klerksdorp. Patient participation in both studies was based on a positive GeneXpert MTB result obtained from the National Health Laboratory Service (NHLS). Patients were recruited into the study before the commencement of treatment. There were several inclusion criteria: adults at least 18 years of age, able to produce a sputum sample of $\geq$ 3 ml, a documented HIV test result and no prior history of treatment for TB. Exclusion criteria included: RIF resistance at baseline and clinical/social characteristics suggesting that the patient may not complete treatment.

One hundred and forty-four (144) patients were enrolled in the BMG phase 1 study and 119 patients were enrolled in the MGIT plus study for a combined total of 263 patients, in this study (Figure 3.1). However, a total of 99 patients (64 from BMG phase 1 and 35 from MGIT plus) were later removed from the studies due to one of several reasons including: technical problems, screen failure, consent withdrawal, previous history of TB, patient relocation, treatment default and/or death. The remaining 160 treatment naïve (baseline) samples, were genotyped using spoligotyping for the further analysis in this study.

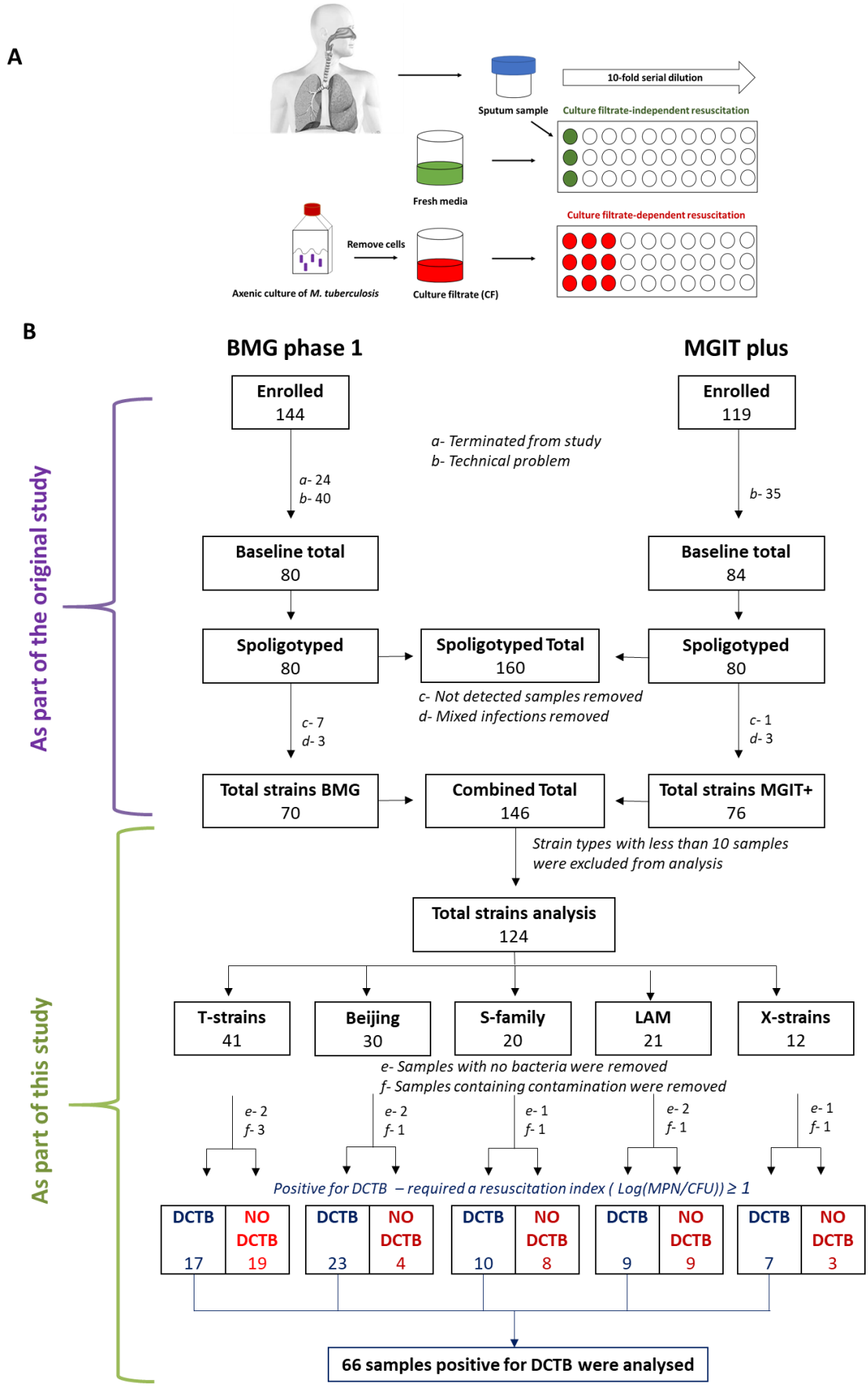


Figure 3.1. Selection criteria flow chart: A flow chart showing the selection process for the clinical samples from BMG phase 1 and MGIT plus studies for *in silico* analysis. Purple brackets indicate the work done by the

authors of the original study and green brackets indicate the work done as part of this study. A total of 233 patients were recruited into both clinical studies through Perinatal HIV Research Unit (PHRU) clinics in Soweto and Klerksdorp. From each study the letters depict patients that were removed from the studies for various reasons.

3.1.2. Strain type distribution

In the remaining participants (n=160), mycobacteria in the sputum samples from both clinical studies were genotyped for classification into strain types using spoligotyping. Spoligotyping is a PCR based method, which can differentiate *M. tuberculosis* strain types based on the spacer sequence in the direct repeat region of *M. tuberculosis* genome. From the 160 patients analysed, strain type distribution patterns indicated that there were five dominant strains in the pooled population between Soweto and Klerksdorp including the T-strain, Beijing, LAM, S-family and X-strains (Figure 3.2). Genotypes of strains could not be determined in 8 patients due to contamination or too little DNA, whilst 6 patients presented with mixed infections.

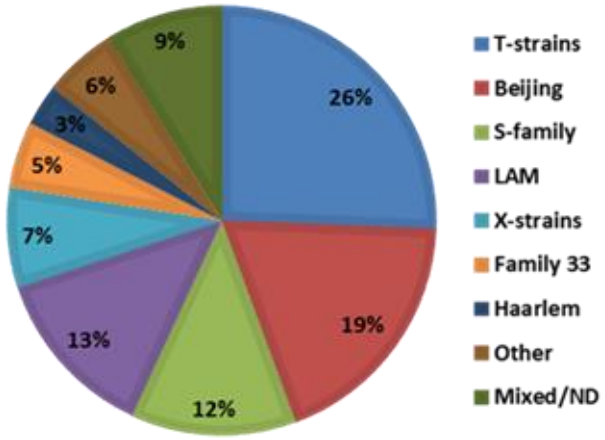


Figure 3.2 Strain type distribution in the BMG phase 1 and MGIT plus cohorts: A pie chart showing the dominant strain types from both BMG phase 1 and MGIT plus and studies (n=160)

3.1.3. Strain type affects the ability of bacteria to adopt the DC state

Next, we investigated the propensity of different clinical strains to adopt the DC state by stratifying the samples according to strain type. Certain samples were excluded from the total population of 146 for further analysis. The exclusions were strain types with less than 10 samples, samples with an unidentified genotype or mixed infections. A total of 124 specimens remained for further analysis. From these, 15 samples were subsequently excluded: 8 samples dues to a lack of bacterial growth in MPN and CFU assays after 6 weeks and 7 samples due to contamination.

After applying these exclusion criteria, 5 strain types dominated the remaining samples: Beijing, LAM, S-family, T-strains and X-strains. Within these five dominant strain types, samples were separated into two categories: sputum samples with or without DCTB. In this study, DCTB positive sputum specimens had either a CF-dependant or CF-independent resuscitation index equal to or greater than one calculated by [log (MPN/CFU)]. The resuscitation index measures the amount of DCTB present by comparing the growth of the bacteria on solid media to growth in liquid media. The ratio of DCTB to no DCTB was examined for each strain type, and results showed that sputum from patients infected with Beijing strains had the highest propensity to contain DCTB (80%), whilst patients infected with T-strains had the lowest (44%) (Figure 3.3). TB sputum samples detected as LAM, S-family and T-strain had significantly lower (p-value ≤0.05) propensity to produce DCTB compared to the Beijing strain using a Chi-squared t-test (Figure 3.3).

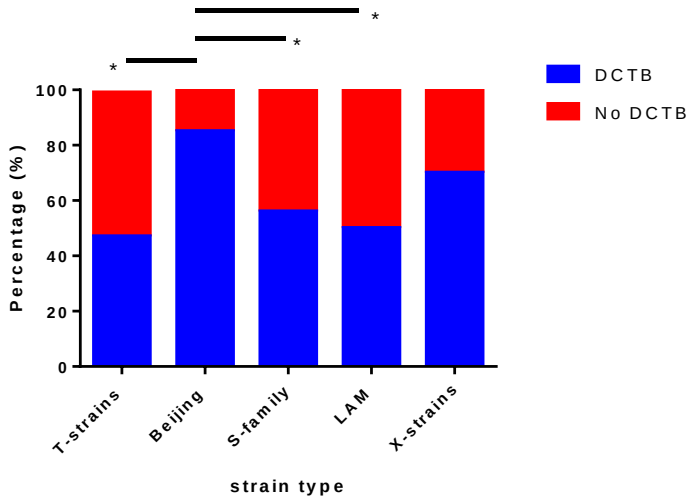


Figure 3.3 Propensity of clinical strains to adopt the DC state. Graph showing the percentage of sputum specimens with DCTB (n=124). The DCTB population was determined by a positive resuscitation index (log (MPN/CFU)) under CF dependant or CF-independent conditions. The resuscitation index needed to be positive only in one of the conditions, not in both. The strains types which had less than 10 samples were exclude from the analysis. Beijing strains induced significantly (p-value ≤0.05) more DCTB infected patients compared to LAM S-family and T-strains, using a chi-squared t-test.

3.1.4. The effect strain type has on the quantity of DCTB induced

The analysis the five dominant clinical strains (Beijing, LAM, S-family, T-strains and X-strains) were analysed for the quantity of DCTB produced (n= 66) in figure 3.3. With the exception of Beijing (p=0.062), most *M. tuberculosis* clinical strains produced increased levels

of DCTB in the presence of CF compared to CF-independent conditions which was statistically significant using a Mann Whitney u test (Figure 3.4). Thus, these data confirm previous data from our group (Chengalroyen et al., 2016) that demonstrated how CF significantly aided the resuscitation of DCTB from sputum of TB patients. Interestingly, in patients infected with Beijing strains, DCTB can be partially resuscitated under CF-independent conditions (Figure 3.4). Furthermore, patients infected with Beijing strains showed the highest median resuscitation index for both CF-dependant and CF-independent DCTB compared to the other clinical strains (Figure 3.4). Patients infected with Beijing strains had higher levels of CF-dependant DCTB in their sputum (p=0.0518) compared to those infected with LAM strains (Figure 3.4). Sputum samples with Beijing strain contained significantly more CF-independent DCTB compared to patients infected with T-strains, LAM strains, and X strains (Figure 3.4). Surprisingly, sputum samples with X-strains did not contain significant levels CF-independent DCTB. Overall, these results indicate Beijing strains have the highest propensity to adopt the DCTB state relative to other clinical strains assessed in this study. This observation was consistent under CF-dependant and CF-independent conditions.

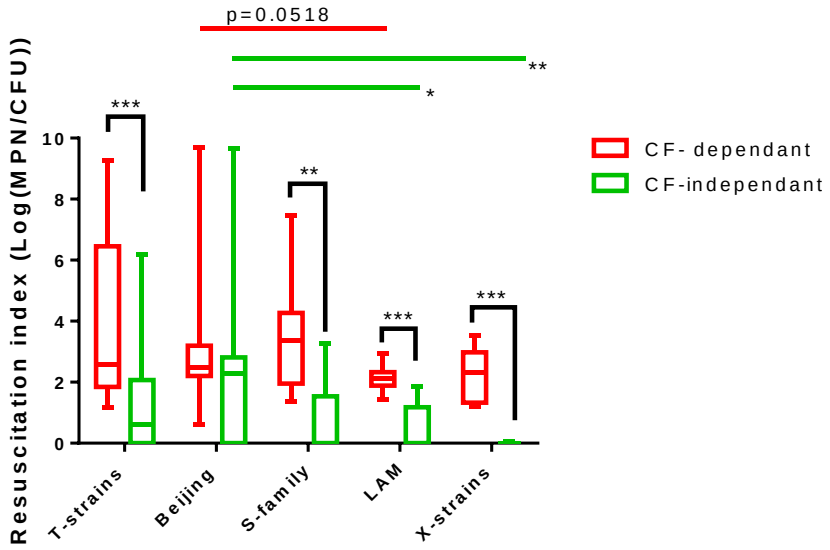


Figure 3.4 Effect of CF on resuscitation of DCTB. For each strain type, the resuscitation index was calculated for CF-independent and CF-dependant DCTB across all samples using log (MPN/CFU) (n=66). The mean and quartile ranges were calculated using GraphPad statistical tool. The ability to resuscitate in CF was significant (p-value <0.05) in Beijing strains compared to LAM and X strains using the Mann Whitney u statistical test. Beijing strains were able to produce more DCTB (p-value =0.0518) when CF was present compared to LAM strains using the Mann Whitney u statistical test (* = p-value <0.05, ** = p-value < 0.01 and ***= p-value < 0.001).

3.2. Optimization of *in vitro* models in *M. smegmatis* to generate DCTB

One of the other objectives of this study was to develop an *in vitro* model to robustly generate DCTB. For this, *M. smegmatis*, a non-pathogenic, model strain for *M. tuberculosis*, was used to test and optimize three *in vitro* stress models for the ability to robustly generate DCTB, carbon starvation, biofilm formation and potassium depletion.

3.2.1. Carbon starvation model

Growth of bacteria under carbon starvation conditions, has previously been shown to induce a non-replicating "dormant" state in mycobacteria (McDonough, Kress, & Bloom, 1993; Nyka, 1974). It has further been shown that when *M. tuberculosis* is cultured in phosphate-buffered saline (PBS), a carbon deplete medium, bacteria gradually shutdown respiration while still remaining viable, as they are recoverable in nutrient rich media (Loebel et al., 1933). The carbon starvation model discovered by *Loebel et al* in 1933 has been refined over the years. One of the well-known variations of the model was developed by Betts and colleagues wherein *M. tuberculosis* was subcultured in PBS for 1 week and as a result, demonstrated downregulation of aerobic respiration, protein translation, cell division and lipid biosynthesis (Betts et al., 2002). A recent adaptation of the carbon starvation model was developed by *Saito et al* that made use of two sequential stresses. The bacteria were incubated in PBS and subsequently treated with RIF to generate DCTB (Saito et al., 2017).

In this study we used this two-step stress model developed by Saito and colleagues to generate DC bacteria in *M. smegmatis* (mc^2155) as described in the materials and methods section 2.2.1.2 and depicted in figure 3.5-A. We termed these bacteria differentially culturable *M. smegmatis* (DCMS) and the quantity of DCMS induced was determined using the resuscitation index (MPN/CFU). *M. smegmatis* produced significantly higher (p-value ≤ 0.01) levels of DCMS after starvation (1^{st} stress event) but exposure to 100 µM RIF (2^{nd} stress event) repeatedly showed a decrease in the amount of DCMS (Figure 3.5B). These observations were in contrast to Saito and colleagues who reported increased levels of DC bacteria after treatment of the carbon starved cells with RIF. The reason for this difference remains unclear and it is plausible that the decrease in resuscitation index could either be due to the RIF concentration being lethal, or that the starved bacteria had an increased sensitivity to what is otherwise a tolerable concentration of RIF under normal conditions in 7H9 media. To test the first

hypothesis, lower concentrations of RIF – 25 µM, 50 µM and 75 µM were utilised as a secondary stress after carbon depletion. However, even at these concentrations there was a significant decline (p-value ≤ 0.01) in the resuscitation index of DCMS compared to untreated starved cells (axenic culture) using a one-way ANOVA statistical test. (Figure 3.5- B). Also, with increasing concentrations of RIF, there was a gradual decline of CFU/ml of the starved cells compared to the untreated cells (Figure 3.5-C) indicating that the starved bacteria are indeed sensitive to RIF. Exposure of starved bacteria to the lowest concentration of RIF (25 µM) resulted in approximately 10^4 CFU/ml remaining, (Figure 3.5-C), which suggested that these are most likely persisters (a population of bacteria that remain viable after exposure to an antimicrobial agent at concentrations that kill the vast majority of a population), and not DC bacteria as the resuscitation index is still significantly lower compared to the untreated starved bacteria (Figure 3.5- B). Therefore, under the laboratory conditions we used, the culturing of bacteria in PBS without any treatment with RIF was sufficient to produce high levels of DCMS. As a result, these conditions were used for all further experiments.

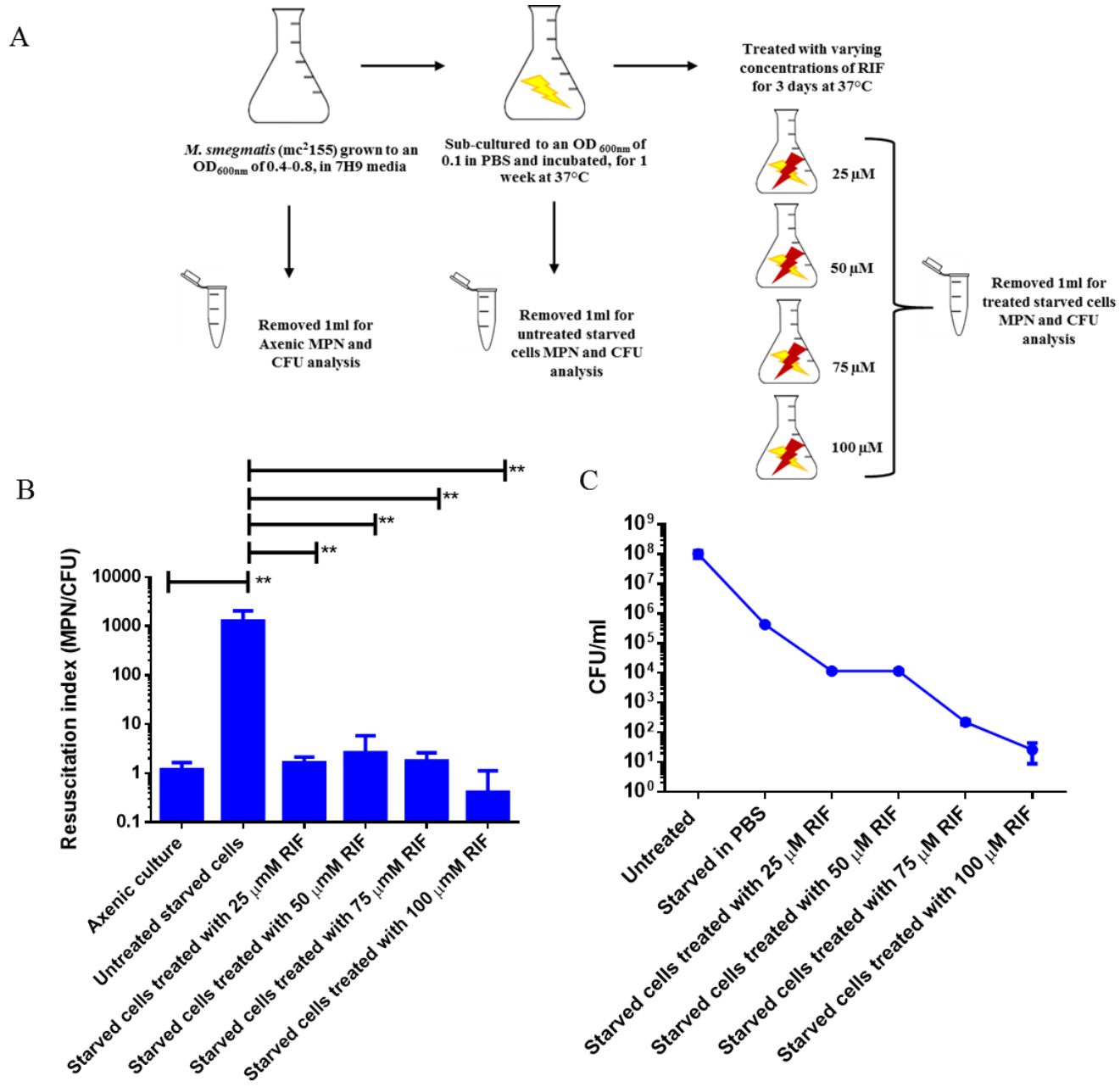


Figure 3.5 RIF negatively affects the generation of differentially culturable (DC) bacteria in starved cells: **A**- A schematic representation of the two sequential stress method for the generation of DC bacteria. The yellow lightning bolt represents the first stress event (bacteria starved in PBS for 1 week) and the red lightning bolt represents the second stress event (treatment with RIF for 3 days). **B**- Resuscitation index comparing untreated bacteria (axenic culture), starved bacteria and starved bacteria treated with different concentrations of RIF compared to an untreated axenic culture using a one-way ANOVA statistical test (** =p value ≤0.01). **C**. MPN and CFU assays were done to determine the amount of DCMS produced by comparing the growth on the MPN plate to the CFU count. The resuscitation index was calculated as the MPN/CFU ratio **C**- Growth kinetics of carbon starved cells showing a drop-in cell count as the concentration of RIF increases. Data represent the average of three independent experiments

3.2.1.1. Metabolic activity of the bacteria produced by the carbon starvation model

A common adaption of bacteria to environmental stress, is a reduction in metabolic activity (Baker & Abramovitch, 2018; Gomez & McKinney, 2004; Kana et al., 2008; Kim et al., 2018; Lipworth et al., 2016; Loebel et al., 1933). Under stressful conditions, bacteria shift to alternative energy metabolism pathways to conserve energy and maximise survival (Gomez & McKinney, 2004; Kato et al., 2008; Kim et al., 2018; Muttucumaru, Roberts, Hinds, Stabler, & Parish, 2004). Thus, a reduction in metabolic activity, is expected to be one of the hallmarks of DCTB. To further explore the metabolic activity of DCMS induced by the two sequential stress model, bacteria generated under these conditions were stained with a fluorescent TAMRA D-alanine probe (TADA). This probe is incorporated into the PG layer of the bacterial cell wall either during mycobacterial replication when new cell wall is synthesised or when the existing PG layer is remodelled. Flow cytometry was used to assess probe incorporation and thus, the metabolic activity of DCMS bacteria.

A sample of DCMS bacteria generated from the two sequential stress model was tested for probe uptake after each stress event and compared to cells grown in axenic culture. The cells at each stage as shown in figure 3.6-A, and were labelled and fixed following the protocol described in the material and methods, section 2.6.1. Labelled DCMS bacteria were analysed for by flow cytometry, and compared to a labelled and unlabelled exponentially grown axenic culture (Figure 3.6-B). A shift of the fluorescent peak for the TADA labelled starved cells towards the unlabelled population was observed (Figure 3.6-B). This suggested that carbon starvation was able to induce a non-replicating population. Whilst for the starved cells treated with RIF, the fluorescent peak position shifted between the labelled and unlabelled population, suggesting that these bacteria have reduced metabolic activity.

In figure 3.6.C, the mean fluorescence intensity of the labelled and unlabelled axenic populations was compared to the starved cells using a one-way ANOVA test. The starved cells showed a significant (p-value ≤ 0.01) lack of metabolic labelling, as these cells displayed the same level of fluorescence as the unlabelled, exponentially grown axenic culture, thus providing definitive evidence for the establishment of a non-replicating state (Figure 3.6-C). Although starved cells treated with RIF showed a reduction in metabolic labelling and cell count, the reduction was insignificant (p-value=0.08) when compared to the labelled exponentially grown culture thus, confirming that in our hands carbon starvation is sufficient for the induction of DCMS.

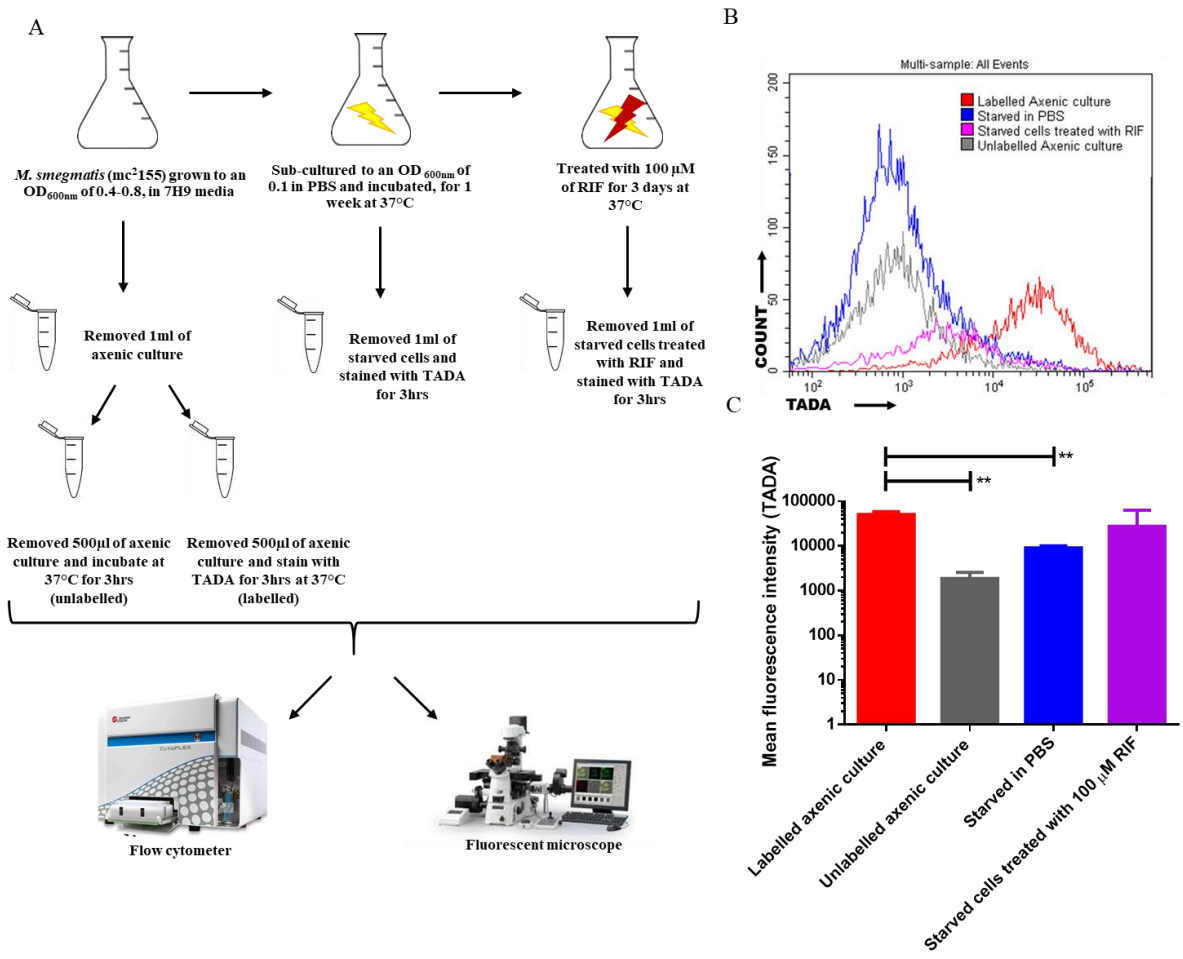


Figure 3.6. DCMS produced by the two sequential stress model displays reduced metabolic activity. A- A schematic representation of the method followed for flow cytometry and microscopy. The yellow lightning bolt represents the first stress event (sub-cultured bacteria in PBS for 1 week) and the red lightning bolt represents the second stress event (treatment with RIF for 3 days). **B-**Flow cytometry graphs of untreated and RIF treated starved bacteria, stained for 3 hrs at 37°C with the TADA probe, compared to a labelled and unlabelled axenic culture grown to an of OD_{600nm} between 0.5- 0.8. **C -** Flow cytometry analysis of the mean fluorescent intensity of treated and untreated starved bacteria strained for 3 hrs with the TADA probe compared to labelled and unlabelled axenic culture grown to an of OD_{600nm} between 0.5- 0.8, using the one-way ANOVA statistical test (**=p-value ≤0.01). Data represent the average of three independent experiments.

3.2.1.2. Cytological profiling of the bacteria produced by the carbon starvation model

In addition to assessing the metabolic activity, the labelled DCMS cells from the two sequential stress model and exponentially grown axenic culture were also analysed for differences in staining patterns by fluorescent microscopy. A sample of DCMS bacteria from the two sequential stress model was removed at each stress event, labelled with the TADA probe and fixed as described in figure 3.6-A. One hundred bacteria were visualised per replicate (experiment done in triplicate), except in the case of the starved cells treated with RIF, where due to low cell number (Figure 3.7-B), a total of 100 cells were visualised across all three

replicates (Figure 3.7-B). The resulting data demonstrate that only 2% of untreated and 5% of treated starved cells were fluorescently stained compared to 95% of staining observed for the axenic cells (Figure 3.7-B). This confirmed that under carbon starvation conditions, DCMS are in a non-replicative state.

In response to environmental stress, bacteria not only alter their metabolic state but also display morphologic differences such as change in cell length, compared to actively growing cells (Anuchin et al., 2009). Moreover, mycobacteria starved in PBS develop a small resting cell (SMRC) phenotype, by shortening their cell length in order to store energy and survive longer under unfavourable conditions (Wu et al., 2016). To test if similar phenotypes prevailed in our model, the cell length of 100 bacteria per replicate (experiment done in triplicate) from the two sequential stress model was measured at each stress event and compared to an exponentially grown culture. Starved cells were significantly shorter relative to the exponentially grown culture (Figure 3.7-A), corroborating a previously study by Wu and colleagues. When these starved bacteria were treated with RIF, the surviving bacteria displayed a similar mean length compared to an exponentially grown culture. The reason for this difference is currently unclear, we speculate that since, carbon treated cells are killed by RIF, it is plausible that the larger cells represent surviving persister cells.

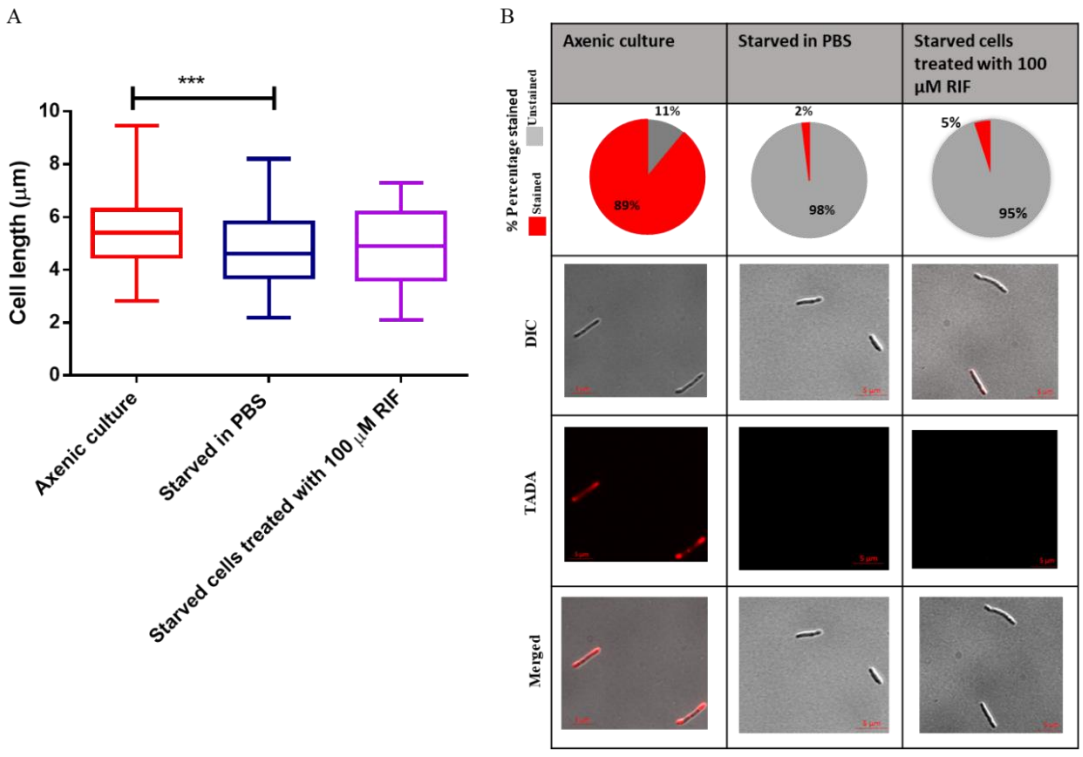


Figure 3.7 Starved DCMS produced by the two sequential stress model have reduced cell length: A- Microscopy analysis of cell length of starved and starved cells treated with RIF, compared to an axenic cultured

using a one-way ANOVA statistical test (*** = p value ≤ 0.001). **B**- Using a fluorescent microscope, 100 bacteria per replicate were analysed for the presence of a fluorescent signal in the TADA channel. The DIC channel, is the phase view of the bacteria and the merge channel is the DIC channel overlapped with the TADA channel. Scale bar represents 5 µm.

3.2.2. The Biofilm model

The biofilm structure is complex and contains regions of hypoxic gradients which is thought to promote persistence and drug tolerance (Esteban & García-Coca, 2018; Kulka et al., 2012; Solokhina et al., 2017). These hypoxic regions mimic conditions found within granulomas and was therefore chosen as a model to test for DCMS generation (Esteban & García-Coca, 2018) (Figure 3.8-A). Biofilms of *M. smegmatis* were formed over 5 days in Sautons media and then DCMS generation was assessed using the MPN and CFU assays. The resuscitation index measured as the ratio of MPN/CFU showed that axenic culture of *M. smegmatis* was unable to produce significant (p-value ≤0.05) amounts of DCMS compared to bacteria from biofilms. We also tested to see if addition of RIF to the biofilm would promote the formation of DCMS as biofilms are more tolerant to antibiotics relative to starved bacteria (Solokhina et al., 2017). Our results suggested that biofilms treated with 100 µM of RIF for 3 days significantly increased (p-value ≤0.05) the resuscitation index compared to an exponentially grown culture (axenic culture) indicating that in the biofilm model, RIF treatment has the potential to generate more DCMS. Higher concentrations of RIF, 150 µM, 200 µM and 300 µM were tested on *M. smegmatis* biofilms for 3 days to establish if DCMS levels could be correlated to higher drug concentrations (Figure 3.8-B). Surprisingly, increasing concentrations of RIF reduced the amount of DCMS produced (Figure 3.8-B). Furthermore, at these higher drug concentrations, the integrity of the biofilm structure was completely lost. The CFU/ml of the biofilm also decreased with increasing concentration of RIF (Figure 3.8-C). These observations suggest that at increased concentrations of RIF, the bacteria in the biofilms become sensitive to RIF. Increasing the concentration of RIF resulted in the decrease of both DCMS and culturable bacteria. Therefore, under the laboratory conditions we tested, biofilms treated with 100 µM of RIF was sufficient to produce high levels of DCMS.

It has been shown previously that biofilms treated with increasing concentrations of RIF had a negative impact on the amount of DCMS produced, however it was hypothesised that instead of increasing the concentration, increasing the exposure to RIF would further improve the amount of DCMS produced (Solokhina et al., 2017). Biofilms were exposed to 100 µM of RIF for 3, 5 and 7 days following the procedure described in materials and methods section 2.4.2.

Our results showed that exposure to RIF over a longer period of time resulted in a decreased amount of DCMS (Figure 3.8-D). The CFU/ml at 3 days, was reduced when compared to an untreated biofilm. However, at 5 days, there is increase in the CFU/ml and then at day 7, CFU/ml drops (Figure 3.8-E). Therefore, despite the steady decrease in the DCMS over a longer period of time, the number of bacteria present in the biofilm does not drop below 10^5 CFU/ml. These observations suggest that the increased length of exposure to RIF, creates an increase in the persister population rather than an increase in the DCMS population. Therefore, biofilms treated with 100 µM of RIF was sufficient to produce DCMS.

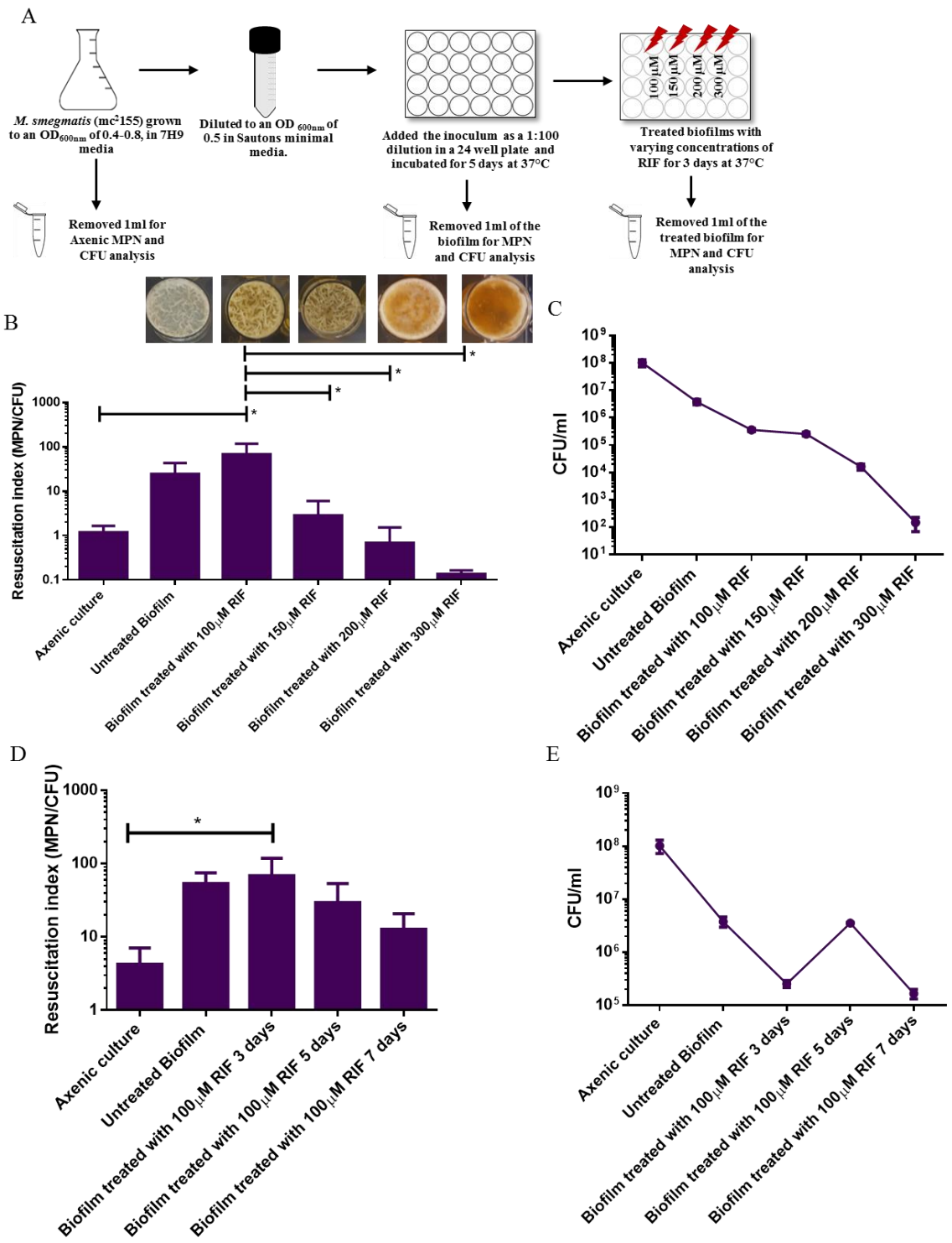


Figure 3.8 RIF negatively affects the generation of differentially culturable bacteria in biofilm cells: **A-** A schematic representation of the biofilm model, at different concentration of RIF. Red lightning bolts indicate the treatment of biofilms with RIF. **B**- Resuscitation index comparing biofilm bacterium treated with different concentrations of RIF to an untreated biofilm and axenic culture, using one-way ANOVA statistical test (* indicates a p-value ≤0.05). An MPN and CFU assay were done to determine the amount of DCMS produced by comparing the growth on the MPN plate to the CFU. Resuscitation index was calculated using (MPN/CFU). **C**- Growth kinetics of biofilm cells treated with RIF showing a drop in cell count as the concentration of RIF increases. **D**- Resuscitation index comparing bacteria exposed to 100 µM of RIF, over a period of 7 days, using a one-way ANOVA statistical test (* =p-value ≤0.05). **E**- Growth kinetics of biofilm cells treated with 100 µM of

RIF showing a fluctuation in cell count as the exposure of bacteria to RIF increases. Data represent the average of three independent experiments

3.2.2.1. Metabolic activity of the bacteria produced by the biofilm model

We sought to assess the metabolic activity of DCMS in untreated and treated biofilms using the TADA probe as described in the materials and methods, section 2.6.1 and graphically depicted in figure 3.9 A. The fluorescent peaks of TADA labelled cells for the treated and untreated biofilms positioned between the labelled and unlabelled axenic population, suggesting that these bacteria have reduced metabolic activity (Figure3.9-B). Probe incorporation measured by mean fluorescence intensity of the TADA probe, revealed there was a significant difference (p-value ≤0.01) between the labelled and unlabelled exponentially grown cultures. However, there was no significant difference in mean fluorescent intensity of labelled cells compared to the untreated and treated biofilms (p-value = 0.12 and p-value = 0.13, respectively) (Figure 3.9-C). Therefore, bacteria from the biofilm model displayed a slightly reduced metabolic activity compared to the exponentially grown culture, and thus did not display a non-replicating phenotype that is akin to that seen in the carbon starvation model.

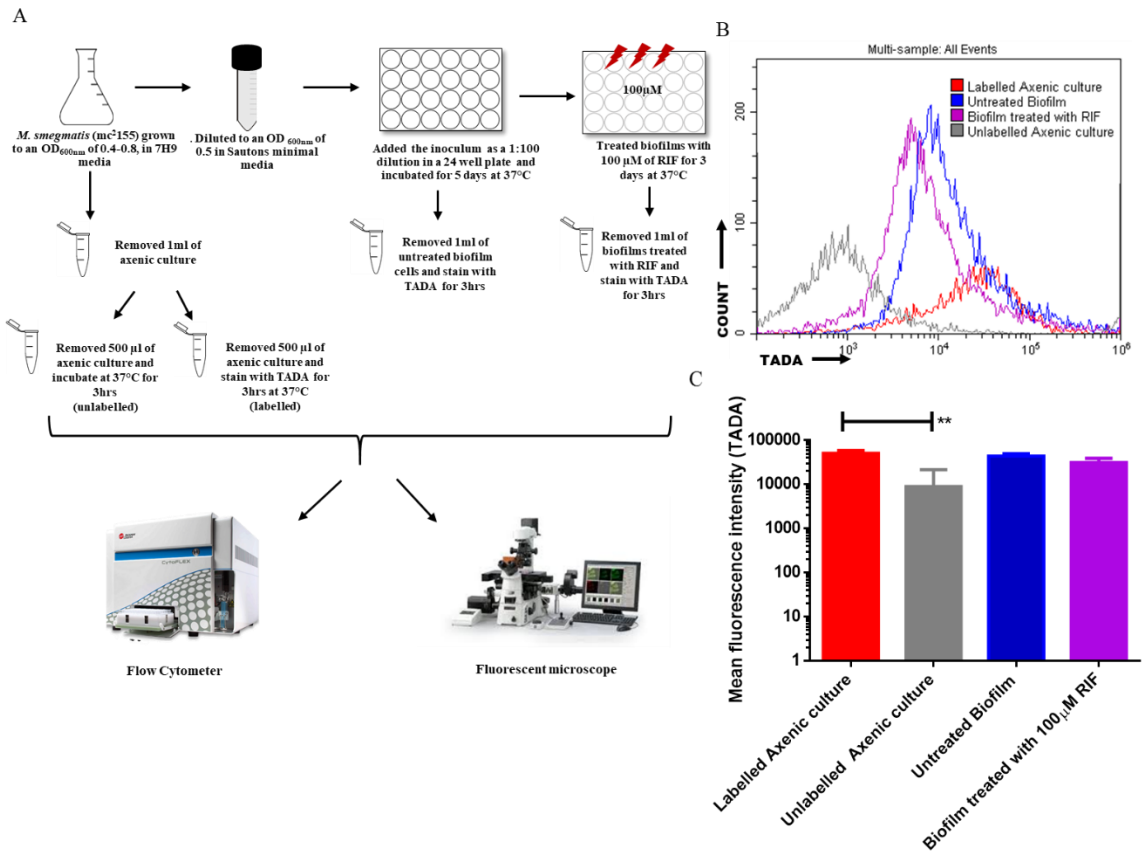


Figure 3.9 Biofilm cells contain a heterogeneous population of replicating and non-replication bacteria A-schematic representation of the method followed for flow cytometry and microscopy. Red lightning bolts indicate the treatment of biofilms with RIF **B**-Flow Cytometry charts of treated and untreated biofilms stained for 3 hrs with the TADA probe compared to labelled and unlabelled axenic culture with an OD_{600nm} between 0.5-0.8**. C**-Flow cytometry analysis of the mean fluorescent intensity in treated and untreated biofilms strained for 3 hrs with the TADA probe compared to labelled and unlabelled axenic culture grown to an of OD_{600nm} between 0.5- 0.8, using a one-way ANOVA statistical test (** indicates a p-value ≤ 0.01). Data represent the average of three independent experiments.

3.2.2.2. Cytological profiling of the bacteria produced by the biofilm model

In addition to metabolic activity, the labelled DCMS cells from untreated, treated biofilms and exponentially grown axenic cultures were analysed for differences in staining patterns as described in materials and methods section 2.8.1 and depicted in figure 3.9-A. One hundred bacteria per replicate (experiment done in triplicate) were analysed to determine the proportion of TADA stained cells to unstained cells (Figure 3.10 -B). Our results showed that a proportion of cells in both the untreated biofilms and biofilms treated with RIF did not stain, even though cells appeared to be metabolically active when assessed by flow cytometry. This result further confirmed that both untreated and treated biofilms induced a heterogeneous population of cells with varying metabolic activity, as previously observed by flow cytometry (Figure 3.10-B).

The cell lengths of 100 bacteria per replicate (experiment done in triplicate) from untreated and RIF treated biofilms was measured and compared to an exponentially grown culture. Cells from untreated biofilms were significantly longer (p-value ≤ 0.001) compared to an exponentially grown culture, (Figure 3.10-A). Furthermore, our results revealed that a longer cell phenotype is not a feature of DCMS bacteria, as these untreated biofilms did not produce a significant amount of DCMS when compared to an exponentially grown culture or the biofilms treated with RIF, as shown previously in results section 3.2.2. Interestingly when these long bacteria derived from the biofilm model were treated with 100 μM of RIF, the surviving bacteria were shorter and had a similar median cell length when compared to the exponentially grown culture. Therefore, the biofilm model produces longer cells but when these were treated with RIF, these decreased in length.

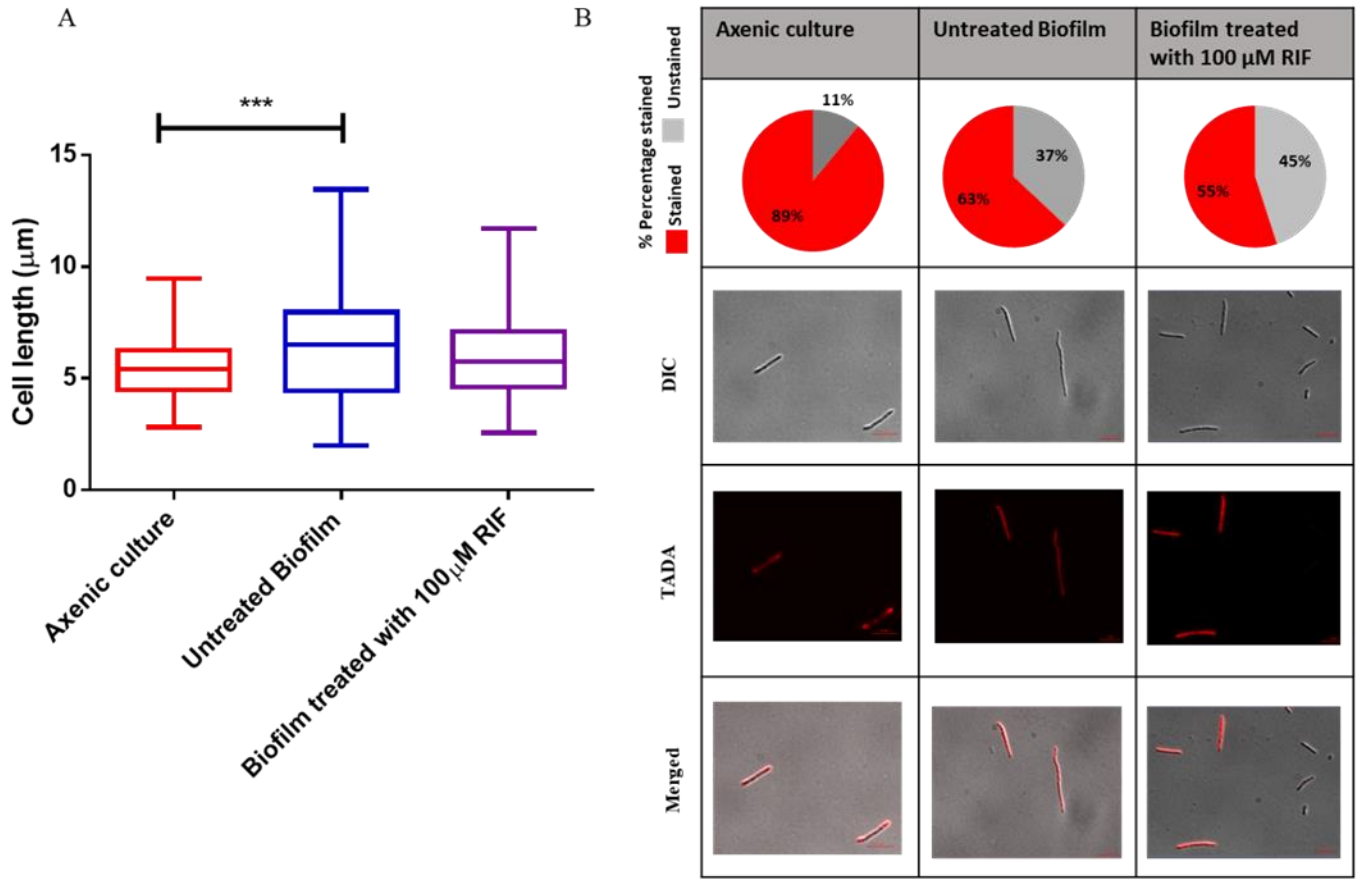


Figure 3.10 DCMS produced by the biofilm model have increased cell length A- Microscopy analysis of cell length of bacteria in untreated biofilms and biofilms treated with RIF, compared to an axenic cultured using a one-way ANOVA statistical test (***p-value= ≤0.001)**. B-** Using a fluorescent microscope, 100 bacteria per replicate were analysed for the presence of a fluorescent signal in the TADA channel. The DIC channel, is the phase view of the bacteria and the merge channel is the DIC channel overlapped with the TADA channel. Scale bar represents 5 µm. Data represent the average of three independent experiments.

3.2.3. The Potassium depletion model

The potassium depletion model developed by Salina and colleagues demonstrated that without the presence of potassium ions required for the maintenance of intracellular pH, *M. tuberculosis* enters a DCTB state (Salina et al., 2019; Salina et al., 2014). Therefore, the effects of potassium, in relation to the production of DCMS were tested. In the initial protocol developed by Salina and colleagues, *M. tuberculosis* bacteria were incubated for a period of 2 weeks in Sautons minimal media depleted of potassium ions (K-depleted Sautons). As *M. smegmatis* is a faster growing pathogen, cells were initially incubated in potassium depleted media over a period of 24 hours. Sautons minimal media is a nutrient limiting media, thus bacteria cultured in Sautons minimal media for 3 days was added as a control to ensure that production of DCMS

seen from the model was from the removal of potassium ion and not from the other components of the media. The model was produced following the procedure described in materials and methods section 2.4.3 and graphically depicted in figure 3.11-A

Our results showed that bacteria cultured for 24 hours without potassium ions had a reduced resuscitation index compared to both bacteria grown exponentially and bacteria grown in Sautons minimal media, indicating that DCMS were not generated under these conditions. Hence, the incubation period in the potassium depleted media was increased to 72 hours, 120 hours, 168 hours and 336 hours to ascertain if the extended incubation period would enhance the production of DCMS. The resulting data suggested that the optimal time for the production of DCMS is 168 hours (Figure 3.11-B). Decreasing the incubation of bacteria in potassium depleted media (24 hours and 72 hours) resulted in significantly less (p-value ≤ 0.05) DCMS bacteria. After 168 hours, there was a decline in the amount of DCMS produced (Figure 3.11-B). There was a decrease in the CFU/ml with increased exposure to the potassium depleted media, suggesting that the bacteria are losing culturability and transiting into the DC state with the prolonged incubation period (Figure 3.11-C). Therefore, under the laboratory conditions we tested, incubation without potassium ions for 168 hrs produced significantly more DCMS bacteria compared to an exponentially grown culture.

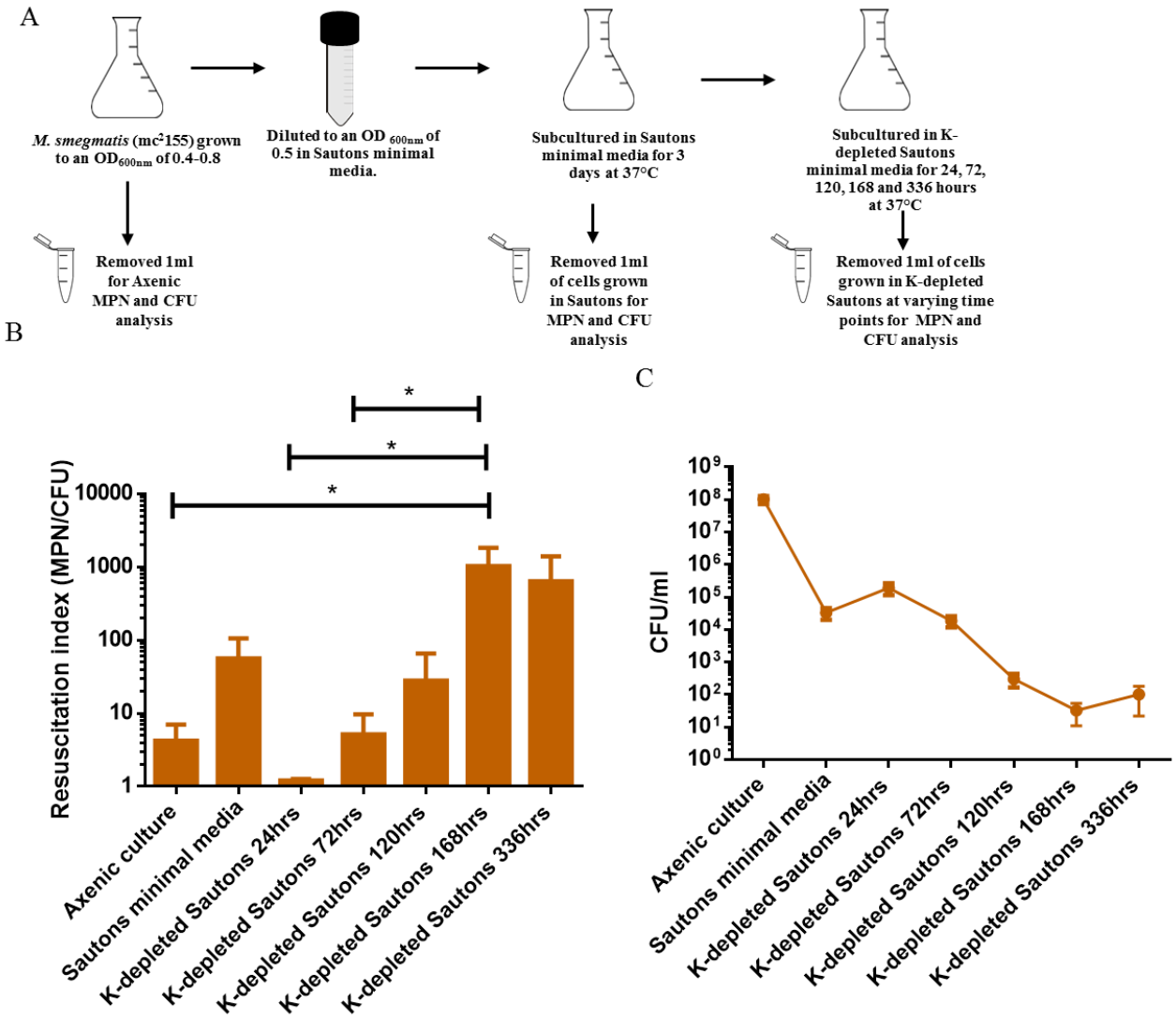


Figure 3.11 Bacteria cultured in potassium depleted Sautons for up to 168 hrs, increases the generation of DCMS A- A schematic representation of the potassium depletion model **B**-Resuscitation index comparing bacteria exposed to potassium depleted media over a period of 336 hrs to an exponentially grown axenic culture with an OD_{600nm} 0.5-0.8, using a one-way ANOVA statistical test (* =p-value ≤0.05). MPN and CFU assays were performed to determine the amount of DCMS produced at each time point by comparing the growth on the MPN plate to the CFU. **C**- Growth kinetics of bacteria cultured in potassium depleted media showing a decrease in cell count with increased exposure of bacteria to the potassium depleted media.

3.2.3.1. The importance of potassium ions in biofilm formation

In the potassium depletion model, the primary media from which potassium ions are removed is Sautons minimal media. Sautons minimal media is also the primary media for biofilm formations and therefore it was hypothesised that in the absence of potassium ion biofilm formation will be disrupted and increase the production of DCMS. Biofilms were cultured with

and without potassium ions following the procedure in materials and methods section 2.4.3.1 and graphically depicted in figure 3.12-A.

After 5 days incubation at 37°C, biofilm formation was hindered in media deplete of potassium ions (Figure 3.12-B). Extended incubation for 7 and 14 days of these plates did not aid in the formation of biofilms. A possible reason for this is that the longer cells are cultured without potassium, there is a reduction in the bacterial population, as seen previously in figure 3.11-C. Therefore, instead of the bacteria growing to form a biofilm, the majority of cells are dying.

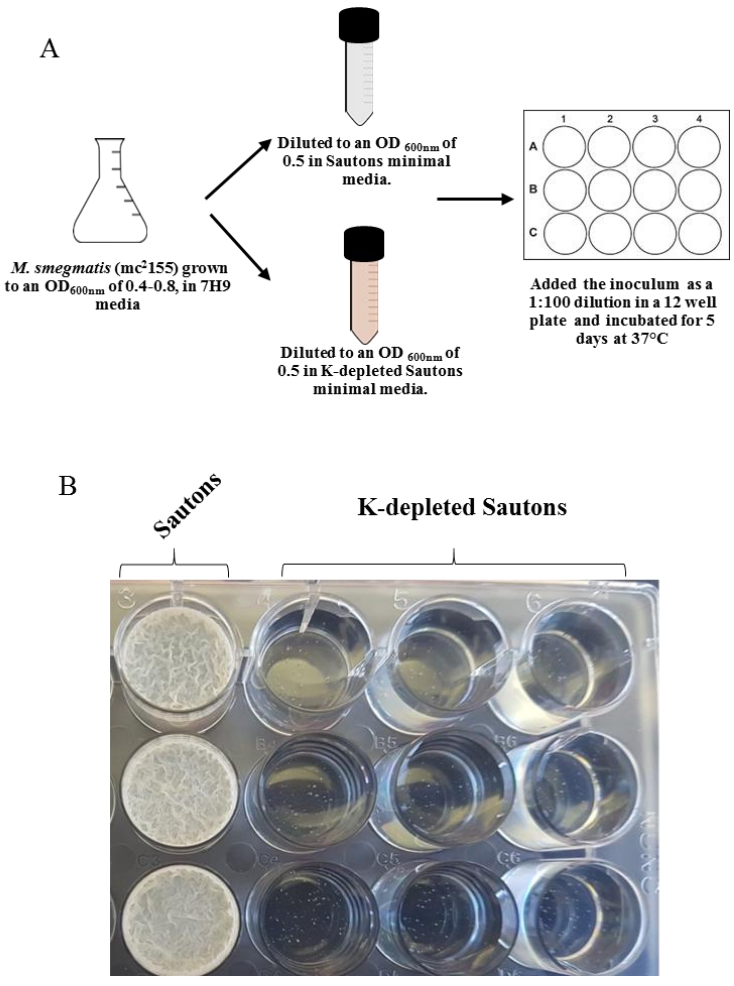


Figure 3.12 Removal of potassium ions from Sautons media prevents the formation of biofilms. A –A schematic representation of the method for potassium depleted biofilm formation**. B-***M. smegmatis* was cultured in 7H9 media, washed and resuspended in Sautons minimal media with and without potassium. The respective bacteria were aliquoted into a 12 well microtiter plate. Plates were incubated for 5, 7and 14 days and viewed for the development of a biofilm. Images show the biofilm formation after incubation for 14 days, wells indicate that the experiment was done in triplicate

3.2.3.2. Metabolic activity of the bacteria produced by the potassium depletion model

Next, the metabolic activity of DCMS induced in Sautons minimal media with and without potassium ions was assessed by measuring the uptake of the TADA probe. A sample of DCMS bacteria cultured in Sautons minimal media with and without potassium ions and an exponentially grown culture were labelled and fixed following the protocol described in the materials and methods section 2.6.1 and graphically depicted in figure 3.13-A. The TADA stained cells were analysed by flow cytometry (Figure 3.13-B). A clear shift in the fluorescent peaks of TADA labelled cells cultured with and without potassium ions was observed, suggesting that these bacteria have reduced metabolic activity. Interestingly, the bacteria cultured in Sautons minimal media displayed two peaks, indicating the presence of two populations: a non-replicating and replicating population (Figure 3.13-B).

Probe incorporation which was, measured as the mean fluorescence intensity of the TADA probe in the labelled and unlabelled cells revealed a significant lack of metabolic labelling of bacteria cultured in Sautons minimal media with and without potassium ions (p-value ≤ 0.01 and p-value ≤ 0.001 respectively), when compared to a labelled exponentially grown culture (Figure 3.13-C). The reduction of metabolic labelling indicated a lack of de novo biosynthesis of the PG, similar to that found in the carbon starvation model (see results section 3.2.1). The mean fluorescence intensity of the bacteria cultured with and without potassium ions was at the same level as the unlabelled exponentially grown axenic culture; thus, providing evidence for the establishment of a non-replicating state in these cells.

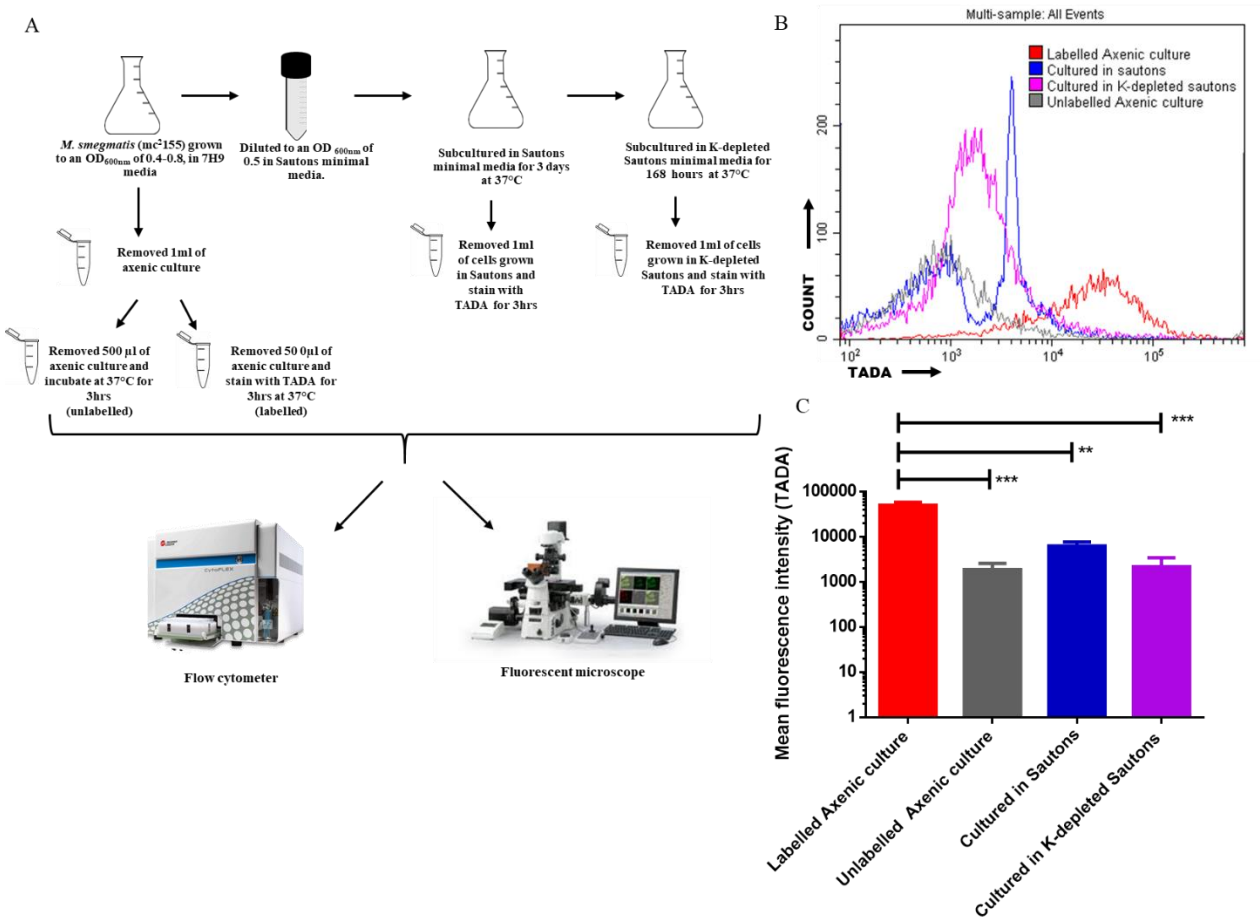


Figure 3.13 Bacteria cultured in potassium depleted media contain a larger population of non-replicating bacteria, compared to an axenic culture. A-A schematic representation of the model followed for flow cytometry and microscopy. **B-**Flow cytometry charts of bacteria cultured with and without potassium ions in Sautons minimal media strained for 3 hrs with TADA probe compared to labelled and unlabelled axenic culture with an OD_{600nm} between 0.5-0.8. **C**- Flow cytometry analysis of the mean fluorescent intensity of bacteria cultured with and without potassium ions, strained for 3hrs with TADA probe and compared to labelled and unlabelled axenic culture grown to an OD_{600nm} between 0.5- 0.8, using a one-way ANOVA statistical test (** = p-value≤0.01 and ***=a p-value ≤0.001).

3.2.3.3. Cytology of the bacteria produced by the potassium depletion model

In addition to metabolic activity, the labelled DCMS cells cultured in Sautons minimal media with and without potassium ions and exponentially grown axenic culture were analysed for the cytology of the bacteria by fluorescent microscopy as described in materials and methods section 2.8.1 and depicted in figure 3.13-A. One hundred bacteria per replicate (experiment done in triplicate) were analysed for the proportion of stained and unstained populations, (Figure 3.14 -B). Our results confirmed the flow cytometry results as only 17% of cells cultured in potassium depleted media showed staining, indicating the establishment of a non-replicative state. As observed previously in section 3.2.3.2, bacteria cultured in Sautons minimal media

confirmed the presence of two populations, a non-replicating population (unlabelled-46%) and a replicating population (labelled-54%).

Salina and colleagues showed that *M. tuberculosis* cells grown under potassium depletion conditions displayed changes in cell morphology resulting in a coccoid shape with intact membranes and condensed cytoplasm that closely resembled forms associated with dormant phenotypes (Salina et al., 2014). Therefore, the cell length of 100 bacteria per replicate (experiment done in triplicate), from cells cultured with and without potassium ions, were measured and compared to an exponentially grown culture. Bacteria cultured in potassium depleted media were significantly shorter compared to an exponentially grown culture but were not coccoid in shape as previously seen by Salina and colleagues (Figure 3.14-A). A possible reason for the difference could be that in this study the model was optimised in *M. smegmatis*. The bacteria cultured in Sautons minimal media appear to have a larger range of cell length, but have a similar median length compared to an exponentially grown culture.

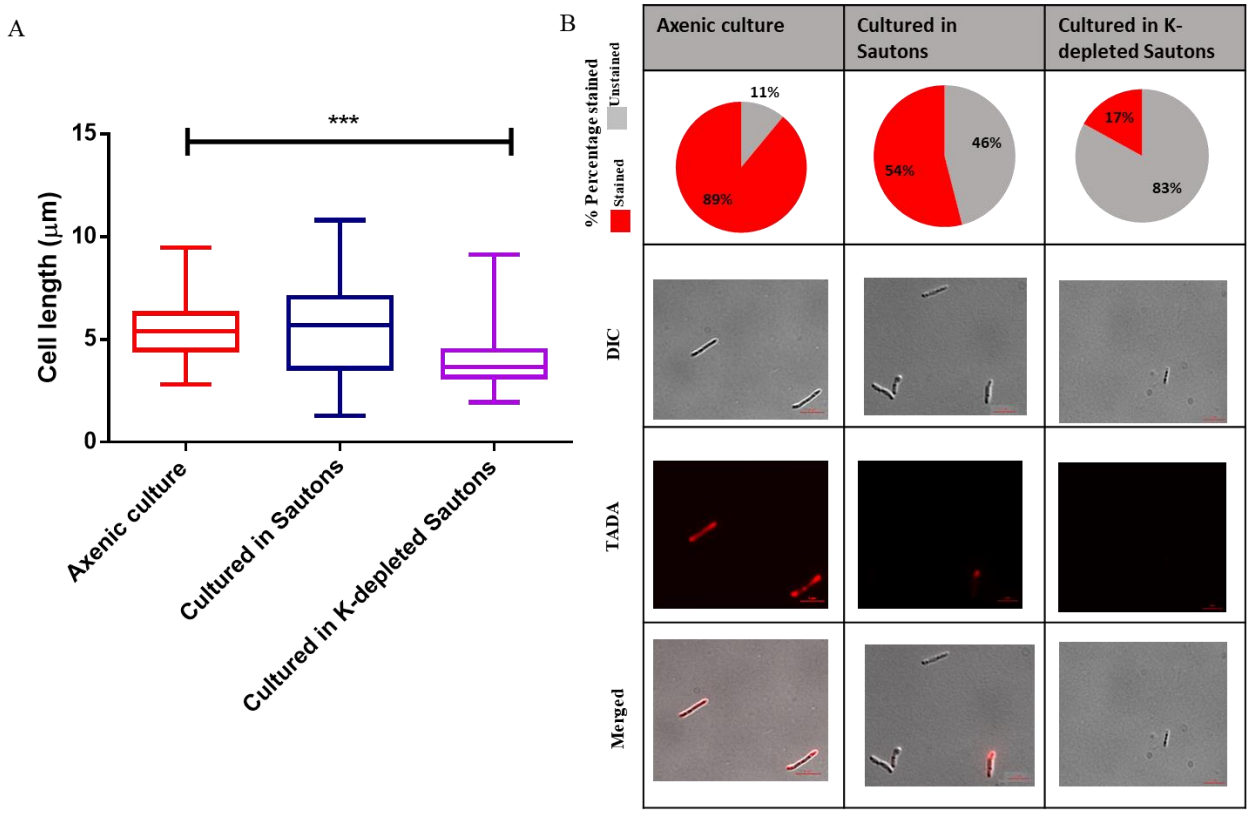


Figure 3.14 DCMS produced under the potassium depletion model have decreased cell length. A- Microscopy analysis of cell length of bacteria cultured with and without potassium ions were compared to an axenic culture using a one-way ANOVA statistical test (***= p-value ≤0.001) **B-** A 100 bacteria per replicate were analysed for the presence of fluorescent signal in the TADA channel. The DIC channel, is the phase view of the bacteria and the merge channel is the DIC channel overlapped with the TADA channel. Scale bar represents 5 µm

3.2.4. The role of CF in the detection of DCMS produced by *in vitro* models

Previous studies have shown that DCTB have reduced metabolic activity and therefore are unable to grow on solid media (Mukamolova, Turapov et al. 2010). However, CF from *M. tuberculosis* has been shown to increase the detection of DCTB in South African TB patients, providing evidence that DCTB require additional growth factors to resume metabolic processes and growth (Chengalroyen et al., 2016). Therefore, we tested whether media supplemented with CF, would enhance the detection of DCMS in the three models discussed above. CF from *M. smegmatis* (mc^2155) was used to supplement 7H9 Middlebrook media in the MPN assay for the enhanced detection of DCMS bacteria in each of the models. The recoverability of the DCMS was determined using two resuscitation conditions: 1) CF-dependant (growth in 7H9 media, supplemented with CF) and 2) CF-independent (growth in 7H9 media without CF supplementation).

In the carbon starvation model, the addition of growth factors in the form of CF did not improve the detection of DCMS (Figure 3.15-B). Resuscitation of these bacteria was equivalent under both CF-dependant and CF-independent conditions. However, bacteria starved in PBS and treated with 100 µM RIF displayed CF-dependant resuscitation, exhibiting significantly improved (p-value ≤ 0.05) detection of DCMS compared to CF-independent resuscitation, using a two-way ANOVA statistical test.

In the biofilm model both the RIF untreated and treated cells showed enhanced detection of DCMS with the addition of growth factors present in CF. However, this increase in detection was insignificant when compared to DCMS detected in media only, using a two-way ANOVA statistical test (Figure 3.15-B). Similarly, the addition of CF did not improve the detection of DCMS, cultured in Sautons minimal media with and without potassium ions, using a two-way ANOVA statistical test (Figure 3.15-B), indicating that in the potassium depletion model, DCMS resuscitation is CF-independent.

Overall, the carbon starvation model produced significantly more bacteria under both CF-dependant and CF-independent conditions compared to the exponentially grown culture and the other DC producing models using a two-way ANOVA statistical test (Figure 3.15-B). Therefore, this model was used for all further work.

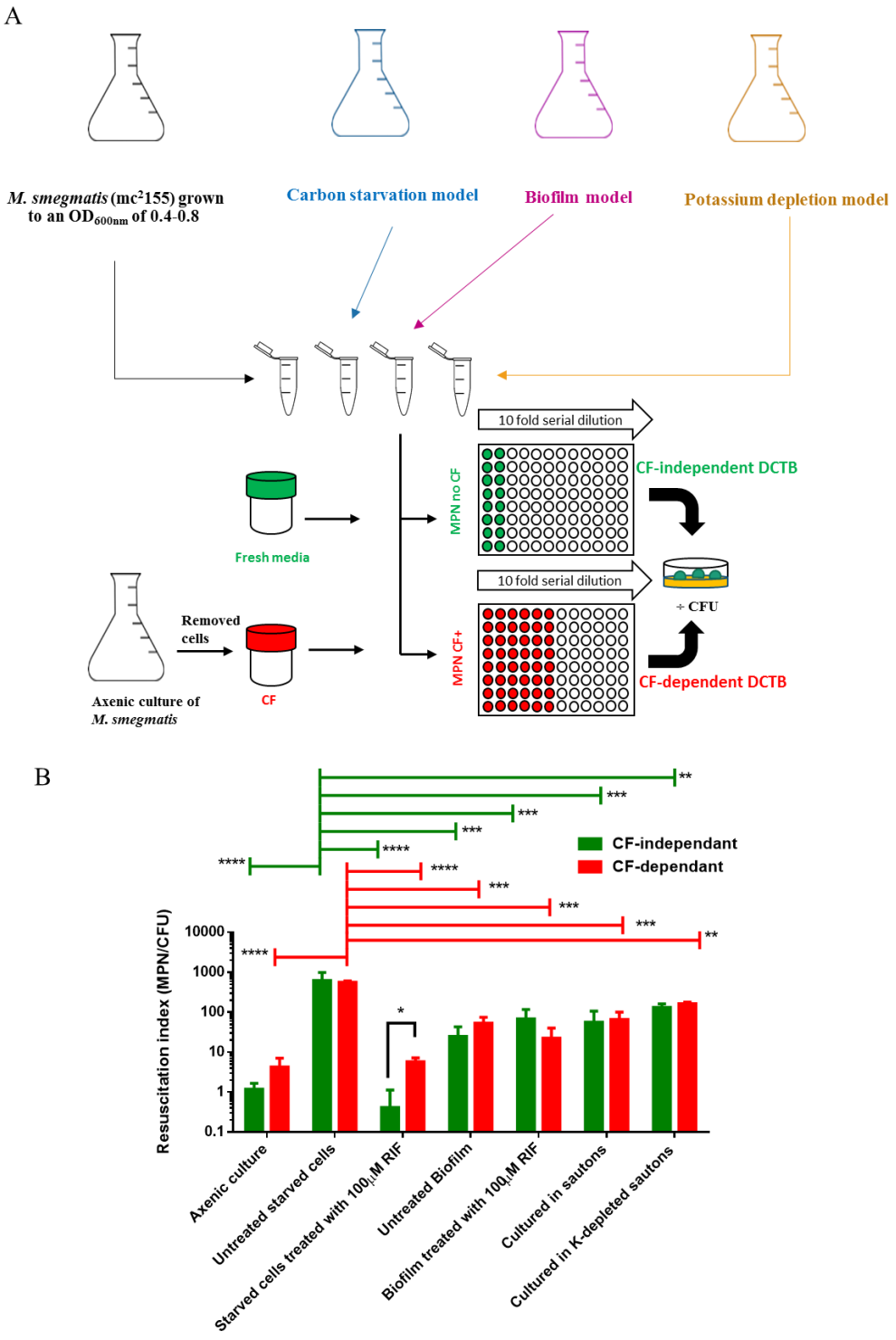


Figure 3.15. The effect of CF on the resuscitation of DCTB in the various models tested. **A**-A Schematic representation of resuscitation of the DC producing model (carbon starvation –blue, biofilm model –pink and potassium depletion model –yellow) with CF-supplementation (CF-dependent: growth in 7H9 media, supplemented with CF-red) and CF-independent (growth in 7H9 media without CF supplementation-green). **B** Resuscitation index was calculated using (MPN/CFU). All models were tested in triplicate. All models showed no significance difference between media and CF when no RIF was added, using a two-way ANOVA statistical test (**= p-value ≤0.01, *** = p-value ≤0.001 and **** = p-value ≤0.0001).

3.2.4.1. Metabolic activity of the bacteria produced by various *in vitro* the models

The metabolic activity of DCMS induced by the carbon starvation model, biofilm model and potassium depletion model were compared using the mean fluorescent intensity data from the flow cytometry experiment discussed in sections 3.2.1.1, 3.2.2.1 and 3.2.3.1. The overall results indicated that the carbon starvation model and potassium depletion model showed the greatest reduction in metabolic activity, evidenced by a reduction in mean fluorescent intensity which was similar to the unlabelled population (Figure 3.16). A non-replicative state was confirmed in the bacteria cultured in these models. Approximately 100 cells per replicate displayed negligible fluorescent signal by microscopy (Figure 3.17). Both data sets confirmed the establishment of a non-replicative state in these two models

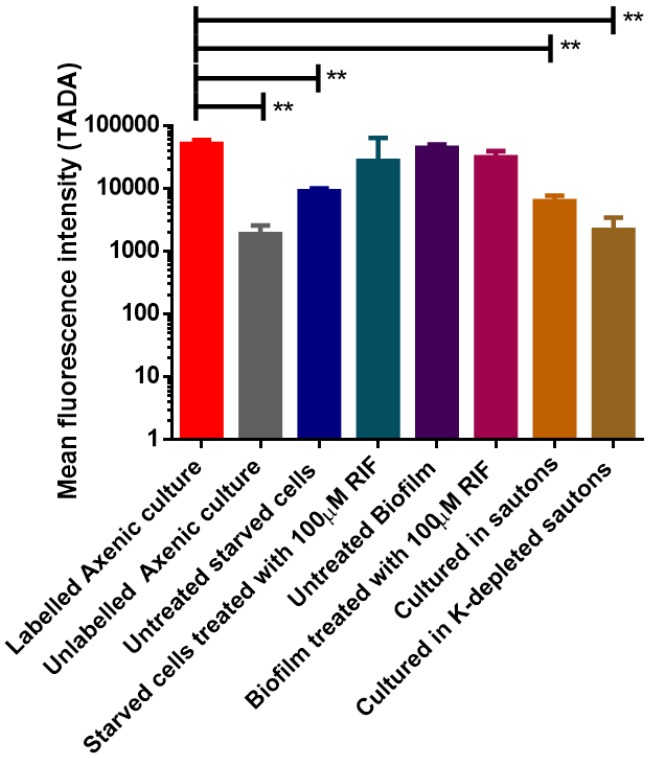


Figure 3.16 Carbon starvation and growth in potassium depleted media both induce non-replicating bacteria. Flow cytometry analysis showing the mean fluorescent intensity of DCMS bacteria produced by the various models. These bacteria were incubated for 3hrs with TADA probe at 37°C in the media of the model. The mean fluorescent intensity for all samples were analysed in triplicate and compared to labelled and unlabelled axenic culture grown to an OD_{600nm} between 0.5- 0.8 using a one-way ANOVA statistical test (** = p-value≤0.01). These data are a secondary analysis of the data presented in figures 3.6, 3.9 and 3.13

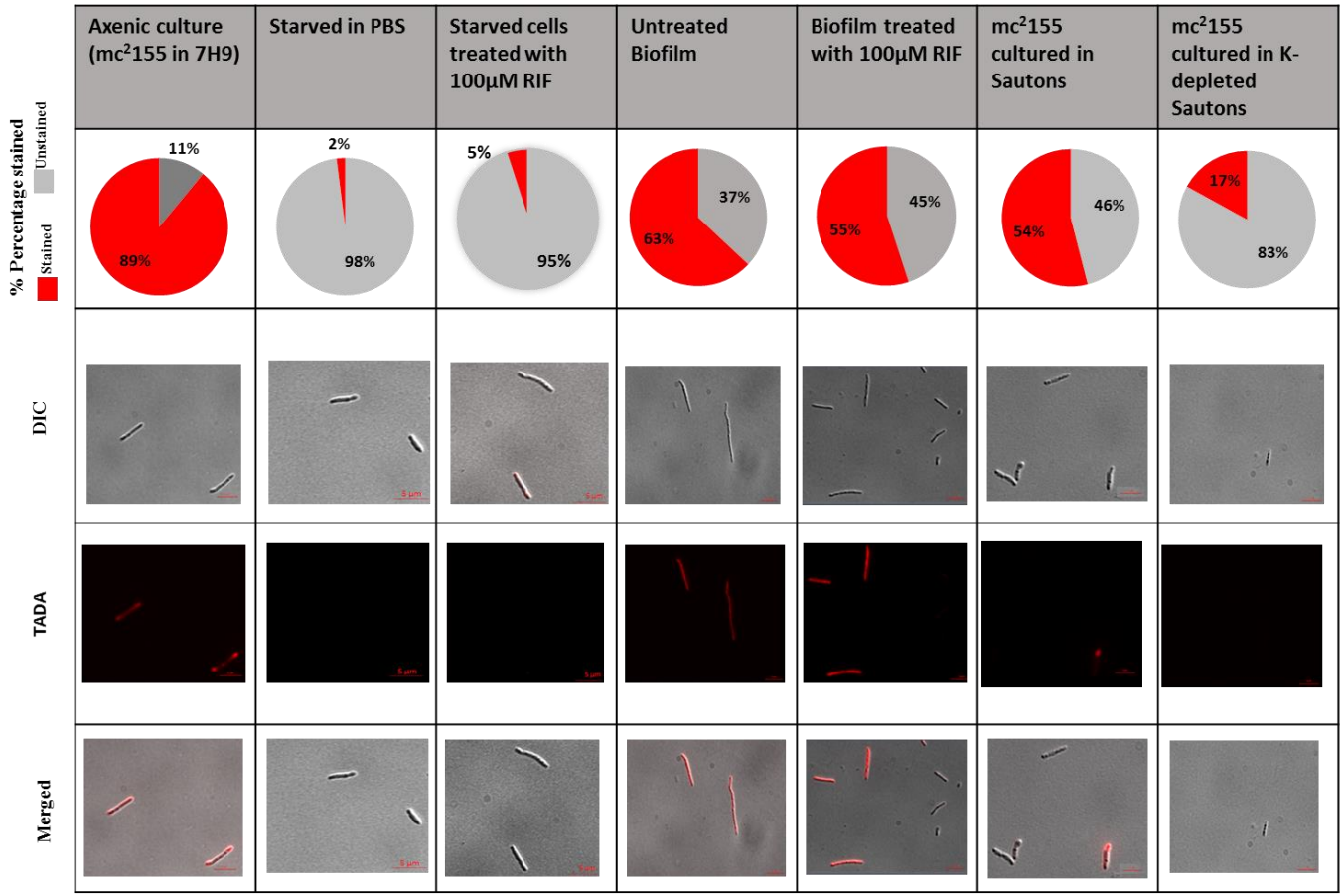


Figure 3.17 Microscopy analysis of probe incorporation in DCMS bacteria from the various models. In all cases, DCMS samples from the various models were incubated for 3 hrs with TADA probe at 37°C in the media of the model. All samples were analysed in triplicate and compared to labelled axenic culture grown to an OD_{600nm} between 0.5- 0.8. One hundred bacteria per replicate were analysed for the presence of fluorescent signal in the TADA channel. The DIC channel, is the phase view of the bacteria and the merge channel is the DIC channel overlapped with the TADA channel. Scale bar represents 5 µm. These data are a secondary analysis of the data presented in figures 3.7, 3.10, 3.14.

.

3.2.4.2. Cytological profiling of the bacteria produced by the various *in vitro* models

In addition to metabolic activity, the staining profile of the labelled DCMS cells from the carbon starvation model, biofilm model and potassium depletion model, compared to exponentially grown axenic culture were analysed by fluorescent microscopy. PBS starved bacteria and bacteria cultured in Sautons minimal media in the absence of potassium ions were significantly shorter compared to an exponentially grown culture (Figure 3.18). In contrast, bacteria from the biofilm model were significantly longer compared to an exponentially grown culture. Our results revealed that a longer cell phenotype is not a feature of DCMS bacteria, as the untreated biofilms did not produce a significant amount of DCMS when compared to an exponentially grown culture as shown previously in results section 3.2.2. The models with the highest DCMS production display a SMRC phenotype. Therefore, bacteria starved in PBS and bacteria cultured in potassium deplete media best resemble the DC state.

In summary, the carbon starvation model produced the highest quantity of DCMS compared to the other *in vitro* DC producing models. The bacteria from the model had a reduction in metabolic activity, which is consistent with a non-replicative state and were shorter compared to exponentially grown culture. Therefore, the carbon starvation model robustly generates DCMS and was used for the generation of DCTB.

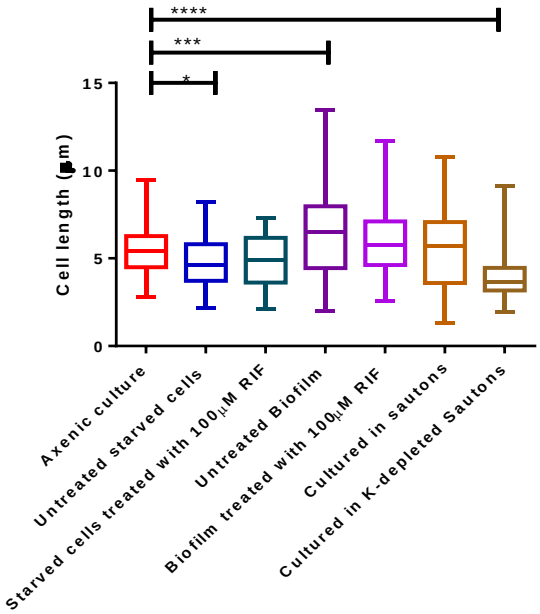


Figure 3.18 Carbon starvation and Potassium-depleted models, produce shorter *M. smegmatis* cells: Box and whisker plots showing the cell length of DCMS from the various models. A 100 cells were measured for each model. Mean and quartile ranges were calculated using GraphPad statistical tool. A one-way ANOVA

statistical test show that the starved cells and bacteria cultured in the absence of potassium are significantly shorter compared to an exponentially grown axenic culture (* =p-value ≤0.05. ** = p-value ≤0.01, ***= p-value ≤0.001 and **** = p-value ≤0.0001)

3.3. Optimization of an *in vitro* carbon starvation model in *M. tuberculosis*

As the carbon starvation model robustly generated DCMS, the methodology was tested and optimized for the generation of differentially culturable bacteria in the *M. tuberculosis* laboratory strain (H37Rv) using the protocol described under materials and method 2.3.1 and depicted in figure 3.19-A. Briefly, H37Rv was grown to exponential phase (OD_{600nm} 0.5-0.8), and a single cell suspension of the culture was created by low speed centrifugation without deceleration. The single cell suspension was subcultured into PBS media supplemented with tyloxapol, and incubated for 1 and 2 weeks at 37°C. The viability and recoverability of the starved *M. tuberculosis* was determined using two resuscitation conditions: CF-dependant (growth in 7H9 media, supplemented with CF) and CF-independent (growth in 7H9 media without CF supplementation). The resuscitation index was counted as a measure of DCTB.

After one week, cells starved in PBS showed an increase in both CF-dependent and CF-independent DCTB, compared to an exponentially grown axenic culture (Figure 3.19-B). This increase was not significant (p-value=0.06 for CF-dependant DCTB and p-value=0.09 for CF-independent DCTB), using a two-way ANOVA statistical test which, suggested that *M. tuberculosis* required longer exposure to starvation conditions compared to *M. smegmatis* to induce the DC state. Indeed, cells starved in PBS for two weeks showed a significantly increased resuscitation index compared to an exponentially grown culture under both CF-dependant and CF-independent conditions, using a two-way ANOVA statistical test (Figure 3.19-B). Under these conditions there are significantly more CF-dependant DCTB (p-value ≤ 0.01) compared to CF independent DCTB, using a one-way ANOVA statistical test, indicating that the DCTB bacteria generated under carbon starvation required growth stimulatory molecules from the CF, in order to exit the DC state. Thus, these findings demonstrated that the carbon starvation model can robustly generate DC

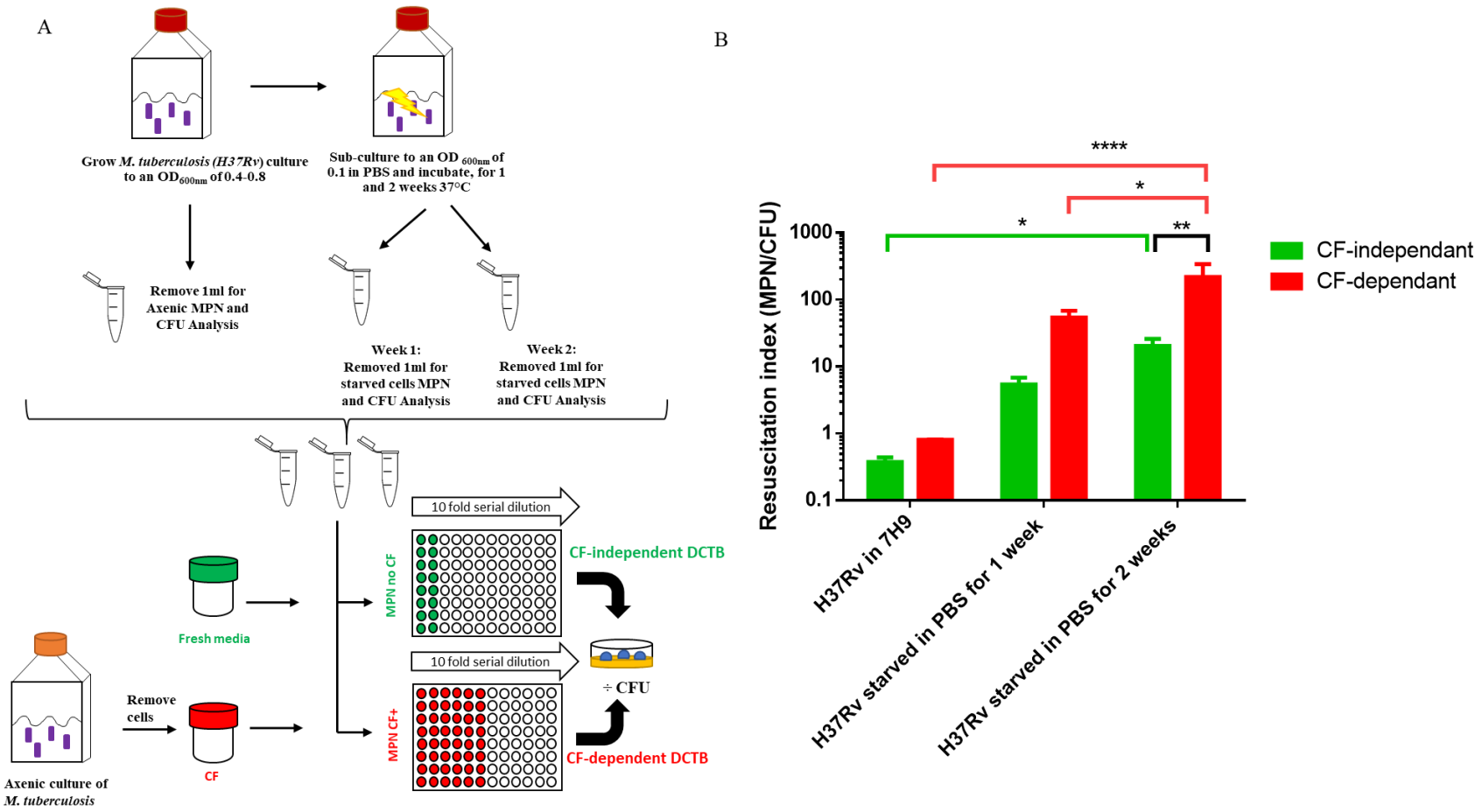


Figure 3.19 The effect of CF in the resuscitation of DCTB in the carbon starvation model: A-Schematic of the carbon starvation model and MPN assays used**.** Yellow light bolt represents the stress of starving bacteria in PBS for 2 weeks**. B-** H37Rv starved in PBS for 1 and 2 weeks compared to an axenic culture of H37Rv in 7H9 with an OD_{600nm} (0.5-0.8). The bacteria were resuscitated with media and CF, in a 96 well plate. Resuscitation index was calculated using the MPN/CFU ratio. The experiment was done in triplicate. Cultures starved for 1 and 2 weeks in PBS and resuscitated in CF and media without CF were significantly different (p-value ≤0.05) compared to an axenic culture of H37Rv grown in 7H9, using a two-way ANOVA statistical test (* = p-value <0.05, **= p-value <0.01, ***= p-value <0.001 and **** = p-value ≤0.0001).

3.3.1. Metabolic activity of *M. tuberculosis* bacteria produced under the carbon starvation model

We next accessed the metabolic activity of bacteria cultured in carbon depleted media using a TADA probe uptake as a proxy. The DCTB generated from the carbon starvation model after 1 and 2 weeks were labelled following the protocol described in material and methods section 2.6.1 and graphically depicted in figure 3.20-A. The starved cells showed a significantly reduced level (p-value ≤0.0001) of metabolic labelling of cells using a one-way ANOVA statistical test, indicating a lack of de novo biosynthesis of the PG (Figure 3.20-B). The cells starved in PBS displayed a similar mean fluorescent intensity relative to the unlabelled exponentially grown axenic culture, thus providing definitive evidence for the establishment of a non-replicating state (Figure 3.20-C).

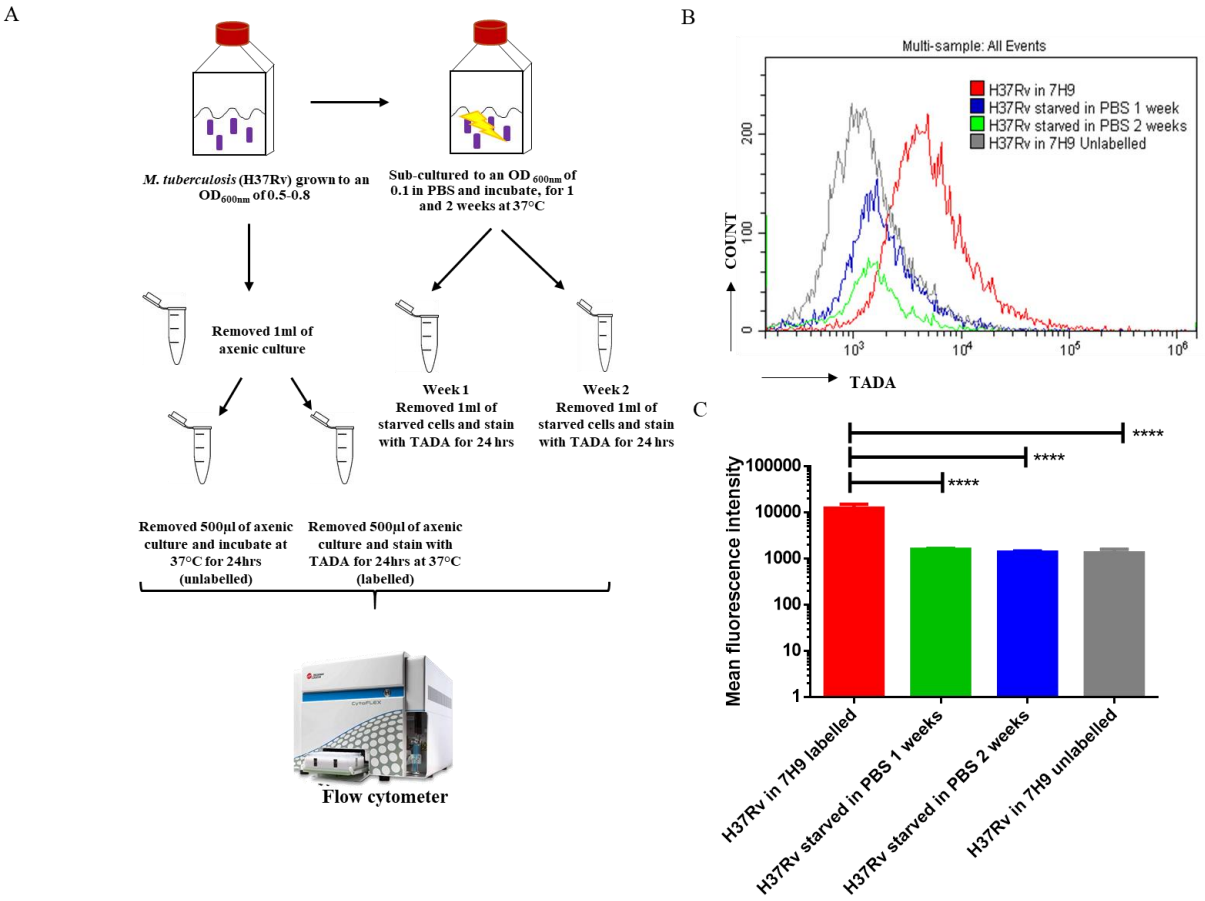


Figure 3.20 Carbon starvation induces non-replicating bacteria. A- A schematic representation of the method followed for flow cytometry. Yellow light bolt represents the stress of starving bacteria in PBS for 2 weeks. **B-** Flow cytometry analysis- H37Rv starved cells for 1 and 2 weeks and H37Rv grown in 7H9 media to an OD_{600nm} between 0.5-0.8 were incubated with the TADA probe for 24 hrs at 37°C. All samples were analysed in triplicate and, compared to labelled and unlabelled axenic culture. H37Rv starved cells produced a fluorescent signal, that was similar to the unlabelled population, thus confirming a non-replicative state. **C**- Mean fluorescent intensity

of starved cells after 1 and 2 weeks compared to a labelled and unlabelled exponentially grown culture using a one-way ANOVA statistical test (****= p-value ≤0.0001). H37Rv starved for 1 and 2 weeks had the same mean fluorescent intensity as the unlabelled population.

In addition to confirming the non-replicative state of DCTB produced using the carbon starvation model, re-incorporation of the metabolic TADA probe during resuscitation in media and CF was also assessed. We speculate that by deciphering the mechanisms of probe uptake during resuscitation, clues as to how bacteria exit the DC state may be obtained. To test this, samples were removed at 3, 5 and 7 days after resuscitation with media and CF, following the protocol described in materials and method section 2.5.4 and depicted graphically in figure 3.21-A. Our results indicated that after 3 days there was no significant difference in the mean fluorescent intensity with cells resuscitated either with 7H9 media (p-value = 0.11) or CF (p-value=0.07) compared to an exponentially grown culture, using a one-way ANOVA statistical test. Analysis of these cells by flow cytometry after 3 days of resuscitation, showed a low cell count, suggesting that the bacteria required a longer period for resuscitation. After 5 days of resuscitation, flow cytometry analysis showed an increase in cell count, represented by a larger peak. The mean fluorescent intensity of the samples indicated that there was a significant difference (p-value ≤0.05) between cells resuscitated in CF after 5 days, compared to an exponentially grown culture using a one-way ANOVA statistical test (Figure 3.21-B&C). Seven days of resuscitation with CF yielded a further increase in bacterial cell count as seen by the shift of the flow cytometry trace to the right indicative of increased metabolic activity (Figure 3.21-B). Measurement of the mean fluorescent intensity showed a significant increase in metabolic activity in bacteria resuscitated both with 7H9 media (p-value ≤0.05) and CF (p-value ≤0.01) compared to an exponentially grown axenic culture, using a one-way ANOVA statistical test (Figure 3.21-C). These results clearly indicated that the reduction in metabolic activity associated with starved cells, can be restored and increased after 7 days of resuscitation with either 7H9 media or CF (Figure 3.21-D&E). Thus, the non-replicating state that bacteria enter during carbon starvation is reversible and the carbon starvation model developed in this study can be used to robustly produce and study DCTB.

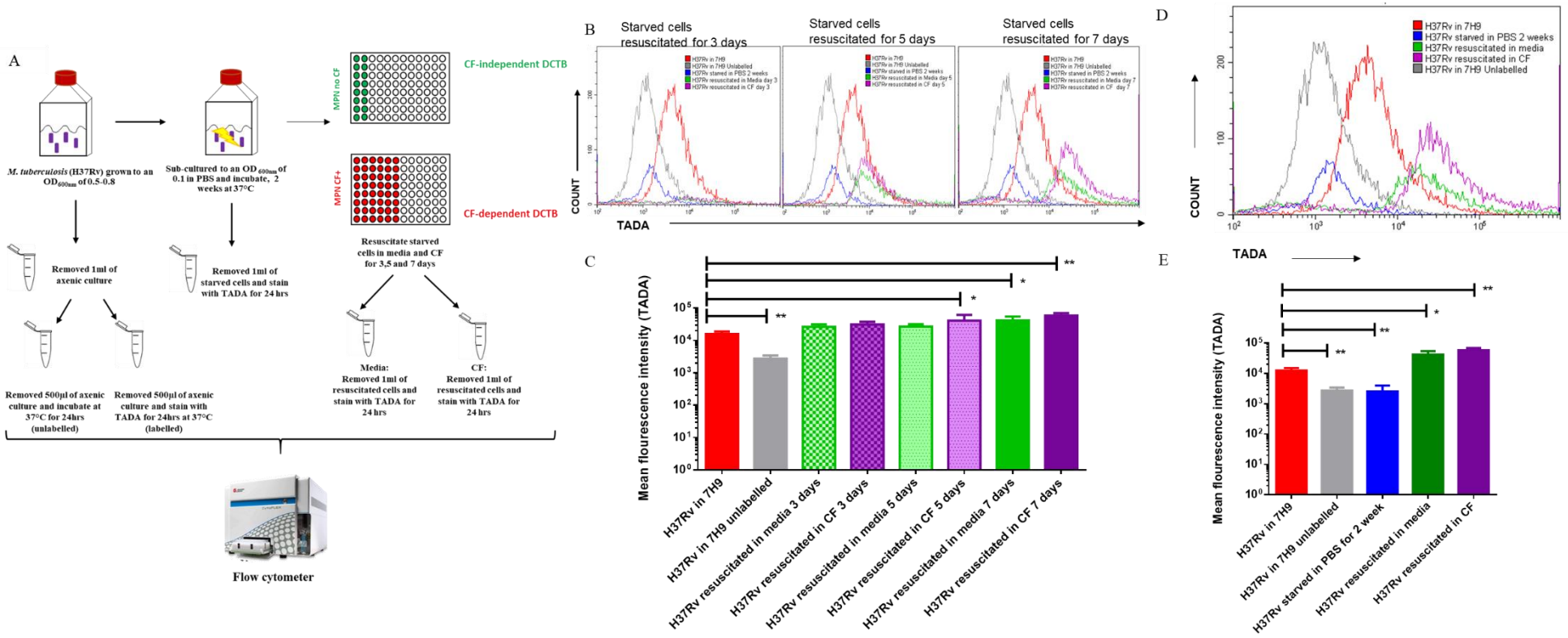


Figure 3.21 Resuscitation of starved bacteria in CF restored the non-replicating bacteria to their active state after 7 days. **A**- A schematic representation of method followed for flow cytometry. Yellow light bolt represents the stress of starving bacteria in PBS for 2 weeks **B**-Flow cytometry analysis. Bacteria resuscitated in media and CF at 3, 5 and 7 days and H37Rv in 7H9 samples were incubated for 24 hrs with TADA probe at 37°C. All samples were analysed in triplicate and, compared to labelled and unlabelled axenic culture grown to an OD_{600nm} between 0.5-0.8 using a two-way ANOVA statistical test (* = p-value ≤0.05, **= p-value ≤0.01). **C**- Mean fluorescent intensity of bacteria resuscitated in media and CF compared to a labelled and unlabelled exponentially grown culture. **E**- Mean fluorescent intensity of cells starved in PBS, bacteria resuscitated in media and CF compared to a labelled and unlabelled exponentially grown culture. **D**- Flow cytometry analysis- H37Rv starved cells at 1 and 2 weeks, resuscitated cells and H37Rv in 7H9. Samples were incubated for 24 hrs with TADA probe at 37°C.

3.3.2. Cytological profiling of DCTB produced by the carbon starvation model

In addition to flow cytometry analysis, fluorescent microscopy was used to confirm incorporation of the metabolic probe. Three experimental conditions were tested: 1) H37Rv starved in PBS, 2) H37Rv resuscitated with 7H9 media and 3) H37RV resuscitated with CF. In each case, cells were stained with TADA and then visualised following the protocol described in material and method section 2.8.2 and depicted in figure 3.22-A. One hundred cells per replicate (experiment done in triplicate) were visualised and analysis for the incorporation of the metabolic TADA probe, and cell length of the bacteria were measured. Incorporation of the TADA probe was measured by the percentage of cells that produced a fluorescent signal. As with *M. smegmatis*, fluorescent microscopy confirmed the lack of metabolic probe uptake in a large proportion of the *M. tuberculosis* (H37Rv) cells cultured in carbon depleted media (labelled-17%), compared to an exponentially grown culture (labelled-70%) (Figure 3.22-D). Additionally, a small subset of cells displayed defective spatial incorporation of the metabolic probe. Metabolic labelling was restored in majority of the population when resuscitated using CF or 7H9 media after 7 days (Figure 3.22-D). Furthermore, microscopy revealed that DCTB from the carbon starvation model were significantly shorter (p-value ≤ 0.0001) compared to an exponentially grown culture. In contrast, bacteria resuscitated in 7H9 media (p-value ≤ 0.0001) and CF (p-value ≤ 0.0001) were significantly longer compared to an exponentially grown culture (Figure 3.22-C).

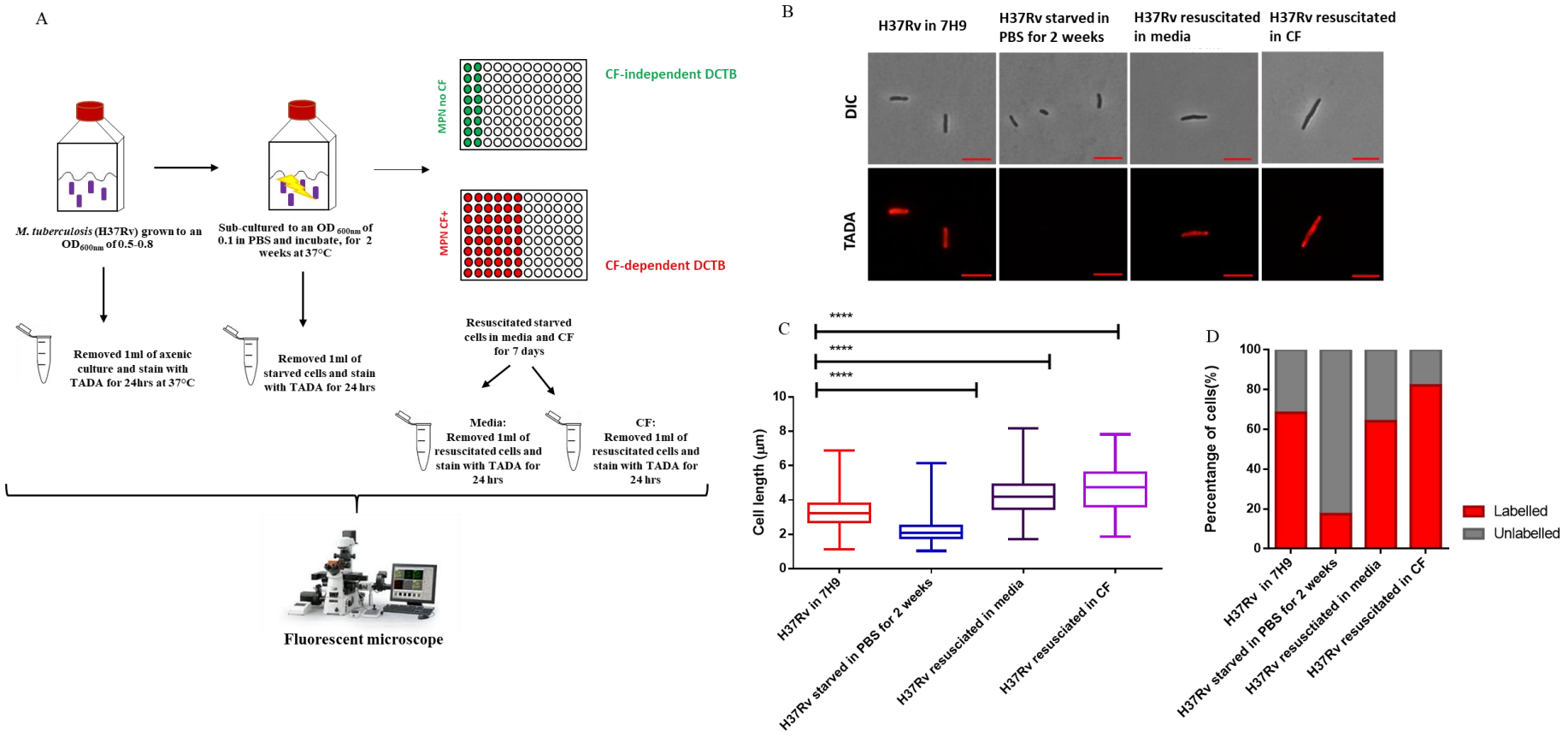


Figure 3.22. H37Rv starved in PBS for 2 weeks produce shorter DCTB cells: A- schematic representation of method followed for microscopy. **B-**H37Rv in 7H9, H37Rv starved in PBS and starved H37Rv resuscitated in media and CF samples were viewed under the microscope. Starved cells were shorter and did not incorporate the probe compared to cells grown in 7H9**. C-** Box and whisker plots showing the length of H37Rv cells starved in PBS, starved H37Rv resuscitated in media and CF compared to cells grown in 7H9. Mean and quartile ranges were calculated, cells starved in PBS were significantly (p-value ≤ 0.0001) shorter, whilst H37Rv resuscitated in media and CF were significantly longer (p-value ≤ 0.0001) compared to cells grown in 7H9, using a one-way ANOVA statistical test. **D-**H37Rv was grown in Middlebrook 7H9, starved in PBS, resuscitated in CF and resuscitated in media after 7 days. Samples were incubated for 24 hrs with TADA probe at 37°C. H37Rv starved in PBS and starved H37Rv resuscitated in CF and media samples were compared to labelled and unlabelled cells grown in 7H9 to an OD_{600nm} 0.5- 0.8. H37Rv starved in PBS appeared within the unlabelled population, whilst starved cells resuscitated in CF were brighter compared to the H37Rv in 7H9. Three hundred cells per sample were analysed for staining using a fluorescent microscope, to confirm flow cytometry results.

An in-depth analysis of PBS starved H37Rv bacteria resuscitated in 7H9 media and CF was performed using a fluorescent super resolution structured illumination microscopy (SR-SIM), following the protocol describe in materials and method section 2.8.2 and compared to an exponentially grown culture. Under all three conditions, SR-SIM microscopy revealed 6 staining patterns: Uniform staining (bacteria were metabolically active, but not actively replicating), Polar staining (bacteria were metabolically active and actively replicating at both poles), cell wall staining cell , polar and septal staining (bacteria which were metabolically active and about to divide), strong and weak pole staining (bacteria were metabolically active, and actively replicating at one pole) and uneven staining (bacteria were metabolic active, and remodelling the cell wall) depicted in figure 3.23-A. One hundred cells per replicate (experiment done in triplicate) were viewed and then categorised into one of the six staining patterns outlined above.

The results showed that the bacteria resuscitated with CF showed higher incorporation of the metabolic probe at the cell pole compared to the exponentially growing culture (Figure 3.3.5-B). In-depth analysis of the incorporation of the metabolic TADA probe in 10% of the bacterial population represented in figure 3.23-C confirmed a strong incorporation of the TADA probe cell poles in bacteria resuscitated in media supplemented with CF, whilst an exponentially grown culture had uniform staining (Figure 3.23-B&C). Bacteria resuscitated in CF had a more distinct polar staining pattern compared to cells resuscitated in media. Mycobacteria replicate by polar extension, therefore an increase in probe incorporation at the pole suggest that cells resuscitated with CF display increased metabolic activity compared to an exponentially grown axenic culture or starved bacteria resuscitated with media.

These combined observations indicate that the carbon starvation model, induces a non-replicative DC state in *M. tuberculosis*, and that culturability can be restored by the addition of CF. This model is therefore ideal model to study the DC state in clinical strains.

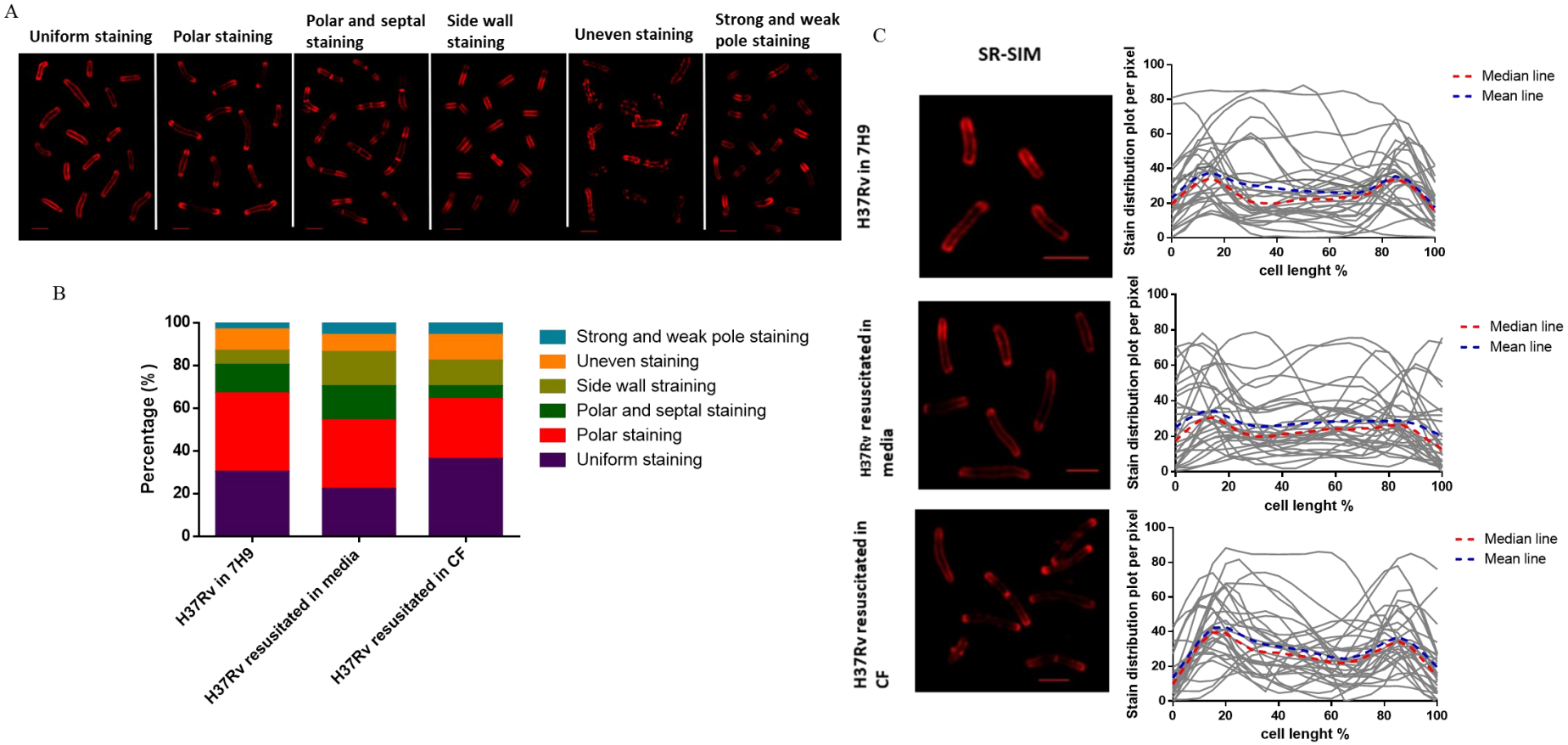


Figure 3.23 Resuscitated bacteria have increase metabolic activity A- Grouped representation of the six staining groups visualised using SR-SIM. **B-** Distribution of the six staining patterns in H37Rv grown in 7H9, starved and resuscitated in CF and media after 7 days. Samples were incubated for 24 hrs with TADA probe at 37°C. Starved and subsequently resuscitated cells in CF and media were compared to cells grown in 7H9 to an OD_{600nm} (0.5- 0.8). One hundred cells per sample (experiment done in triplicate) were analysed for staining using SR-SIM fluorescent microscopy. C- Staining distribution plots, 10% of the total population of resuscitated bacteria were analysed and compared to an exponentially grown axenic culture, with a mean (blue line) and median (red line) trend line.

3.4. The propensity of clinical *M. tuberculosis* strains to adopt the differentially culturable (DC) state

Another objective of this study was to test the propensity of *M. tuberculosis* clinical strains to adopt the DC state using the previously optimised *in vitro* carbon starvation model (see results section 3.3) for the laboratory strain *M. tuberculosis* H37Rv. The carbon starvation model generated DCTB robustly, when H37Rv was cultured in carbon depleted media for two weeks. Thus, the carbon starvation model was tested on clinical *M. tuberculosis* strains for the ability to generate DCTB.

3.4.1. Selection and confirmation of *M. tuberculosis* clinical strains

Previous data from the meta-analysis of two clinical studies: BMG phase one and MGIT plus described in results section 3.1 indicated that Beijing strains had the highest propensity to produce CF-independent and CF-independent DCTB compared to other clinical strains. Our data further suggested that Beijing strains were better adapted to produce DCTB relative to LAM and other clinical strains. Hence, we decided to test the optimised *in vitro* carbon starvation model on clinical isolates of LAM and Beijing stains. Consequently, five Beijing clinical strains and five LAM clinical strains were selected and passaged through multiple culturing steps following the protocol described in materials and methods section 2.2.3. Single colonies for each clinical strain were selected and spoligotyped following the protocol described in materials and methods section 2.3.2, to reconfirm the strain type. As depicted in figure 3.24 and figure 3.25, the spoligotypes of the five Beijing and five LAM strains matched the previously annotated spoligotypes, with the exception of the third LAM strain (Figure 3.25). In this case, the mismatched LAM strain was initially classified as a LAM 3 strain, whereas subsequent testing suggested it was a LAM 8 genotype. The reason for this discrepancy remains unclear but it may be due to human error when interpreting the spoligotype pattern. This discrepancy should not have a significant impact on the groupings.

3.4.1.1. Growth kinetics of *M. tuberculosis* clinical strains

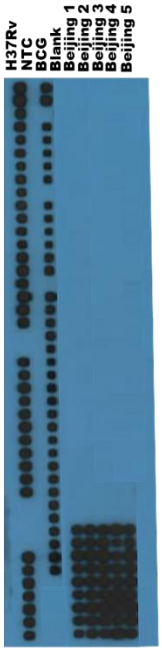
To determine the growth kinetics of LAM and Beijing strains, the growth rates of all 10 clinical isolates in 7H9 media were analysed and compared to the laboratory strain H37Rv, following the protocol described in materials and methods section 2.2.1. As indicated in figure 3.24,

Beijing strains showed identical growth rates to the laboratory strain H37Rv, whilst LAM strains showed reduced growth rate during the exponential growth phase compared to the H37Rv laboratory strain (Figure 3.25). These differences in growth rates between the LAM and Beijing strains could be associated with the many other variations noted between these strains in the literature (Hanekom et al., 2011; Kong et al., 2007; G. Kumar et al., 2017; Parwati et al., 2010). Several studies have previously assessed the intracellular growth of Beijing clinical strains in macrophages and have reported that Beijing genotypes grow significantly faster than non-Beijing genotype strains and therefore, have been associated with hypervirulence (Hanekom et al., 2011; Parwati et al., 2010; Reed et al., 2007).

A

Strain	Patient number	1st spoliogotyping results	2nd spoliogotyping results	Octal number
Beijing 1	57165	Beijing	Beijing	000000000003771
Beijing 2	59129	Beijing	Beijing	000000000003771
Beijing 3	57134	Beijing	Beijing	000000000003771
Beijing 4	57154	Beijing	Beijing	000000000003771
Beijing 5	59014	Beijing	Beijing	000000000003771

B



C

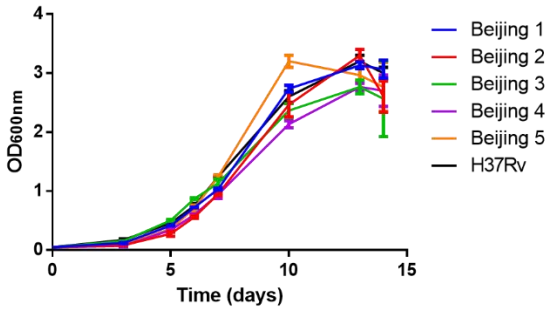
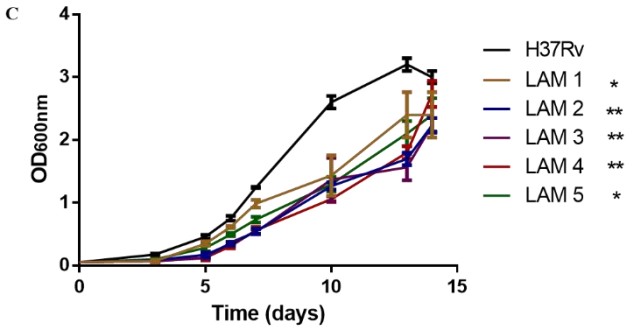


Figure 3.24 Genetic Confirmation and growth kinetics of Beijing strains. **A**- Table of the 5 Beijing strains selected, the patient identification number, spoligotyping results and octal numbers (represent a unique banding pattern) **B**-Spoligotyping results of the repeated spoligotyping for the 5 Beijing strains and controls (H37Rv, BCG and no template control [NTC]). C- Growth kinetics of the 5 Beijing stains compared to H37Rv, showing that the Beijing strains and H37Rv have a similar growth rate. Data are representative of three independent experiments.

A

Strain	Patient number	1st spoliotyping results	2nd spoliogotyping results	Octal number
LAM 1	57150	LAM 9	LAM 9	777777607760771
LAM 2	57149	LAM 8	LAM 8	777775606060731
LAM 3	59007	LAM 3	LAM 8	777775606060731
LAM 4	59028	LAM 9	LAM 9	777777607760771
LAM 5	59002	LAM 10	LAM 10	777761007760770



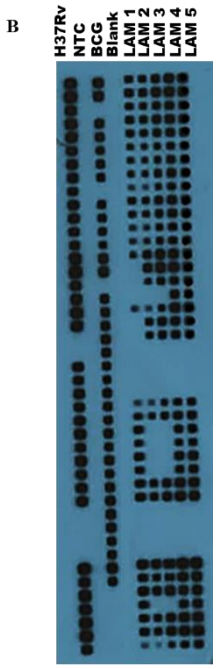


Figure 3.25. Genetic confirmation and growth kinetics of LAM strains. A-Table of the 5 LAM strains selected, the patient number, spoligotyping results and octal numbers represent a unique banding pattern). **B**-Spoligotyping results from the repeated spoligotyping membrane of the 5 LAM strains and controls (H37Rv, BCG and no template control [NTC]). **C**-Growth kinetics of the 5 LAM stains compared to H37Rv, showing that LAM strains have a significantly slower growth rate compared to H37Rv.

3.4.2. The propensity of starved clinical strains to adopt the DC state in carbon depleted media

DCTB were generated for the clinical Beijing and LAM strains and compared to DCTB produced by the laboratory strain (H37Rv) using the carbon starvation model as described in materials and method section 2.3.1. A sample of exponentially grown axenic culture of Beijing, LAM and H37Rv strains were assessed for the presence of DCTB as a control. The results indicated that cultures of Beijing, LAM and H37Rv did not contain any DCTB bacteria before undergoing carbon starvation (Supplementary figure C-1). Beijing and H37Rv strains incubated in carbon depleted media for 2 weeks produced both CF-dependant and CF-independent DCTB (Figure 3.26-A). Under these conditions, LAM strains did not show any CF-independent DCTB (resuscitation index was less than 1, represented by the back line on Figure 3.26-A & C), but did produce CF-dependant DCTB. LAM 1 and LAM 2 produced significantly less CF-dependant DCTB compared to Beijing 1 and H37Rv. Only one isolate of the Beijing strains (Beijing 1) showed a significant difference (p-value≤0.01) in the detection of DCTB bacteria between media and CF-supplementation, using the two-way ANOVA

statistical test. Overall, there was a significant difference between the CF-dependant resuscitation and CF-independent resuscitation between Beijing and LAM stains, using statistical t-test as depicted in Figure 3.26 B & C). These results suggested that clinical strains of *M. tuberculosis* starved of carbon sources robustly generate DCTB. The ability of Beijing strains to produce both CF-dependant and CF-independent DCTB whilst LAM strains only produced CF-dependant DCTB, somewhat reflects the results from section 3.1 where sputum samples carrying Beijing strains were more likely to have DCTB when compared to the LAM strain.

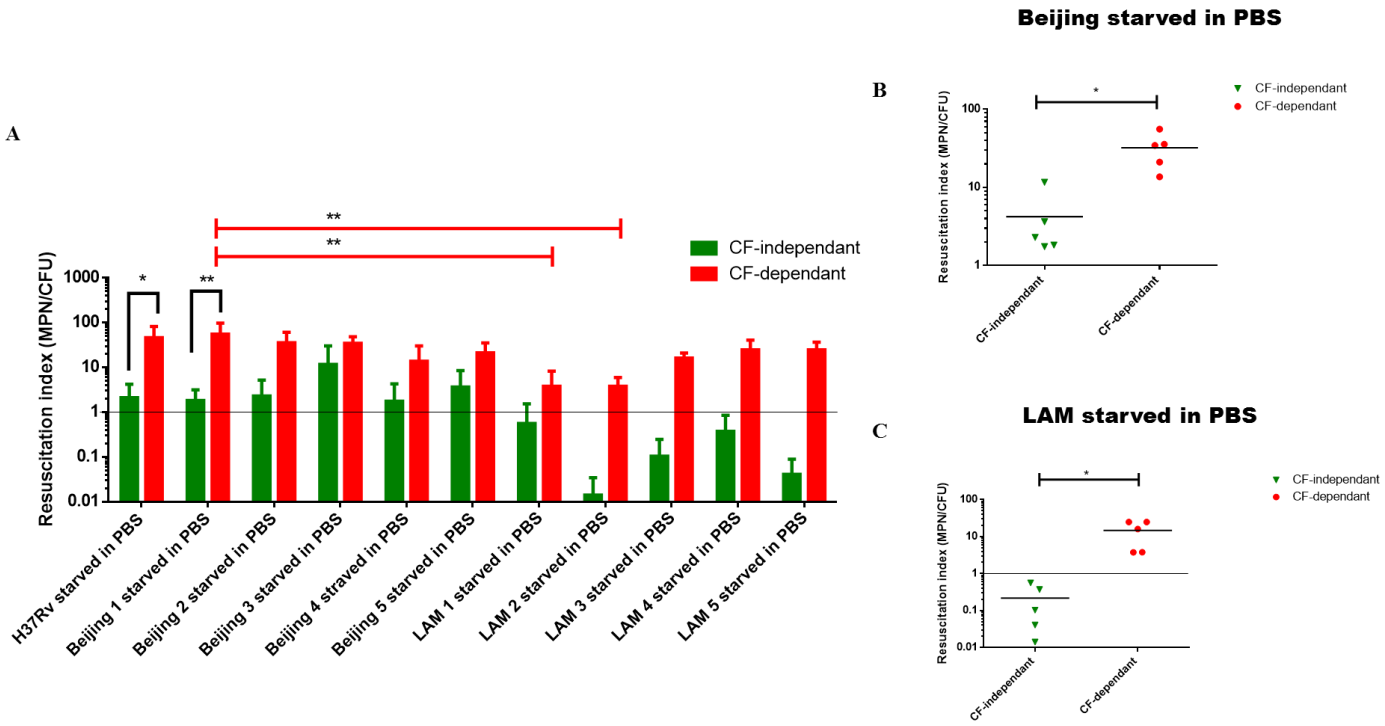


Figure 3.26 Beijing strains have an increased propensity to produce DCTB compared to LAM strains - Beijing and LAM strains starved in PBS for 2 weeks were compared to H37Rv starved in PBS for the same period. The bacteria were resuscitated with media and CF, in a 96 well plate. Resuscitation index was calculated using MPN/CFU ratio. The experiment was done in triplicate. Beijing 1 and H37Rv resuscitated in CF and media detected significantly more (p-value ≤0.01) DCTB compared to starved cultures of LAM 1 and LAM 2, using a two-way ANOVA statistical test **B**- Grouped analysis based on figure A, comparing the effect of CF in all the Beijing strain **C** -Grouped analysis based on figure A, comparing the effect of CF in all the LAM strains. Grouped analysis showed that both Beijing and LAM strains resuscitated significantly more CF-dependant DCTB compared to CF-independent DCTB.

3.4.2.1. Metabolic activity of the *M. tuberculosis* clinical bacteria produced by the carbon starvation model

Next the metabolic activity of DCTB from clinical isolates of Beijing and LAM strains were investigated using the TADA probe. Due to time constraints only one Beijing strain (Beijing 2) and one LAM strain (LAM 5) were selected at random. For each of the strains a sample of

DCTB from the carbon starvation model as well as an exponentially grown culture was labelled with the TADA probe and fixed following the protocol from materials and methods 2.6.1. Labelled DCTB bacteria from starved Beijing and LAM strains were analysed for TADA probe incorporation, and compared to a labelled and unlabelled exponentially grown axenic culture for the respective strain using flow cytometry (Figure 3.27-B and Figure 3.28-B) and these results were confirmed by microscopy.

Beijing 2 and LAM 5 had a significant reduction (p-value ≤ 0.01) in metabolic activity, which is consistent with a non-replicative state, when cultured in carbon depleted media using a one-way ANOVA statistical test (Figure 3.27-A and Figure 3.28-A). However, when the starved Beijing and LAM bacteria were resuscitated in media, there was an increase in metabolic activity, but the increase was significantly lower (p-value ≤ 0.05) compared to an exponentially grown culture. These findings were in contrast to previous data observed for the laboratory strain (results section 3.3.4) suggesting that LAM and Beijing strains require additional growth factors in order to exit the non-replicative state to become metabolically active. Subsequently, when the starved Beijing and LAM bacteria were resuscitated in CF, the metabolic activity of the bacteria was restored to that of an exponentially grown culture (Figure 3.27-A and Figure 3.28-A). These results were in contrast to previous data from results section 3.3, where the starved laboratory strain (H37Rv) displayed restored metabolic activity when resuscitated in media and increased metabolic activity when resuscitated in CF compared to an exponentially grown culture. This indicates that clinical strains need additional growth factors in order to shift from the DCTB state to an active growth.

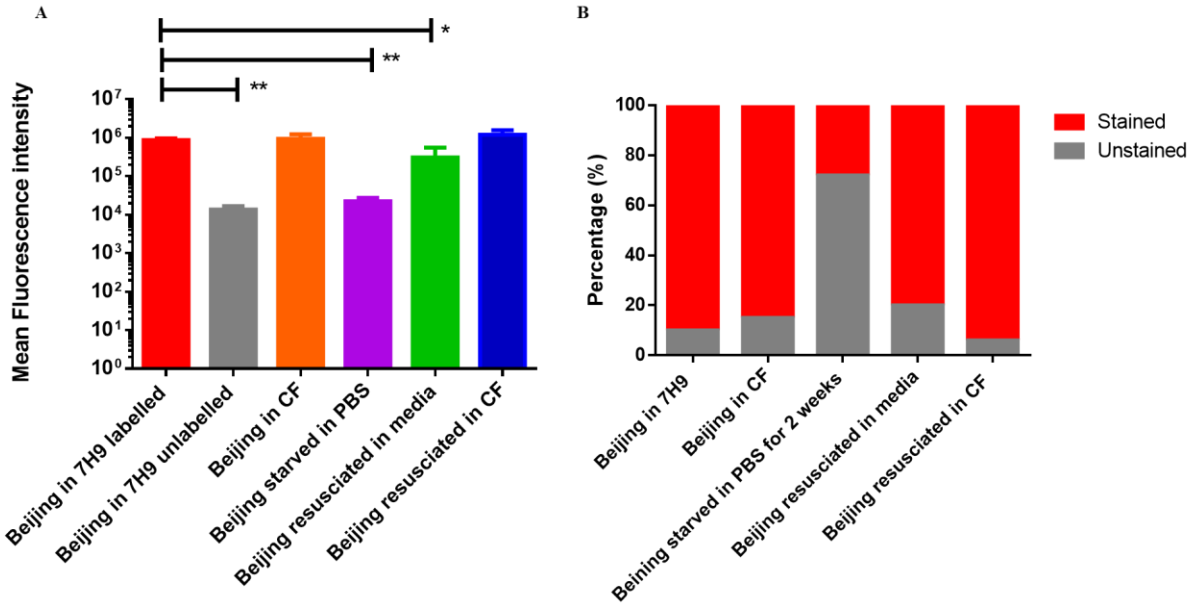


Figure 3.27 Metabolic activity of Beijing analysed by flow cytometry and microscopy. A- Flow cytometry analysis showing mean fluorescent intensity of Beijing cells cultured in 7H9 (labelled and unlabelled), Beijing cells starved cells for 2 weeks, starved Beijing cells resuscitated in media and CF. Analysis was done in triplicate and all samples were incubated for 24 hrs with the TADA probe at 37°C and compared to an unlabelled exponentially grown culture of Beijing, using a one-way ANOVA statistical test (*=p-value ≤0.05, **=p-value ≤0.01 and ***= p-value ≤0.001). **B**-One hundred cells per replicate (experiment done in triplicate) were analysed for staining using a fluorescent microscope.

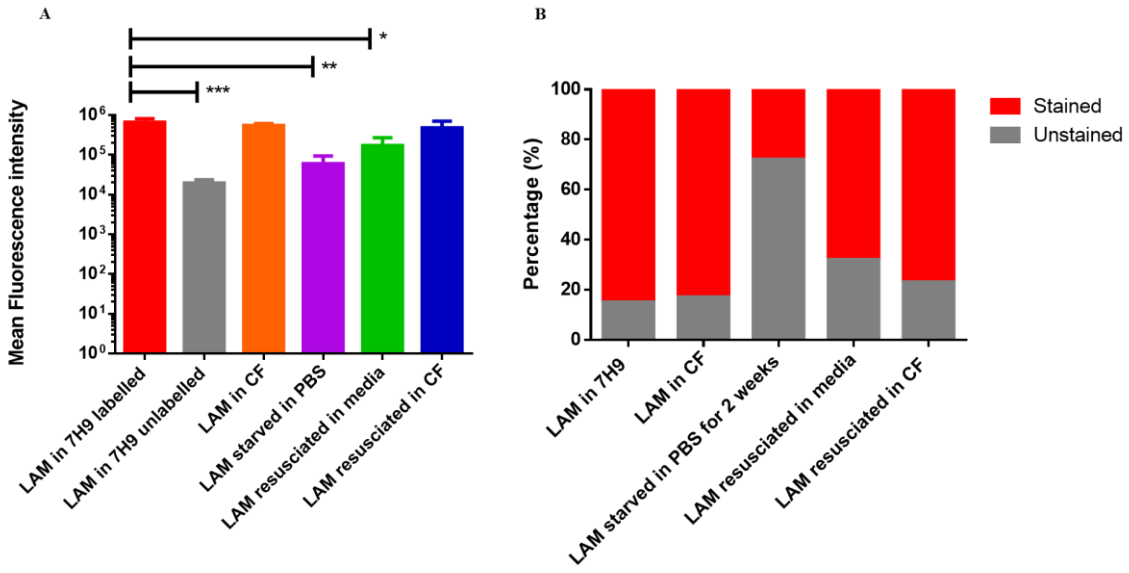


Figure 3.28 Metabolic activity of LAM analysed by flow cytometry and microscopy. A- Flow cytometry analysis showing mean fluorescent intensity of LAM cells cultured in 7H9 (labelled and unlabelled), starved cells for 2 weeks, resuscitated in media and CF. Analysis was done in triplicate and all samples were incubated for 24 hrs with the TADA probe at 37°C, and compared to an unlabelled exponentially grown culture of LAM using a one-way ANOVA statistical test (* = p-value ≤0.05, **= p-value ≤0.01 and ***= p-value ≤0.001). **B**-One hundred cells per replicate (experiment done in triplicate) were analysed for staining using a fluorescent microscope.

3.4.3. Cytological profiling of the *M. tuberculosis* clinical bacteria produced by carbon starvation the model

Beijing and LAM strains grown in 7H9, grown in CF (as a control), and resuscitated with media and with CF were stained with the TADA probe and visualised using SR-SIM. Furthermore, a random 10 % of the bacterial population was selected and analysed for the distribution of staining along the cell length to determine the mean and median staining pattern, as described in materials and methods section 2.7.3. Under all four conditions, SR-SIM microscopy revealed 6 staining patterns: uniform staining, polar staining, side wall staining, polar and septal staining, strong and weak pole staining and uneven staining (Figure 3.23-A).

Beijing cells cultured in 7H9 had the highest proportion of cells with uniform staining and strong staining at the poles with starved Beijing cells resuscitated in media also displaying a similar phenotype (Figure 3.29-B). A closer look at the incorporation of the metabolic TADA probe in 10% of the bacterial population is represented in figure 3.30 and confirms the strong incorporation of the probe at the cell poles. Starved Beijing bacteria resuscitated in CF displayed a mixture of uniform staining, strong polar staining and a portion of uneven staining. A closer look of the incorporation of the metabolic TADA probe in 10% of the bacterial population represented in figure 3.30 confirmed that Beijing bacteria cultured in CF have strong incorporation of the TADA probe at mid-cell of the bacterium whilst starved Beijing cells resuscitated in CF had a strong interaction of the TADA probe along the side wall of the bacterium, but the distribution of probe incorporation was uneven. These results suggested that bacteria grown and resuscitated in CF have a heterogenous population, with a high metabolic rate, as a result of the growth stimulatory molecules found in CF.

When viewed under the microscope, starved Beijing cells were significantly shorter (p-value ≤ 0.0001) compared to an exponentially grown Beijing culture. When these starved bacteria were resuscitated in media, the cell length increased slightly, nonetheless the bacteria were still significantly shorter (p-value ≤ 0.01) compared to an exponentially grown Beijing culture. However, when the starved bacteria were resuscitated in CF, the cell length was restored to that of an exponentially grown culture (Figure 3.29-C). These results compared well to the laboratory strain (H37Rv) tested under the same conditions.

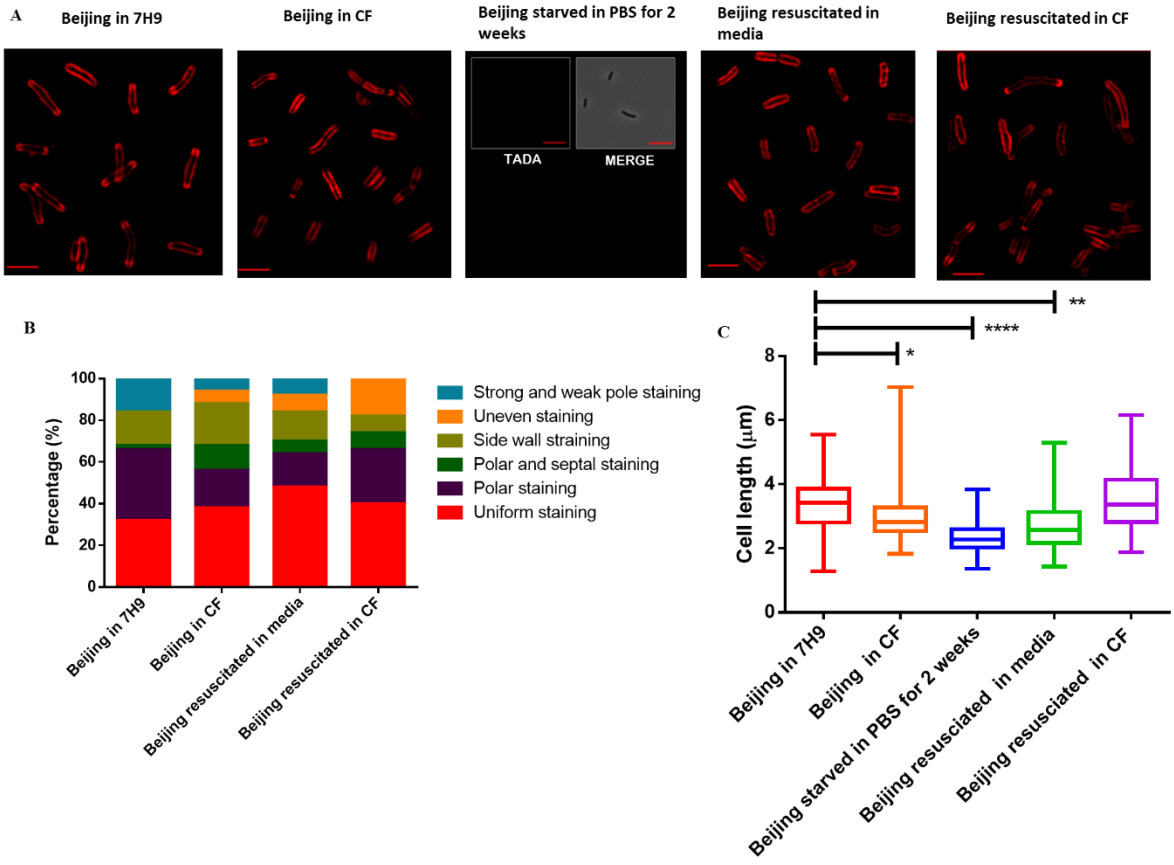


Figure 3.29 Cytological profiling of Beijing strain analysed by fluorescent microscopy. Beijing samples grown in 7H9 with CF, starved in PBS and resuscitated in media and CF were viewed under the microscope, using SR-SIM. Scale bare represents 2 µM. **B-** Distribution of the six staining patterns in cells resuscitated in CF and media after 7 days. Samples were incubated for 24 hrs with the TADA probe at 37°C. Starved Beijing cells resuscitated in CF and media samples were compared to Beijing grown in 7H9 to an OD_{600nm} (0.5- 0.8). One hundred cells per sample (experiment done in triplicate) were analysed for staining using a SR-SIM fluorescent microscope. **C-** Box and whisker plots showing the length of Beijing cells starved in PBS, starved Beijing cells resuscitated in media and CF compared to Beijing cells grown in 7H9. Mean and quartile ranges are shown, Beijing cells starved in PBS and resuscitated in media were significantly shorter (p-value ≤0.0001and p-value ≤0.01 respectively), whilst starved Beijing cells resuscitated in CF, had a similar cell length compared to cells grown in 7H9, using a one-way ANOVA statistical test (*= p-value ≤0.05, **= p-value ≤0.01 and ***= p-value ≤0.001).

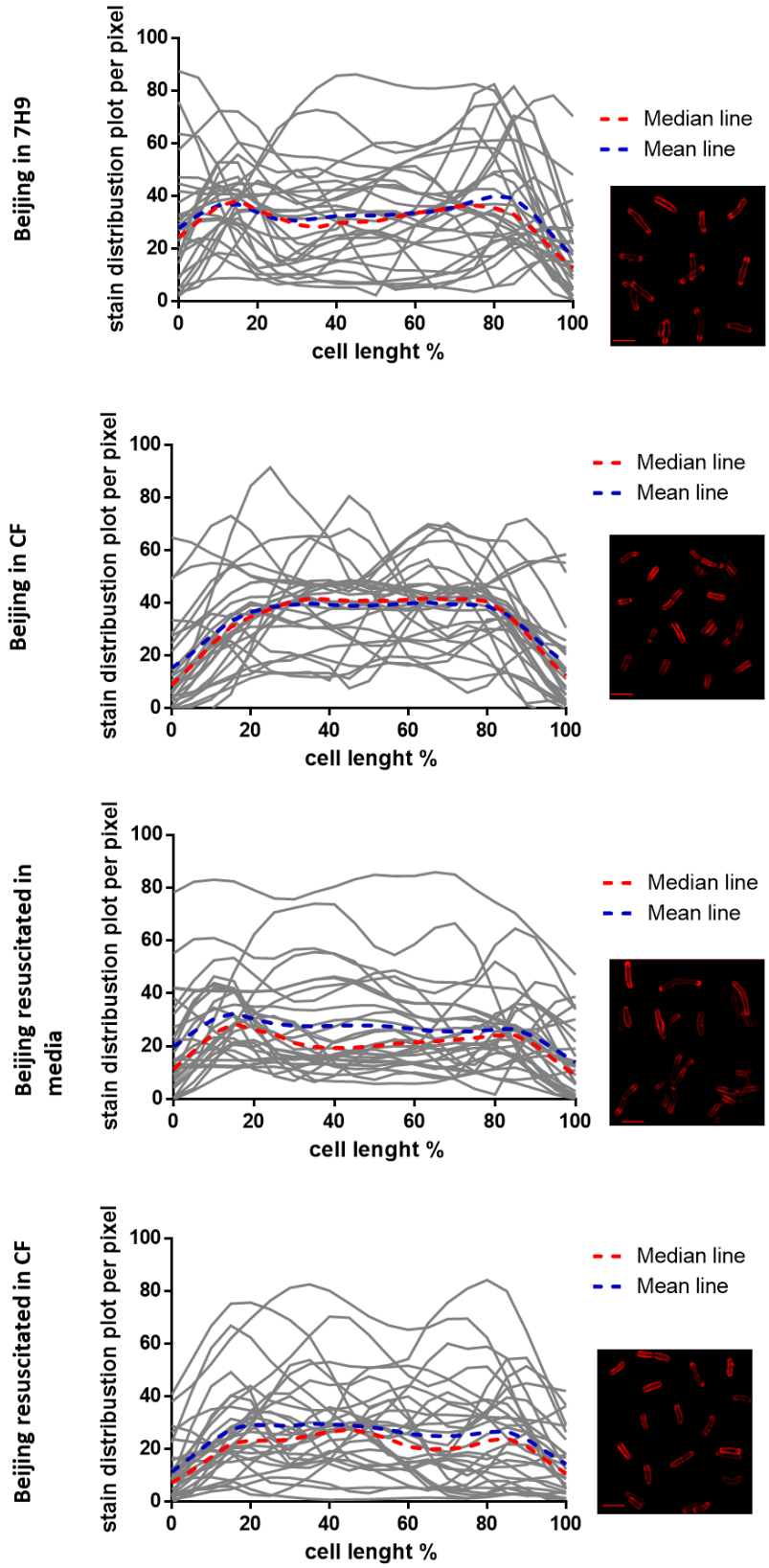


Figure 3.30 Incorporation of the metabolic probe along the side wall in Beijing cells- Staining distribution plots, 10% of the total population of resuscitated bacteria were analysed and compared to an exponentially grown axenic culture using the data from figure 3.29. A mean trend line (blue) and median trend line (red) was calculated on 30 cells to determine general pattern of probe incorporation along the cell wall

LAM cells cultured in 7H9 to exponential phase had the highest proportion of cells with uniform staining and strong staining at the poles, and displayed a similar phenotype to starved LAM cells resuscitated in media (Figure 3.31-B and Figure 3.32). These results were similar to those obtained for the Beijing strain and H37Rv and suggested that bacteria grown or resuscitated in media are actively replicating. LAM cells grown and resuscitated in CF displayed uniform staining and strong staining at the poles whilst starved LAM bacteria resuscitated in CF, displayed large proportions of cell with uniform staining. A closer look of the incorporation of the metabolic TADA probe in 10% of the bacterial population represented in figure 3.32 confirmed that LAM bacteria cultured in media has a strong interaction of the TADA probe at the poles of the bacterium whilst LAM bacteria cultured and resuscitated in CF also had a strong interaction of the TADA probe at the mid-cell of the bacterium. These results were in parallel to the data obtained for the Beijing strains, suggesting that LAM and Beijing bacteria grown and resuscitated with CF are metabolically active.

Starved LAM cells were not significantly shorter (p-value=0.07) compared to an exponentially grown LAM culture. However, LAM cells grown in CF were significantly shorter (p-value $\leq$0.01) but the cell length increased slightly (p-value $\leq$0.05) when these starved bacteria were resuscitated with media, compared to the exponentially grown LAM culture. However, when the starved bacteria were resuscitated in CF, the cell length was restored to that of an exponentially grown culture (Figure 3.31-C). These results were in contrast to Beijing and H37Rv, suggesting strain-specific effects. However, the LAM strains grown in 7H9 had a lower median cell length (2.53µM) when compared to Beijing cultured in 7H9 (3.48µM) and H37Rv cultured in 7H9 (3.65µM). This decrease in cell length may be attributable to the reduction in growth rate described in results section 3.4.1.1 and depicted in figure 3.4.2.

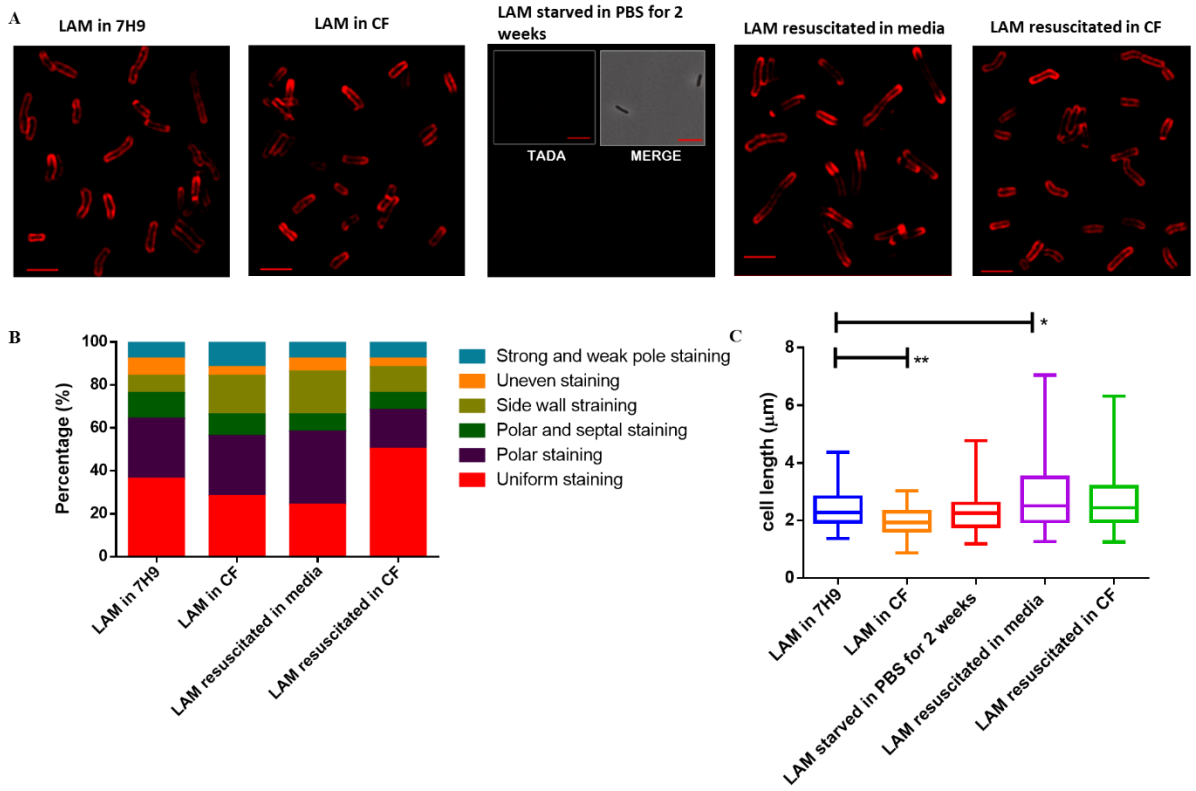


Figure 3.31 Cytological profiling of LAM strain analysed by fluorescent microscopy. LAM samples grown in 7H9, in CF, starved in PBS, resuscitated in media and CF were viewed under the microscope, using SR-SIM. Scale bar represents 2 µM. **B-** Distribution of the six staining patterns in CF and media after 7 days. Samples were incubated for 24 hrs with the TADA probe at 37°C. Starved LAM cells resuscitated in CF and media samples were compared to LAM grown in 7H9 to an OD_{600nm} (0.5- 0.8). One hundred cells per sample (experiment done in triplicate) were analysed for staining using SR-SIM fluorescent microscope. **C-** Box and whisker plots showing the length of LAM cells starved in PBS, starved LAM cells resuscitated in media and CF compared to LAM cells grown in 7H9. Mean and quartile ranges are shown, LAM cells starved in PBS were not significantly (p-value=0.07) shorter, whilst LAM cells cultured in CF were significantly shorter when compared to cells grown in 7H9. LAM cells resuscitated in media were significantly longer compared to cells grown in 7H9. All analysis done using a one-way ANOVA statistical test (* =p-value ≤0.05, **=p-value ≤0.01 and ***= p-value ≤0.001).

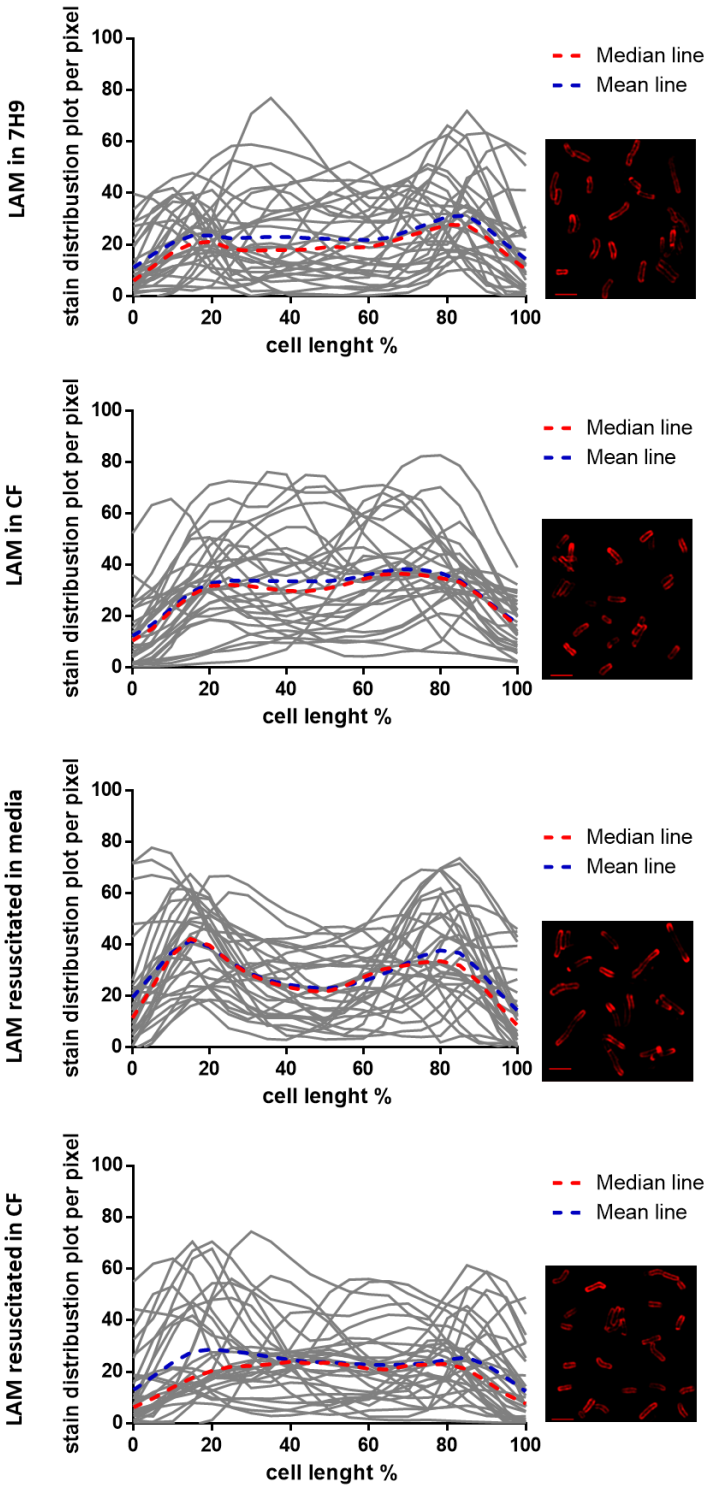


Figure 3.32 The incorporation of the metabolic probe along the cells wall in LAM cells- Staining distribution plots, 10% of the total population of resuscitated bacteria were analysed and compared to an exponentially grown axenic culture using the data from figure 3.31. A mean trend line (blue) and median trend line (red) was calculated to determine general pattern of probe incorporation along the cell wall.

3.4.4. The effect of clinical Beijing and LAM culture filtrate on the resuscitation of DCTB.

Previous results indicated that the number of bacteria resuscitated from clinical isolates, was lower than that seen in the carbon starvation model. This suggested that clinical strains need additional growth factors in order to shift from DCTB to actively growing bacteria. Our results from section 3.4.2 indicated that CF generated from the laboratory strain (H37Rv) improved resuscitation of DCTB bacteria in clinical isolates. However, it was hypothesised that the addition of culture filtrate from the cognate clinical isolates would further enhance the resuscitation of DCTB. Unpublished data from the CBTBR has shown that the addition of CF to MGITs, decreased time to positivity (TTP) in HIV infected patients with low bacterial loads (Amanda Mclvor, manuscript in progress). Therefore, we decided to use this method on starved H37Rv to determine whether CF from the Beijing or LAM strains would improve detection of DCTB. To evaluate this hypothesis, CF from all five Beijing and LAM strains was prepared following the protocol described in material and methods section 3.2.1.2. The CF from the different clinical isolates was added in a 1:1 ratio to mycobacterial growth indicator tubes (MGIT) following the protocol described in materials and method section 2.9.1 and graphically depicted in figure 3.33-A. To the MGIT tubes, starved H37Rv (produced following the protocol described in materials and method section 2.5.1) was added and incubated in a MGIT BACTEC 960 until it flagged positive.

Overall, CF from clinical isolates of Beijing and LAM strains decreased time to positivity (TTP) in starved H37Rv in MGIT culture (shown by a lower value on Figure 3.33-B) compared to MGIT tubes supplemented with media and H37Rv-CF. MGIT tubes supplemented with CF from Beijing 1 and Beijing 2 significantly decreased (p-value ≤ 0.05 and p-value ≤ 0.001, respectively) TTP of starved cells compared to MGIT tubes containing normal media, using a one-way ANOVA statistical test. This suggested that either Beijing 1 or 2 CF could be used to further resuscitate clinical isolates. While the MGIT tubes supplemented with CF from LAM 1 and LAM 5 also significantly reduced TTP (p-value ≤ 0.05) of starved cells when compared to MGIT tubes containing media, using a one-way ANOVA statistical test. This suggested that either LAM 1 or LAM 5 could also be used to further resuscitate clinical isolates. Therefore, we selected Beijing 2 and LAM 5 strains, for all further experiments. A sample of exponentially grown axenic culture of H37Rv was assessed for TTP in MGITs supplemented with media, H37Rv-CF, Beijing-CF and LAM-CF. Results showed that CF had no effect on TTP in

exponentially grown clinical isolates and the effect was only seen with starved DCTB (Supplementary Figure C-4)

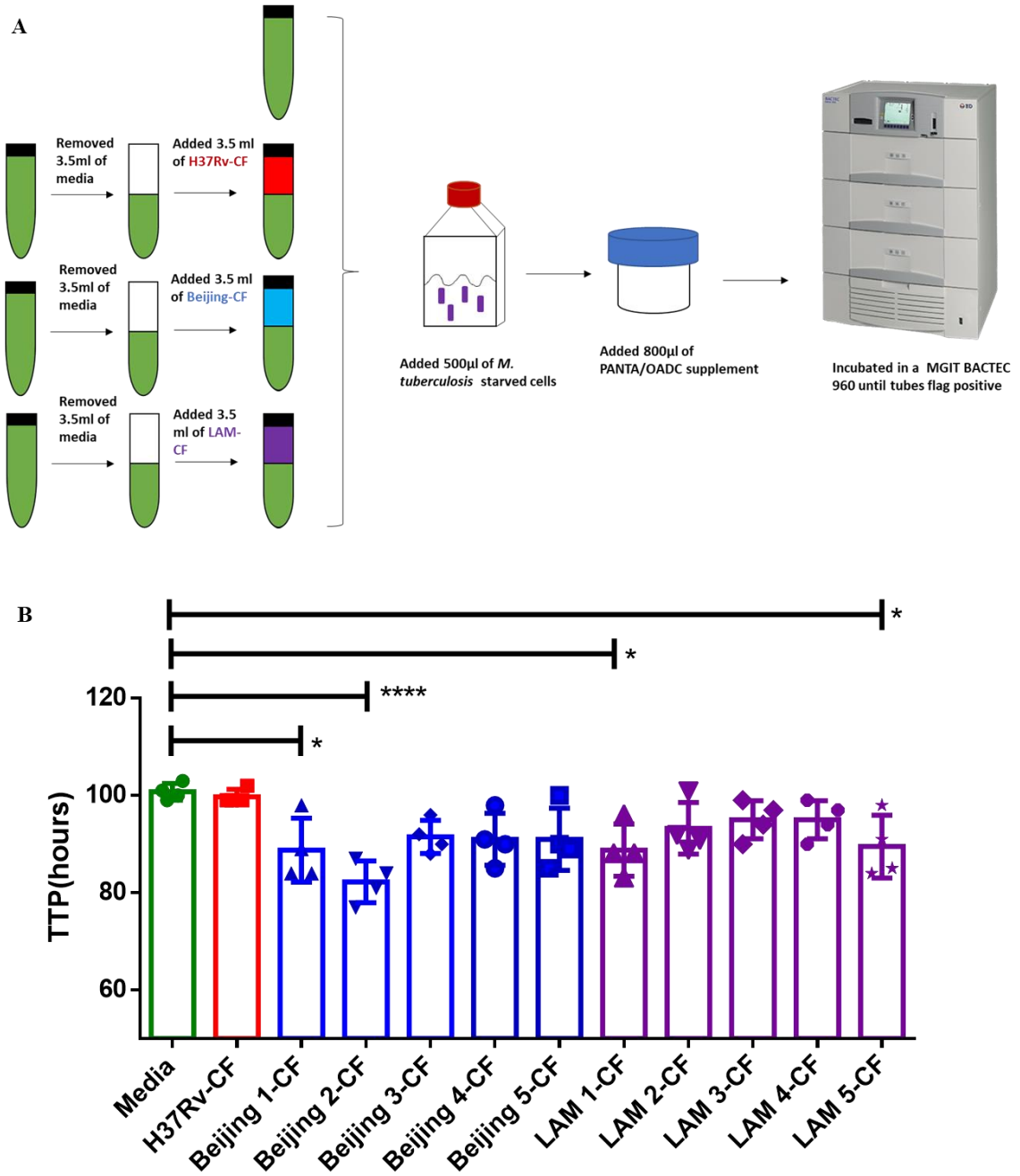


Figure 3.33 Addition of clinical CF decreases TTP in starved H37Rv bacteria A- A schematic representation of the procedure followed to supplement MGIT tubes with CF from clinical isolates. Media noted in green, H37Rv-CF supplementation is noted in red, Beijing-CF supplementation in noted in blue and LAM-CF supplementation is noted in purple. **B**- Graphs showing the TTP of starved H37Rv supplemented with CF from 5 Beijing strains and 5 LAM strains compared to media and CF from H37RV to determine optimal resuscitation with the respective CFs. CF from Beijing 1, Beijing 2, LAM 1 and LAM 5 significantly decreased TTP compared to media and CF from H37Rv using a one-way ANOVA statistical test (* =p-value ≤0.05, **= p-value≤0.01 and ****= p-value≤0.0001).

Since, the carbon starvation model robustly generated DCTB in clinical strains, the methodology was tested for the effect of CF on the resuscitation of DCTB in Beijing, LAM and H37Rv using the protocol described in materials and method section 2.3.1.1. and graphically depicted in figure 3.34-A. CF from H37Rv, Beijing 2 and LAM 5 was used to supplement 7H9 media, following the procedure described in materials and methods section 2.5.2 and graphically depicted in figure 3.34-A. Due to time constraints H37Rv and Beijing strains were resuscitated with CF from Beijing 2 and H37Rv and LAM strains were resuscitated with CF from LAM 5.

A sample of exponentially grown axenic culture of Beijing, LAM and H37Rv strains prior to starvation were assessed for the presence of DCTB bacteria as controls. All strains contained no DCTB bacteria, when resuscitated with Beijing-CF and LAM-CF (Supplementary figure C-2 & C-3). DCTB from starved Beijing and H37Rv strains were detected at higher levels when resuscitated in Beijing 2-CF (Figure 3.34-B). Interestingly DCTB from starved LAM strains showed no change in recovery of DCTB when resuscitated with LAM5-CF. Analysing each strain individually showed that Beijing 2-CF significantly improved the detection of DCTB in Beijing 1 and Beijing 4 strains, using a two-way ANOVA statistical test (p-value ≤ 0.001 and p-value ≤ 0.05 respectively). Overall, there was a significant increase in Beijing CF-dependant resuscitation compared to H37Rv-CF dependant and CF-independent resuscitation between Beijing strains and H37Rv stains, using statistical t-test as depicted in Figure 3.34-D (p-value ≤ 0.05). These results suggested that the addition of Beijing-CF to Beijing strains cultured in carbon depleted media improved the detection of DCTB. Further work needs to be done to investigate if the addition of Beijing-CF will improve detection of DCTB in non-Beijing strains.

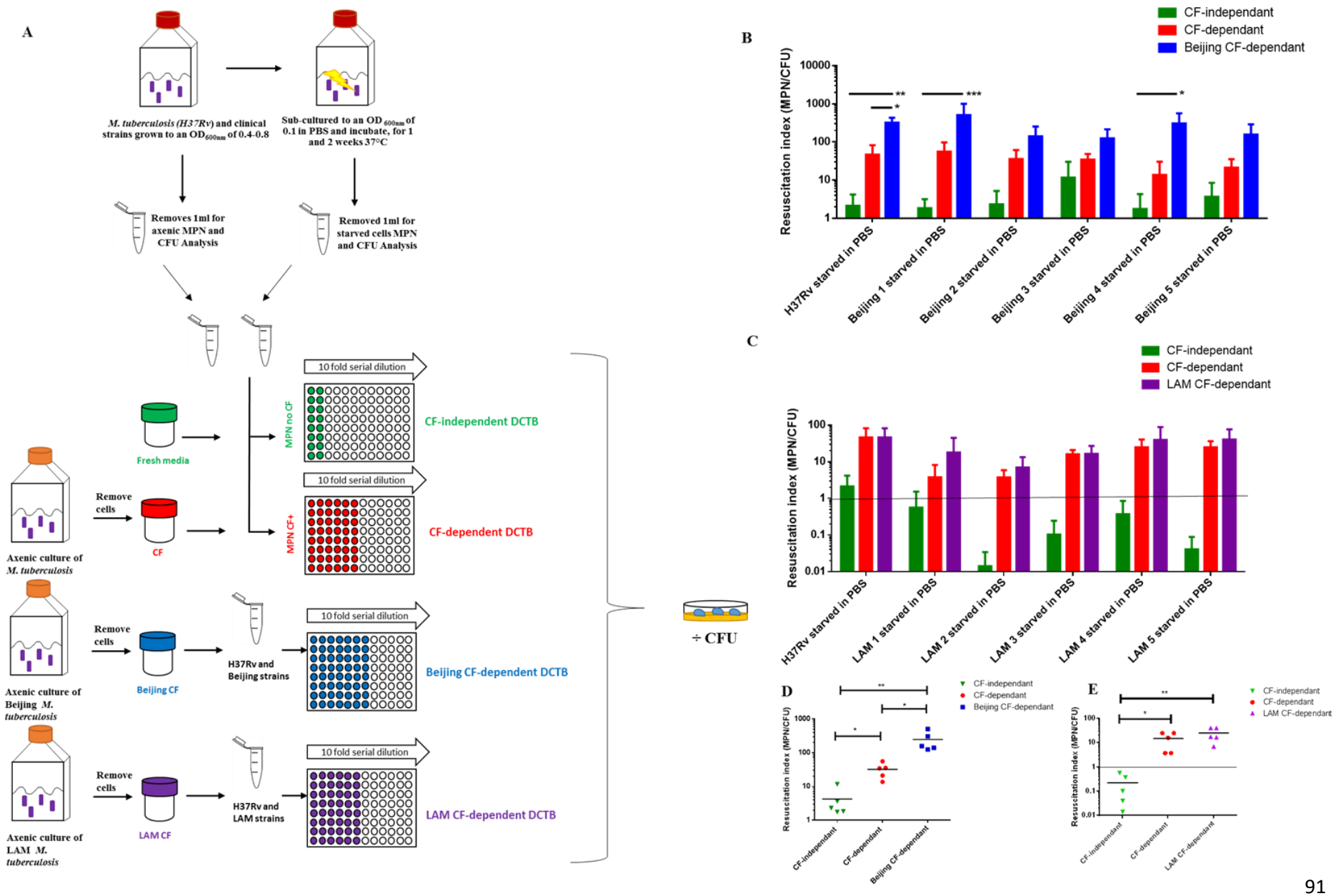

A
M. tuberculosis (H37Rv) and clinical strains grown to an OD600nm of 0.4-0.8
Sub-cultured to an OD 600nm of 0.1 in PBS and incubate, for 1 and 2 weeks 37°C
Removes 1ml for axenic MPN and CFU Analysis
Removed 1ml for starved cells MPN and CFU Analysis
Fresh media
MPN no CF
10 fold serial dilution
CF-independent DCTB
Remove cells
CF
MPN CF+
10 fold serial dilution
CF-dependent DCTB
Axenic culture of M. tuberculosis
Remove cells
Beijing CF
H37Rv and Beijing strains
10 fold serial dilution
Beijing CF-dependent DCTB
Axenic culture of Beijing M. tuberculosis
Remove cells
LAM CF
H37Rv and LAM strains
10 fold serial dilution
LAM CF-dependent DCTB
Axenic culture of LAM M. tuberculosis
÷ CFU
B
CF-independant
CF-dependant
Beijing CF-dependant
Resuscitation index (MPN/CFU)
H37Rv starved in PBS
Beijing 1 starved in PBS
Beijing 2 starved in PBS
Beijing 3 starved in PBS
Beijing 4 starved in PBS
Beijing 5 starved in PBS
C
CF-independant
CF-dependant
LAM CF-dependant
Resuscitation index (MPN/CFU)
H37Rv starved in PBS
LAM 1 starved in PBS
LAM 2 starved in PBS
LAM 3 starved in PBS
LAM 4 starved in PBS
LAM 5 starved in PBS
D
CF-independant
CF-dependant
Beijing CF-dependant
Resuscitation index (MPN/CFU)
E
CF-independant
CF-dependant
LAM CF-dependant
Resuscitation index (MPN/CFU)

Figure 3.34- Beijing-CF enhances the resuscitation of DCTB from Beijing strains A-Schematic of the carbon starvation model and MPN assays used. Yellow light bolt represents the stress of starving bacteria in PBS for 2 weeks. Media is noted in green, H37Rv-CF supplementation is noted in red, Beijing-CF supplementation to media is noted in blue and LAM-CF supplementation to media is noted in purple **B**-Resuscitation index of Beijing strains starved in PBS for 2 weeks compared to H37Rv starved in PBS, with resuscitation in media, H37Rv-CF and Beijing CF. H37Rv and Beijing strains were resuscitated with CF from Beijing 2. Resuscitation index was calculated using the MPN/CFU ratio. The experiment was done in triplicate and starved Beijing 1, Beijing 4 and H37Rv cells resuscitated in Beijing-CF detected significantly more DCTB compared to starved cultures resuscitated in media and H37Rv-CF, using a two-way ANOVA statistical test (*= p-value ≤0.05, **=p-value ≤0.01 and ***=p-value ≤0.001). **C**- Resuscitation index of LAM strains starved in PBS for 2 weeks compared to H37Rv starved in PBS, with resuscitation in media, H37Rv-CF and LAM-CF. H37Rv and LAM strains were resuscitated with CF from LAM 5. The experiment was done in triplicate and starved LAM strains showed no significant resuscitation of DCTB compared to starved cultures resuscitated in media and H37Rv-CF, using a two-way ANOVA statistical test. **D**- Grouped analysis based on panel B, comparing the effect of the different CF's in all the Beijing strains **E** -Grouped analysis based on panel C, comparing the effect of the different CF's on all the LAM strains. Grouped analysis showed that both Beijing and LAM strains resuscitated significantly more bacteria when CF was present compared to CF-independent DCTB. However, Beijing-CF significantly resuscitated more DCTB compare to both media and H37RV-CF.

3.4.5. The resuscitation capacity of clinical CF to change time to positivity in starved *M. tuberculosis* strains

Previous results from section 3.4.3 indicated that the number of bacteria resuscitated from clinical isolates, detected was higher in H37Rv-CF, Beijing-CF and LAM-CF compared to media. Therefore, it was hypothesised that the addition of Beijing-CF and LAM-CF to MGIT tubes will increase the TTP in starved Beijing and LAM clinical strains. To evaluate this hypothesis, Beijing-CF, LAM-CF and H37Rv-CF were purified following the protocol described in material and methods section 2.5.2. The various CFs from the clinical isolates were added to MGIT tubes in a 1:1 ratio following the protocol described in materials and method section 2.8.1 and graphically depicted in figure 3.35-A. To the MGIT tubes, starved H37Rv, Beijing and LAM strains (produced following the protocol described in materials and method section 2.5.1) was added and incubated in MGIT BACTEC 960 the until a positive result was obtained.

A sample of exponentially grown axenic culture of Beijing, LAM and H37Rv strains was assessed for TTP in MGITs supplemented with media, H37Rv-CF, Beijing-CF and LAM-CF. Results showed that CF had no effect on TTP in exponentially grown clinical isolates (Supplementary Figure C-5). Analysing each strain individually showed that Beijing 2-CF significantly decreased TTP in Beijing 2 and Beijing 4 strains starved in PBS, using a two-way ANOVA statistical test, the TTP increased with Beijing 1 (Figure 3.35-B). Overall there was a significant decrease in TTP when starved Beijing and H37Rv strains were cultured with Beijing-CF compared to H37Rv-CF, using statistical t-test as depicted in figure 3.35-D. LAM

5-CF significantly increased the TTP in LAM 4 starved in PBS and significantly decreased TTP in H37Rv starved in PBS (Figure 3.35-C). Overall, there was no difference in TTP when LAM and H37Rv strains were cultured with LAM-CF, using a statistical t-test as depicted in figure 3.35-E. These results suggested that the addition of Beijing-CF to Beijing strains cultured in carbon depleted media, improved detection of DCTB. Further work needs to be done to investigate if the addition of Beijing-CF will improve TTP and detection of DCTB in non-Beijing strains.

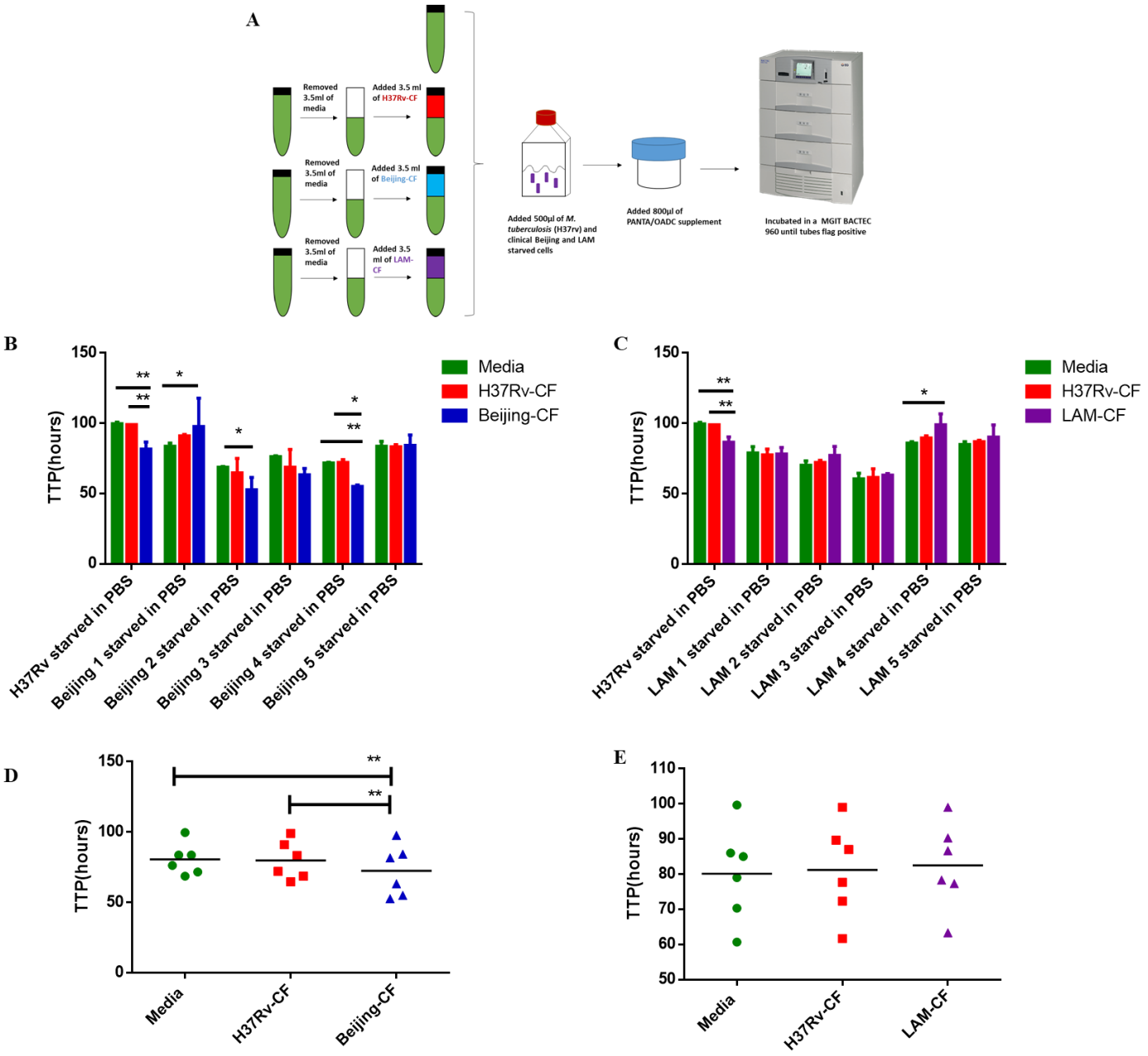


Figure 3.35 Addition of Beijing-CF decreases TTP in starved Beijing bacteria A- A schematic representation of the procedure followed to supplement MGIT tubes with CF from clinical isolates. Media noted in green, H37Rv-CF supplementation is noted in red, Beijing–CF supplementation in noted in blue and LAM supplementation is noted in purple. **B**- Graphs showing the TTP of 5 clinical Beijing isolates supplemented with H37Rv-CF and Beijing-CF compared to media. Beijing 2 and Beijing 4 showed a significant decrease in TTP when supplemented with Beijing- CF, using a two-way ANOVA statistical test (*p-value ≤0.05, **p-value≤0.01 and ***p-value≤0.001). **C**- Graphs showing the TTP of 5 clinical LAM isolates supplemented with H37Rv-CF and LAM-CF compared to media. LAM 4 showed a significant increase in TTP when supplemented with LAM-CF, however H37Rv showed a significant decrease in TTP when supplemented with LAM-CF, using a two-way ANOVA statistical test. **D**- Grouped analysis based on panel B, comparing the effect of media, H37Rv-CF Beijing- CF's on TTP in starved Beijing strains **E** -Grouped analysis based on the panel C, comparing the effect of media, H37Rv-CF and LAM-CF on TTP in starved LAM strains.

4. Discussion

Culturability has traditionally been defined as the growth of colonies on an agar plate (Pienaar, Singh, & Barnard, 2016; Bamford et al., 2017). However, in 2010 Mukamolova and colleagues described that 80 to 99.9% of viable *M. tuberculosis* in the sputa were undetectable by a standard agar plate assay (Mukamolova, Turapov, Malkin, Woltmann, & Barer, 2010). There are two possible explanations for this observation: (1) either the deficiency in culturability is a result of damage that the organism encounters during pathogenesis and expectoration and is unable to establish growth or (2) the DCTB state may be the result of metabolic changes associated with non-culturability providing the organism with a selective advantage allowing it to be protected from the host immune system until conditions are favourable (Chengalroyen et al., 2016; Kim et al., 2018; Mukamolova et al., 2010). Multiple studies provide evidence for the second hypothesis, illustrating that the previously hidden population of bacteria that cannot be detected on solid media can be detected in liquid media or in the presence of CF (Chin et al., 1995; Kana & Mizrahi, 2010; Rosser, Stover, Pareek, & Mukamolova, 2017; Rubin, 2018). At present, little is known about the metabolism of DCTB and it is hypothesized that conditions within granulomas lead to the establishment of these heterogeneous populations (Actor et al., 2008; Ayrapetyan et al., 2015; Chao & Rubin, 2010).

The physiology of *M. tuberculosis* is diverse and complex which creates a large number of challenges for scientists trying to unravel the biology of DC bacteria (Gibson et al., 2018; Kato et al., 2008; Lipworth et al., 2016). Mycobacteria continuously adapt to changes in their environment, as the basic requirements for growth are not always accessible (Actor et al., 2008; Baker & Abramovitch, 2018; Betts et al., 2002; Glickman & Jacobs, 2001). Therefore, in these instances, many bacteria have developed the "cellular quiescence" survival strategy in order adapt to growth limiting conditions (Actor et al., 2008; Anuchin et al., 2009; Bloom et al., 2017). Once exposed to the stress conditions, the majority of the bacterial population reduce their growth and enter a viable but not culturable (VBNC) state, with the exception of "scout cells" (Buerger et al., 2012). The scout cells are differentiated from the remaining population as they have nominal metabolic activity, and do not undergo morphological differentiation into the VBNC state (Buerger et al., 2012; Honeyborne et al., 2016; Kim et al., 2018). Scout bacteria are adept in sensing and adapting to their environmental conditions and are responsible for the revival of the bacterial population once environmental conditions become favourable again (Buerger et al., 2012; Dietrich et al., 2015). Thus, laboratory models that establish this DC state

are important for studying these bacteria to ultimately develop new diagnostic tests for detection and methods to eradicate these bacteria.

4.1 Optimization of nutrient depletion models

To model the conditions within the granuloma, the following conditions need to be mimicked: hypoxia, nutrient deprivation, limited carbon sources and high concentration of nitric oxide (Alnimr, 2015; Betts et al., 2002; Bhatt & Salgame, 2007; Glickman & Jacobs, 2001; Honeyborne et al., 2016). There are several *in vitro* models in the literature which describe the induction of the differentially culturable (DC) state. Most of these models have been shown to induce a non-replicating state in mycobacteria that are morphologically and metabolically distinct (Betts et al., 2002; Ojha et al., 2008; Saito et al., 2017; Salina et al., 2014). Consistent with this, *M. tuberculosis* isolated from the granuloma of infected patients have a different morphology compared to bacteria grown *in vitro* and nutrient starved bacteria have a similar morphology to mycobacteria found in sputum (Keane et al., 2000; Lipworth et al., 2016). In this study three nutrient limiting *in vitro* models were tested for the induction of DC bacteria including: carbon starvation, biofilm formation and potassium depletion *in M. smegmatis*. During optimization of each of the models, the bacteria produced had to (1) induce differentially culturable bacteria (2) have a reduced metabolic function and (3) display a change in the morphology.

From the three nutrient limiting models optimized, the biofilm model did not meet any of the above criteria. Bacteria analysed from biofilms were not in a DC state, suggesting that the environmental stress within the biofilm is insufficient to induce the DC state. Research has shown that the oxygen concentrations at the biofilm-fluid interface is approximately 40% (Brennan, 2017; Esteban & García-Coca, 2018) and mycobacteria enter a non-replicating state only under 0.01% oxygen, as described in the Wayne model (Wayne & Hayes, 1996) suggesting that the reduced oxygen levels and depletion of nutrients in the biofilm do not appear low enough to induce non-replicating bacteria. However, when biofilms were treated with RIF, there was an increase in DC bacteria. This increase is likely related to the precedent for ribosome-binding drugs to differentially affect the proteome of the bacteria rather than block protein synthesis (Polikanov, Aleksashin, Beckert, & Wilson, 2018). Furthermore, the bacteria from the biofilm had reduced metabolic activity with only 50% of bacteria incorporated the metabolic probe.

Bacteria cultured in potassium depleted media, produced a significant amount of differentially culturable bacteria with reduced metabolic activity, suggesting that growth under these conditions generated non-replicative bacteria. Under these conditions Salina and colleagues observed ovoid shaped bacteria however, our results indicated that the cell length decreased but the bacteria still maintained the rod shape (Salina et al., 2014). A study by Ioerger and colleagues showed genetic variation of laboratory strains in different geographical locations (Ioerger et al., 2010). This genetic variation amongst laboratory strains could provide a possible explanation to the absence of an ovoid shape phenotype observed in potassium depleted bacteria from our laboratory. However, further investigations need to be done to confirm this hypothesis. In addition, bacteria cultured in potassium depleted media were tolerant to INH and BTZ antibiotics which target cell wall biosynthesis pathways but were sensitive to RIF (Salina et al., 2014). This suggests that potassium depletion induces reduce metabolic activity and cell length in order for the mycobacteria to survive adverse conditions. In this study, the antibiotic tolerance of potassium depleted cells to INH and BTZ was not tested. Therefore, further investigation of these rod-shaped bacteria generated in this study, would improve our understanding on their tolerance to INH and BTZ.

Using the carbon starvation model, we were able to robustly generate DCTB in the laboratory strain (H37Rv) and study the resuscitation of the starved bacteria in both media and CF. The bacteria cultured in carbon depleted media enter a starvation induced resting state. In other work, this non-replicative state is characterised by reduced ATP concentration, reduced oxygen consumption, and increased survival under anaerobiosis (Betts et al., 2002; Dietrich et al., 2015; Wu et al., 2016). In this study metabolism was characterised by the incorporation of a metabolic probe into the cell wall of the bacterium. Our results indicate that bacteria cultured in carbon depleted media have a reduced metabolic activity, which was consistent with the bacteria entering a non-replicative state.

One of the observations in the literature that we were not able to reproduce, was the increased tolerance to antibiotics in bacteria cultured in carbon depleted media. Betts and colleagues noted that nutrient starved *M. tuberculosis* was resistant to both first line TB treatment drug RIF and INH whilst Saito and colleague established a starvation model that included treatment with RIF as a secondary stress (Betts et al., 2002; Saito et al., 2017). A point to note is that the concentration of RIF in both these studies differed. In the Betts model, bacteria cultured in carbon depleted media were resistant to both RIF and INH, at the minimum inhibitory concentration (MIC) of 0.01-0.08 µM, whilst, in the Saito et al. model, RIF at 100X MIC (100

μM) was used. The authors argued that the RIF concentration was increased to reflect impaired uptake of RIF by starved cells or the phenotypic RIF resistance, which results from stress induced protein mistranslations (Saito et al., 2017). In contrast our data indicated that treating starved bacteria with 100 μM RIF resulted in killing of the DC bacteria.

Saito and colleagues speculated that the addition of RIF was important to selectively affect the transcription of different genes, in order to induce the DC state (Saito et al., 2017). Therefore, we tested the effect of lower concentrations of RIF as a secondary stress to starvation to see if we could achieve a similar result. Our results indicated that treatment of starved cells with low concentrations of RIF (25 μM -25X MIC), the starved bacteria were still sensitive to RIF. Our results are in concordance with the observations of Betts and colleagues who showed that starved cells treated with 10X the MIC of RIF showed a 3.5 log drop in CFU (Betts et al., 2002). Taken together our results indicated the decreased CFU after treatment with higher than MIC concentrations of RIF does not induce increased DC bacteria.

We also demonstrated that *M. tuberculosis* cultured in carbon depleted media were significantly shorter compared to an exponentially grown culture. The removal of carbon sources triggered the development of a SMRC morphotype (Wu et al., 2016). The morphological change has been hypothesised to occur as a survival mechanism, that is to decrease permeability and enter a more protective state which, likely contributes to the increased survival of the bacteria in a hostile environment (Wu et al., 2016).

The SMRC morphotype previously described by Wu and colleagues, showed the production of ovoid bacteria in mycobacteria under potassium depleted media and in nitrogen limiting conditions (Anuchin et al., 2009; Salina et al., 2014; Wu et al., 2016). These ovoid shaped cells displayed a VBNC phenotype and when resuscitated in nutrient rich media, restarted growth through a budding pattern (Anuchin et al., 2009). In contrast our results showed that bacteria resuscitated in media and CF, showed regrowth by the incorporation of new cell wall at the poles as is the growth process in mycobacteria (Scanga et al., 1999). No budding regrowth patterns or any other abnormal defects were seen in the resuscitated bacteria. However, the metabolic activity of H37Rv resuscitated in CF was significantly higher compared to an exponentially grown culture. This suggested that resuscitated bacteria are not incorporating the metabolic probe abnormally, but rather at an increased rate.

4.2 Clinical DCTB and disease progression

Beijing strains have been associated with hyper-virulence and increased transmission in the population (Hanekom et al., 2010; Hanekom et al., 2011; Kong et al., 2007; Parwati et al., 2010). However, little is known about their ability to produce DCTB. Therefore, in this study we investigated the propensity of different clinical strains to adopt the DC state using data from two clinical studies (1) BMG phase 1 and (2) MGIT plus, conducted at the Centre of Excellence for Biomedical TB research (CBTBR). Both clinical studies collected and processed treatment naïve sputum samples from South African infected TB-patients for the presence of DCTB and allocating the various samples to the strain type. Using meta-analysis of the data from these two clinical studies we were able to determine that sputum specimens from patients infected with the Beijing strain have an 80% chance of having DCTB bacteria, as well as the highest quantity of DCTB produced compared to other clinical isolates. This suggested that the Beijing stains have a greater propensity to adopt the DC state compared to other clinical strains.

One possible reason for the ability of Beijing strains to produce more DCTB compared to other clinical strains could be due to their increased expression of the Dos regulon. The Dos genes are involved in the adaptive response of the bacterium under hypoxia and stress from reactive nitrogen intermediates, with basal levels of the regulon 50–fold higher in Beijing stains compared to non-Beijing strains (Reed et al., 2007). This increased expression is due to a naturally occurring frameshift mutation in the DosT sensor kinase which results in the appearance of a constitutively active Dos regulon phenotype found in Beijing sublineages, whilst other Beijing sub-lineages have multiple copies of the DosR gene which demonstrate the overexpression phenotype (Reed et al. 2010). Gerasimova and colleagues suggested that increased expression of Dos genes protects the bacteria and poises organisms for survival in the extracellular environment (Gerasimova, Kazakov, Arkin, Dubchak, & Gelfand, 2011). The mechanism surrounding this phenomenon is still unclear. We decided to use the *in vitro* carbon starvation model to assess DCTB production, metabolic activity and cell morphology in clinical Beijing and LAM strains.

Although there is evidence that Beijing strains have greater virulence and transmission potential compared to other clinical strains, it is still strain dependent as there is a high amount of heterogeneity amongst Beijing stains. Therefore, in this study we randomly picked five Beijing strains and five LAM strains for further analysis. The five Beijing and five LAM strains were cultured in carbon depleted media to induce the DC state. Our results indicated that Beijing strains produced more DCTB compared to LAM when cultured under carbon starvation

conditions. Interestingly DCTB produced by both LAM and Beijing strains had increased resuscitation with CF supplementation compared to CF-independent DCTB. The type of resuscitation is important, as spontaneously culturable organisms are normally associated with symptomatic disease whilst differentially culturable bacteria are expected to be associated with asymptotic disease or latent TB infection (Chengalroyen et al., 2016; Mukamolova et al., 2010). This observation suggests that the nutrient deprivation stress exerted on these organisms induces a metabolic shift into a CF-dependent DCTB state (Chengalroyen et al., 2016; Kim et al., 2018).

Furthermore, when the Beijing strains cultured in carbon depleted media were resuscitated using CF from a Beijing strain, there was a significant increase in the number of resuscitated bacteria compared to resuscitation with CF from the laboratory strain (H37Rv). LAM strains cultured in carbon depleted media resuscitated with CF from a LAM strain did not display the same outcome. Collectively these observations indicated that Beijing strains are more adapted to enter and exit the DC state compared to LAM strains and resuscitation of bacteria from the DC state is dependent on growth stimulatory molecules from CF. In addition, the growth stimulatory molecules found in Beijing-CF appear to be more effective in resuscitation of bacteria, compared to H37Rv-CF.

The metabolic profile of Beijing and LAM strains indicated that growth under carbon deplete conditions results in a reduction in metabolic activity consistent with a non-replicative state. However, when these starved bacteria were resuscitated in media, the metabolic activity of the bacteria increased but was not restored to the level of a logarithmic growing culture. Restoration of metabolic activity was only achieved when the bacteria were resuscitated using CF. These observations provided additional evidence that the exit of starved clinical isolates from a non-replicative state requires growth factors from CF. Addition of CF known to contain growth stimulatory molecules, restarted growth by incorporation of new cell wall material at the polar regions in the starved bacteria. There was no difference between LAM and Beijing strains with regards to metabolic activity, or incorporation of the metabolic probe in the cell wall of the bacterium.

4.3 Using CF from clinical strains to improve current diagnosis test

Currently, the gold standard for TB diagnosis is culturing of the bacteria using the MGIT system, which detects the growth of *M. tuberculosis* by measuring oxygen consumption in a tube. The turnaround time of this test is 2-4 weeks, depending on the number of bacteria present, but can also take up to 6 weeks to confirm a positive result. This long duration is problematic and attempts to shorten the detection of TB disease using this system is expected to have benefit, especially in specimens with low bacterial loads. An unpublished study by Mcvlor and colleagues demonstrated that the addition of CF form laboratory *M. tuberculosis* strain (H37Rv) decreased time to positivity in HIV patients with a low bacterial load. Thus, it was hypothesised that the addition of clinical CF to MGIT tubes would have a similar effect with DCTB generated *in vitro*. In order to accomplish this, we supplemented MGIT tubes with clinical CF in a 1:1 ratio and inoculated the tubes with DCTB. The supplementation of Beijing clinical CF to MGITs of starved Beijing strains decreased the TTP. Previous research on Beijing-CF has indicated that the CF contained overexpression of various proteins responsible for metabolism and respiration, lipid metabolism, virulence, detoxification, adaptation, cell wall and cell processes, and conserved hypothetical interacting partners for proteins involved in these pathways (G. Kumar et al., 2017). We speculate that the over expression of these proteins, aid the resuscitation of DCTB to actively growing bacteria with a resultant decrease TTP in clinical strains.

4.4 Limitations and future studies

Literature and our research have shown that there is high range of diversity among clinical isolates of the same strain. Therefore, the analysis of one Beijing strain cannot sufficiently represent the entire population. In future studies we hope to analysis all the Beijing and LAM isolates of this cohort for their metabolic profile and cytology.

Moreover, in this study we used spoligotyping to classify the clinical strains, which has low discriminatory power. Therefore, whole genome sequencing in the future of all 10 clinical isolates could provide detailed insights for the variations observed in the DCTB production amongst the Beijing and LAM isolates. Furthermore, whole genome sequencing will also provide SNP and indel differences between the five Beijing strains, which could explain the observed phenotypical differences.

In addition, the propensity of clinical strains to adopt the DC state was only analysed in drug sensitive isolates, and little has been done on the role of drug resistance in the formation of DC bacteria. It is currently unknown whether stable genetic drug resistance, as displayed by clinically drug resistant strains, affects the ability of *M. tuberculosis* to adopt a DC state. Thus, future studies, will inform whether the propensity of drug resistant clinical strains to generate DCTB is different compared to their drug sensitive counterparts.

4.5 Concluding remarks

Herein we demonstrated that there is a significant relationship between clinical strains and the propensity to produce DCTB. Both experimental and bioinformatics analysis has demonstrated that Beijing strains have greater propensity to produce DCTB compared to LAM strains, however, the mechanistic basis that underpins this is still unknown. The difference in propensity of Beijing and LAM strains to adopt the DC state possibly lies in a combination of transcriptional and metabolic responses that will form the basis of future studies.

5. Appendices

5.1 Appendix A-Materials

Table 1-Culturing media

7H9 (*M. smegmatis*)	4.7 g of 7H9 Difco™ Middlebrook, 10 ml 100X glucose salt (20 g glucose, 8.5 g NaCl dissolved in 100 ml dH_2O autoclaved), 2 ml glycerol and 2 ml 25% Tween®80	Powder was dissolved in 300 ml of dH_2O and the remaining dH_2O and glycerol was added to a total volume of 988ml before the media was autoclaved. The media autoclaved then cooled to 55°C before the Tween®80 and glucose salts were added.
7H9 (*M. tuberculosis*)	4.7 g of 7H9 Difco™ Middlebrook, 100 ml Middlebrook™ oleic acid-albumin-dextrose-catalase (OADC), 2 ml glycerol and 2 ml 25% Tween®80	Powder was dissolved in 300 ml of dH_2O and the remaining dH_2O and glycerol was added to a total volume of 900ml before the media was autoclaved. The media was cooled to 55°C before the Tween®80 and OADC were added. The media was filter sterilised in a stericup
7H10	19 g of 7H10 Difco™ Middlebrook media, 10 ml of 100X glucose salts (GN) and 5 ml of glycerol.	Powder was dissolved in 300 ml of dH2O and the remaining dH2O and glycerol was added to a total volume of 985ml before the media was autoclaved. The media was cooled to 55°C before the Tween®80 and GN were added. The media was poured into plates
7H11	19 g of 7H11 BBL™ Middlebrook media, 100 ml of OADC and 5 ml of glycerol.	Powder was dissolved in 300 ml of dH2O and the remaining dH2O and glycerol was added to a total volume of 900ml before the media was autoclaved. The media was cooled to 55°C before the Tween®80 and OADC were added. The media was poured into plates
Sautons minimal media	0.5 g of KH_2PO_4, 0.5 g of $MgSO_4$, 4 g of L-Asparagine, 2 g of Citric acid, 0.05 g of Ferric Ammonium Citrate and 60 ml of glycerol	All components were dissolved in 800 ml of dH_2O, and the pH of the solution was adjusted to 7.0 with NaOH. Distilled water was added to a total volume of 1 L, and the solution was autoclaved, cooled and, sterile $ZnSO_4$ to a final concentration of 0.1 % w/v was added to the media.
Phosphate buffer saline (1XPBS-Tx)	8 g of NaCl, 0.2 g of KCl, 1.44 g of Na_2HPO_4, 0.24 g of KH_2PO_4 and 2 ml of tyloxapol	All components were dissolved in 800 ml of dH_2O, and the pH of the solution was adjusted to 7.2 with HCl. Distilled water was added to a total volume of 1 L, and the solution was autoclaved, cooled and tyloxapol was added. The media was filtered in a stericup
Potassium depleted Sautons	0.5 g of Na_2PO_4, 0.5 g of $MgSO_4$, 4 g of L-Asparagine, 2 g of Citric acid, 0.05 g of Ferric Ammonium Citrate, 60 ml of glycerol and sterile $ZnSO_4$ to a final concentration of 0.1 % w/v	All components were dissolved in 800 ml of dH_2O, and the pH of the solution was adjusted to 7.0 with NaOH. Distilled water was added to a total volume of 1 L, and the solution was autoclaved, cooled and, sterile $ZnSO_4$ to a final concentration of 0.1 % w/v was added to the media. The media was filtered in a stericup.

Table 2-DNA extraction reagents

Reagent	Components	Description
TE buffer	10 mM Tris-HCl (pH 8), 10 mM EDTA	Dissolved in 500 ml of distilled water and autoclaved
CTAB/NaCl	4.1% NaCl, 10% N-cetl-N,N,N-trimetyl ammonium bromide	Dissolved in 300 ml of distilled water and filter sterilised.

Table 3-Spoligotyping reagents

Reagent	Components	Description
Stock solutions		
10X SSPE	13.7 g sodium di-hydrogen phosphate, 105.19 g sodium chloride. 3.36 g EDTA	All components were dissolved in 900 ml of dH_2O, and the pH of the solution was adjusted to 7.4 with NaOH. Distilled water was added to a total volume of 1 L
10% SDS	50g sodium dodecyl sulphate	Dissolved in 500 ml of distilled water
0.5 M Ethylenediaminetetraacetic acid (EDTA)	93 g EDTA	Dissolved in 500 ml of distilled water
Working solutions		
2x SSPE/0.1%SDS	200 ml of SSPE, 10ml of 10% SDS	All reagents and distilled water were added to a total volume of 1 L
2x SSPE/0.5%SDS	200 ml of SSPE, 20ml of 10% SDS	All reagents and distilled water were added to a total volume of 1 L
1% SDS	20 ml of 10% SDS	Added to distilled water to a volume of 200 ml
20 mM EDTA	20 ml of 0.5M EDTA	Added to distilled water to a volume of 500 ml

Table 4- Spoligotyping materials

Product	Supplier
Spoligotyping membrane	Mapmygemone (Hyderabad, India)
Spoligotyping primers (DRa and DRb)	Mapmygemone (Hyderabad, India)
Streptavidin	GE Healthcare
ECL detection kit	GE Healthcare

Table 5- Flow cytometry and Microscopy

Reagent	Components	Description
2.5% Glutaraldehyde	25% Glutaraldehyde (SIGMA-G5882)	Diluted to 2.5% in PBS

PBS	8 g of NaCl, 0.2 g of KCl, 1.44 g of Na_2HPO_4, 0.24 g of KH_2PO_4	All components were dissolved in 800 ml of dH_2O, and the pH of the solution was adjusted to 7.2 with HCL. Distilled water was added to a total volume of 1 L, and the solution was autoclaved

5.2 Appendix B – Bioinformatics and software used for data analysis

Table- Software used for data analysis

Program	Description
Graphpad prism statistical tool (version 6)	GraphPad prism 6 is a data management and analysis software. This software was used to construct graphs and figures for data analysed in this study. Additionally, it was used for statistical analysis to compare statistically significant differences between data groups (http://www.graphpad.com/scientificsoftware/prism/)
Zen black and blue software	Zen software is an image processing application linked to the Zeiss microscope. This software was used for the analysis of microscope images taken from the Zeiss Elyra super-resolution fluorescence confocal microscope.
Image J (Fiji)	Fiji software is an open source image processing package. This software was used for analysis of microscope images taken using the Zeiss or Nikon fluorescence microscope (http://imagej.net/Fiji)
CytExpert	CytExpert is a data processing application linked to the cytoflex flow cytometer. This software was used for the analysis and gating of data generated from the cytoflex
SPOTCLUST TB	Open access online website used for Tuberculosis evolution and epidemiology mathematical models for genotyping and epidemiological data on infectious diseases. The website was used for the spoligotyping of clinical isolates http://tbinsight.cs.rpi.edu/run_spotclust.html
Most probable number (MPN) calculator (version 2)	The MPN calculator is an open access tool for estimating the population density of viable microorganisms in a test sample. In this study the MPN calculator was used to calculate the total number of bacteria recovered from the MPN assay (available at http://www.wiwiss.fuberlin.de/fachbereich/vwl/iso/ehemalige/wilrich/index.html

5.3 Appendix C –Supplementary Figures

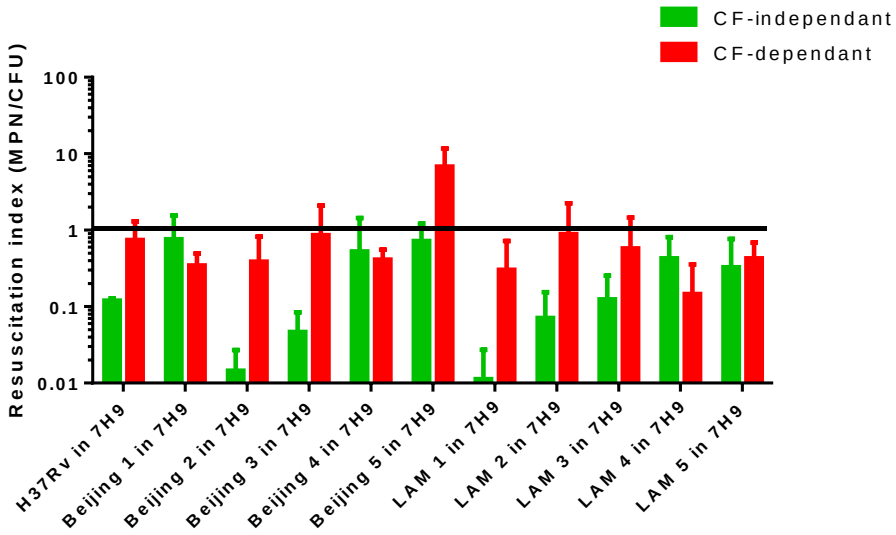


Figure C-1 The exponentially grown cultures of Beijing and LAM strains do not contain DCTB -Beijing and LAM strains exponentially grown to and OD_{600nm} 0.5-0.8 and compared to H37Rv. The bacteria were resuscitated with media and CF, in a 96 well plate. Resuscitation index was calculated using MPN/CFU ratio. The experiment was done in triplicate. The black line represents the threshold for DCTB (resuscitation index greater than 1)

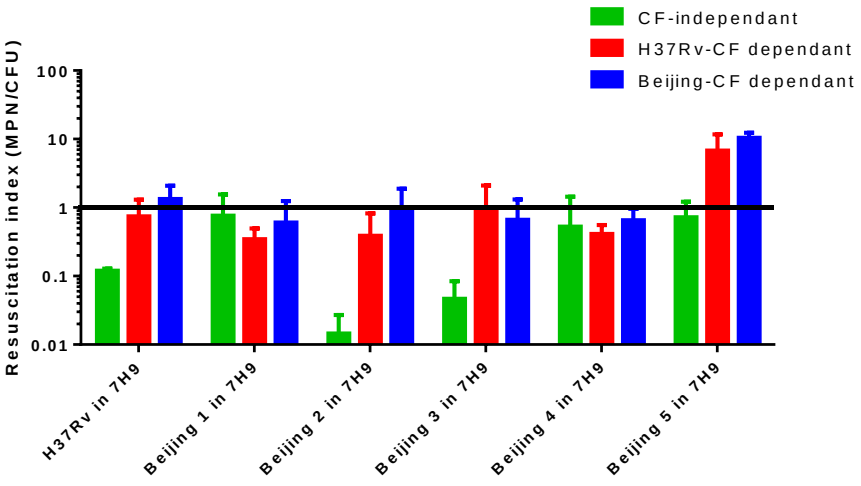


Figure C-2 The exponentially grown cultures of Beijing strains do not contain DCTB, when resuscitated with Beijing CF –Beijing strains exponentially grown to and OD_{600nm} 0.5-0.8 and compared to H37Rv. The bacteria were resuscitated with media, H37Rv-CF and LAM-CF, in a 96 well plate. The resuscitation index was calculated using the MPN/CFU ratio. The experiment was done in triplicate. The black line represents the threshold for DCTB (resuscitation index greater than 1)

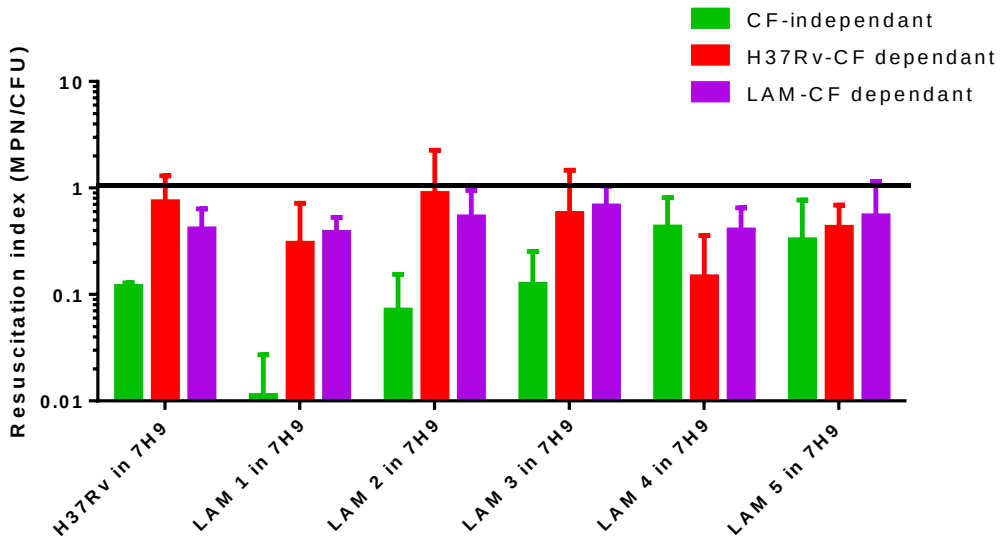


Figure C-3 The exponentially grown cultures of LAM strains do not contain DCTB, when resuscitated with LAM-CF -LAM strains exponentially grown to and OD_{600nm} 0.5-0.8 and compared to H37Rv. The bacteria were resuscitated with media, H37Rv-CF and LAM-CF, in a 96 well plate. The resuscitation index was calculated using the MPN/CFU ratio. The experiment was done in triplicate. Black line represents the threshold for DCTB (resuscitation index greater than 1)

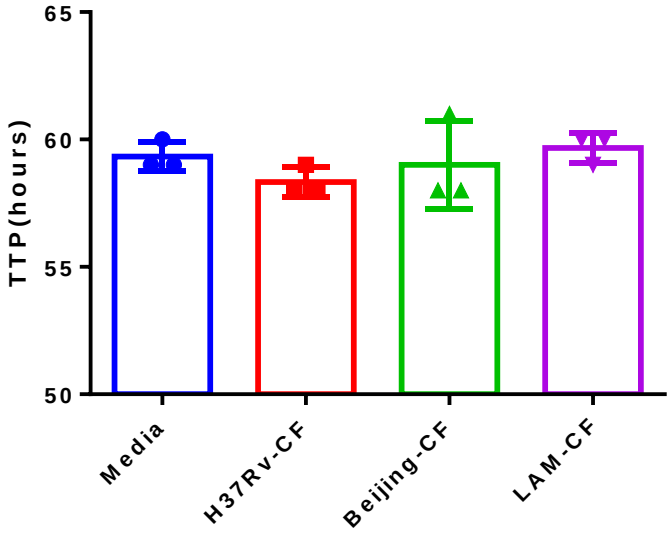


Figure C-4 Addition of clinical CF has no effect on time to positivity in axenic H37Rv bacteria - Graph showing the time to positivity (TTP) of axenically grown H37Rv supplemented with Beijing-CF and LAM-CF compared to media and H37Rv-CF.

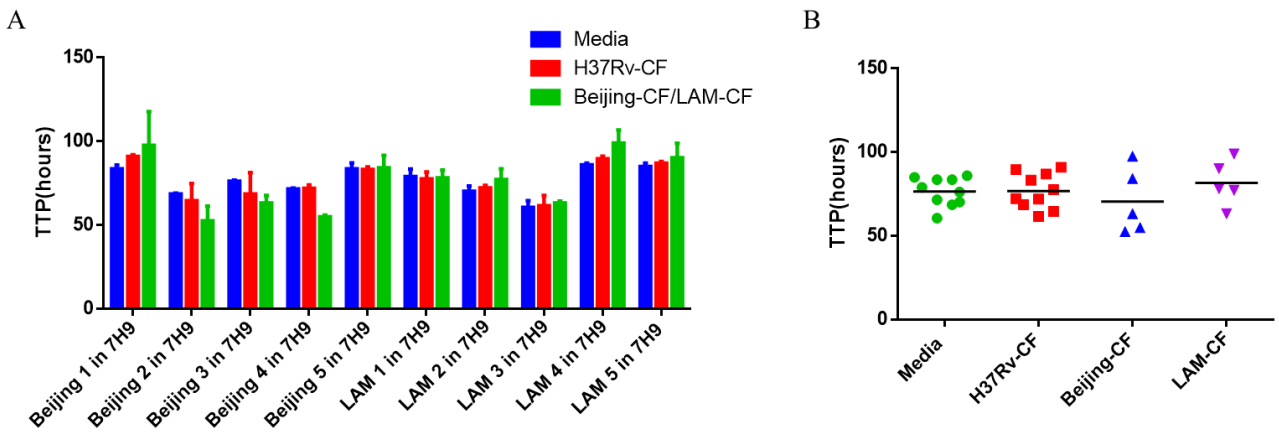


Figure C-5 Addition of clinical CF has no effect on time to positivity in axenic Beijing, LAM and H37Rv strains – A Graph showing the time to positivity (TTP) of axenically grown Beijing, LAM and H37Rv supplemented with Beijing-CF and LAM-CF compared to media and H37Rv-CF. B. Grouped analysis based on panel A comparing the effect of the different CF's in all the LAM strains. Grouped analysis showed that both Beijing-CF and LAM-CF had no effect on TTP

5.4 Appendix D- Ethic certificates

BMG phase 1 renewed ethic certificate

UNIVERSITY OF THE WITWATERSRAND JOHANNESBURG

R14/49 Dr Z Waja and Professor B Kana

HUMAN RESEARCH ETHICS COMMITTEE (MEDICAL)
CLEARANCE CERTIFICATE NO. M200164

NAME: (Principal Investigator)	Dr Z Waja and Professor B Kana
DEPARTMENT:	Schools of Clinical Medicine (Waja) and Pathology (Kana) Perinatal HIV RU (Waja) & CoE in Biomedical TB Res (Kana) CHBAH (Waja) and NHLS (Kana)
PROJECT TITLE:	Sputum and oral swab collection for novel mycobacteriology testing techniques (SNT study)
DATE CONSIDERED:	Ad hoc
DECISION:	Approved unconditionally
CONDITIONS:	
SUPERVISOR:	Not applicable
APPROVED BY:	Dr CB Penny, Chairperson, HREC (Medical)
DATE OF APPROVAL:	2020/03/18

This clearance certificate is valid for 5 years from date of approval. Extension may be applied for.

DECLARATION OF INVESTIGATORS

To be completed in duplicate and **ONE COPY** returned to the Research Office Secretary on the 3rd Floor, Phillip Tobias Building, Parktown, University of the Witwatersrand, Johannesburg.
I/we fully understand the conditions under which I am/we are authorized to carry out the above-mentioned research and I/we undertake to ensure compliance with these conditions. Should any departure be contemplated, from the research protocol as approved, I/we undertake to submit details to the Committee. I agree to submit a yearly progress report. When a funder requires annual re-certification, the application date will be one year after the date when the study was initially reviewed. In this case, the study was initially reviewed in **January** and will therefore reports and re-certification will be due early in the month of **January** each year. Unreported changes to the application may invalidate the clearance given by the HREC (Medical).

Principal Investigator Signature Date

PLEASE QUOTE THE CLEARANCE CERTIFICATE NUMBER IN ALL ENQUIRIES

MGIT plus ethics certificate

R14/49 Miss Amanda McIvor

HUMAN RESEARCH ETHICS COMMITTEE (MEDICAL)

CLEARANCE CERTIFICATE NO. M161058

NAME: (Principal Investigator)	Miss Amanda McIvor
DEPARTMENT:	Centre of Excellence for Biomedical TB Research
PROJECT TITLE:	Characterisation of Differentially Culturable Bacteria in Axenic Culture and from Tuberculosis Patients
DATE CONSIDERED:	Adhoc
DECISION:	Approved unconditionally
CONDITIONS:	Sub-study under M140265 and M110833 Dr Neil Martinson
SUPERVISOR:	Bavesh Kana
APPROVED BY:	Prof C Feldman, Co-Chairperson, HREC (Medical)
DATE OF APPROVAL:	20/12/2016

This clearance certificate is valid for 5 years from date of approval. Extension may be applied for.

DECLARATION OF INVESTIGATORS

To be completed in duplicate and **ONE COPY** returned to the Research Office Secretary in Room 301, Third floor, Faculty of Health Sciences, Phillip Tobias Building, 29 Princess of Wales Terrace, Parktown, 2193, University of the Witwatersrand. I/we fully understand the conditions under which I am/we are authorized to carry out the above-mentioned research and I/we undertake to ensure compliance with these conditions. Should any departure be contemplated, from the research protocol as approved, I/we undertake to resubmit the application to the Committee. **I agree to submit a yearly progress report**. The date for annual re-certification will be one year after the date of convened meeting where the study was initially reviewed. In this case, the study was initially reviewed in October and will therefore be due in the month of October each year. Unreported changes to the application may invalidate the clearance given by the HREC (Medical).

Principal Investigator Signature _____ Date _____

PLEASE QUOTE THE PROTOCOL NUMBER IN ALL ENQUIRIES

5.5 Appendix E- Turn-it-in report

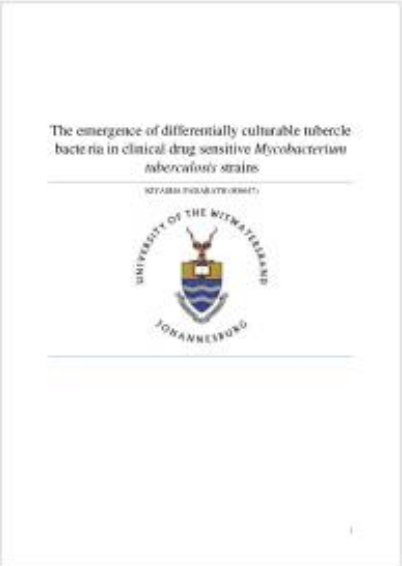
turnitin

Digital Receipt

This receipt acknowledges that Turnitin received your paper. Below you will find the receipt information regarding your submission.

The first page of your submissions is displayed below.

Submission author:	Kiyasha Padarath
Assignment title:	Submit here
Submission title:	806617:Masters_dissertation-80661…
File name:	965-1bcf-4bb5-a7b3-5ef0b03e04e0…
File size:	12.06M
Page count:	108
Word count:	29,431
Character count:	160,483
Submission date:	24-Mar-2020 08:05AM (UTC+0200)
Submission ID:	1280971775


The emergence of differentially culturable tubercle bacteria in clinical drug sensitive *Mycobacterium tuberculosis* strains

Copyright 2020 Turnitin. All rights reserved.

806617:Masters_dissertation-806617.docx

ORIGINALITY REPORT

13%	7%	6%	9%
SIMILARITY INDEX	INTERNET SOURCES	PUBLICATIONS	STUDENT PAPERS

PRIMARY SOURCES

1	Submitted to University of Witwatersrand Student Paper	2%
2	www.escholar.manchester.ac.uk Internet Source	1%
3	epubs.rcsi.ie Internet Source	1%
4	Submitted to University of Birmingham Student Paper	<1%
5	Submitted to University of Ulster Student Paper	<1%
6	www.mdpi.com Internet Source	<1%
7	Bhavna Gowan Gordhan, Julian Peters, Bavesh Davandra Kana. "Application of model systems to study adaptive responses of Mycobacterium tuberculosis during infection and disease", Elsevier BV, 2019 Publication	<1%

Submitted to Higher Education Commission

6. References

Abdool, S. S., Churchyard, G. J., Karim, Q. A., & Lawn, S. D. (2009). HIV infection and tuberculosis in South Africa: an urgent need to escalate the public health response. *Lancet, 374*(9693), 921-933. doi:10.1016/s0140-6736(09)60916-8

Actor, J. K., Hunter, R. L., & Jagannath, C. (2008). Immunopathology of Tuberculosis. In D. S. Zander, H. H. Popper, J. Jagirdar, A. K. Haque, P. T. Cagle, & R. Barrios (Eds.), *Molecular Pathology of Lung Diseases* (pp. 419-428). New York, NY: Springer New York.

Ahmad, S. (2010). New approaches in the diagnosis and treatment of latent tuberculosis infection. *Respir Res, 11*, 169. doi:10.1186/1465-9921-11-169

Alnimr, A. M. (2015). Dormancy models for *Mycobacterium tuberculosis*: A minireview. *Braz J Microbiol, 46*(3), 641-647. doi:10.1590/s1517-838246320140507

Anuchin, A. M., Mulyukin, A. L., Suzina, N. E., Duda, V. I., El-Registan, G. I., & Kaprelyants, A. S. (2009). Dormant forms of *Mycobacterium smegmatis* with distinct morphology. *Microbiology, 155*(Pt 4), 1071-1079. doi:10.1099/mic.0.023028-0

Ashiru, O. T., Pillay, M., & Sturm, A. W. (2010). Adhesion to and invasion of pulmonary epithelial cells by the F15/LAM4/KZN and Beijing strains of *Mycobacterium tuberculosis*. *Journal of medical Microbiology, 59*(5), 528-533.

Ayrapetyan, M., Williams, T., & Oliver, J. D. (2018). Relationship between the Viable but Nonculturable State and Antibiotic Persister Cells. *J Bacteriol, 200*(20). doi:10.1128/jb.00249-18

Ayrapetyan, M., Williams, T. C., Baxter, R., & Oliver, J. D. (2015). Viable but Nonculturable and Persister Cells Coexist Stochastically and Are Induced by Human Serum. *Infect Immun, 83*(11), 4194-4203. doi:10.1128/iai.00404-15

Baker, J. J., & Abramovitch, R. B. (2018). Genetic and metabolic regulation of *Mycobacterium tuberculosis* acid growth arrest. *Scientific Reports, 8*(1), 4168. doi:10.1038/s41598-018-22343-4

Bamford, R. A., Smith, A., Metz, J., Glover, G., Titball, R. W., & Pagliara, S. (2017). Investigating the physiology of viable but non-culturable bacteria by microfluidics and time-lapse microscopy. *BMC Biology, 15*(1), 121. doi:10.1186/s12915-017-0465-4

Barry, C. E., 3rd, Boshoff, H. I., Dartois, V., Dick, T., Ehrt, S., Flynn, J., . . . Young, D. (2009). The spectrum of latent tuberculosis: rethinking the biology and intervention strategies. *Nat Rev Microbiol, 7*(12), 845-855. doi:10.1038/nrmicro2236

Betts, J. C., Lukey, P. T., Robb, L. C., McAdam, R. A., & Duncan, K. (2002). Evaluation of a nutrient starvation model of *Mycobacterium tuberculosis* persistence by gene and protein expression profiling. *Mol Microbiol, 43*(3), 717-731.

Bhatt, K., & Salgame, P. (2007). Host innate immune response to *Mycobacterium tuberculosis*. *J Clin Immunol, 27*(4), 347-362. doi:10.1007/s10875-007-9084-0

Bloom, B. R., Atun, R., Cohen, T., Dye, C., Fraser, H., Gomez, G. B., . . . Yadav, P. (2017). Tuberculosis. In rd, K. K. Holmes, S. Bertozzi, B. R. Bloom, & P. Jha (Eds.), *Major Infectious Diseases*. Washington (DC): The International Bank for Reconstruction and Development / The World Bank (c) 2017 International Bank for Reconstruction and Development / The World Bank.

Brennan, M. J. (2017). Biofilms and *Mycobacterium tuberculosis*. *Infect Immun, 85*(10), e00411-00417. doi:10.1128/iai.00411-17

Buerger, S., Spoering, A., Gavrish, E., Leslin, C., Ling, L., & Epstein, S. S. (2012). Microbial scout hypothesis, stochastic exit from dormancy, and the nature of slow growers. *Appl Environ Microbiol, 78*(9), 3221-3228. doi:10.1128/aem.07307-11

Castelnuovo, B. (2010). A review of compliance to anti tuberculosis treatment and risk factors for defaulting treatment in Sub Saharan Africa. *Afr Health Sci, 10*(4), 320-324.
Chao, M. C., & Rubin, E. J. (2010). Letting sleeping dos lie: does dormancy play a role in tuberculosis? *Annu Rev Microbiol, 64*, 293-311. doi:10.1146/annurev.micro.112408.134043
Chee, C. B., Sester, M., Zhang, W., & Lange, C. (2013). Diagnosis and treatment of latent infection with *Mycobacterium tuberculosis*. *Respirology, 18*(2), 205-216. doi:10.1111/resp.12002
Chengalroyen, M. D., Beukes, G. M., Gordhan, B. G., Streicher, E. M., Churchyard, G., Hafner, R., . . . Kana, B. D. (2016). Detection and Quantification of Differentially Culturable Tubercle Bacteria in Sputum from Patients with Tuberculosis. *Am J Respir Crit Care Med, 194*(12), 1532-1540. doi:10.1164/rccm.201604-0769OC
Chihota, V. N., Niehaus, A., Streicher, E. M., Wang, X., Sampson, S. L., Mason, P., . . . Warren, R. M. (2018). Geospatial distribution of *Mycobacterium tuberculosis* genotypes in Africa. *PloS one, 13*(8), e0200632-e0200632. doi:10.1371/journal.pone.0200632
Cholo, M. C., van Rensburg, E. J., & Anderson, R. (2008). Potassium uptake systems of *Mycobacterium tuberculosis*: genomic and protein organisation and potential roles in microbial pathogenesis and chemotherapy. *Southern African Journal of Epidemiology and Infection, 23*(4), 13-16. doi:10.1080/10158782.2008.11441327
Coscolla, M., & Gagneux, S. (2014). Consequences of genomic diversity in *Mycobacterium tuberculosis*. *Semin Immunol, 26*(6), 431-444. doi:10.1016/j.smim.2014.09.012
Dartois, V. (2014). The path of anti-tuberculosis drugs: from blood to lesions to mycobacterial cells. *Nat Rev Microbiol, 12*(3), 159-167. doi:10.1038/nrmicro3200
Desikan, P. (2013). Sputum smear microscopy in tuberculosis: is it still relevant? *The Indian journal of medical research, 137*(3), 442-444.
Dietrich, J., Roy, S., Rosenkrands, I., Lindenstrom, T., Filskov, J., Rasmussen, E. M., . . . Andersen, P. (2015). Differential influence of nutrient-starved *Mycobacterium tuberculosis* on adaptive immunity results in progressive tuberculosis disease and pathology. *Infect Immun, 83*(12), 4731-4739. doi:10.1128/iai.01055-15
Erie, H., Kaboosi, H., Javid, N., Shirzad-Aski, H., Taziki, M., Kuchaksaraee, M. B., & Ghaemi, E. A. (2017). The high prevalence of *Mycobacterium tuberculosis* Beijing strain at an early age and extra-pulmonary tuberculosis cases. *Iranian journal of microbiology, 9*(6), 312-317.
Esteban, J., & García-Coca, M. (2018). Mycobacterium Biofilms. *Frontiers in Microbiology, 8*, 2651-2651. doi:10.3389/fmicb.2017.02651
Fonseca, D. M. d., Silva, C. L., Wowk, P. F., Paula, M. O. e., Ramos, S. G., Horn, C., . . . Bonato, V. L. D. (2009). *Mycobacterium tuberculosis* Culture Filtrate Proteins plus CpG Oligodeoxynucleotides Confer Protection to *Mycobacterium bovis* BCG-Primed Mice by Inhibiting Interleukin-4 Secretion. *Infect Immun, 77*(12), 5311-5321. doi:10.1128/iai.00580-09
Gagneux, S. (2013). Genetic diversity in *Mycobacterium tuberculosis*. *Curr Top Microbiol Immunol, 374*, 1-25. doi:10.1007/82_2013_329
Gagneux, S., & Small, P. M. (2007). Global phylogeography of *Mycobacterium tuberculosis* and implications for tuberculosis product development. *Lancet Infect Dis, 7*(5), 328-337. doi:10.1016/s1473-3099(07)70108-1
Gandhi, N. R., Moll, A., Sturm, A. W., Pawinski, R., Govender, T., Lalloo, U., . . . Friedland, G. (2006). Extensively drug-resistant tuberculosis as a cause of death in patients co-infected with tuberculosis and HIV in a rural area of South Africa. *Lancet, 368*(9547), 1575-1580. doi:10.1016/s0140-6736(06)69573-1
Gerasimova, A., Kazakov, A. E., Arkin, A. P., Dubchak, I., & Gelfand, M. S. (2011). Comparative genomics of the dormancy regulons in mycobacteria. *J Bacteriol, 193*(14), 3446-3452. doi:10.1128/JB.00179-11
Gibson, S. E. R., Harrison, J., & Cox, J. A. G. (2018). Modelling a Silent Epidemic: A Review of the *In Vitro* Models of Latent Tuberculosis. *Pathogens, 7*(4). doi:10.3390/pathogens7040088
Glickman, M. S., & Jacobs, W. R., Jr. (2001). Microbial pathogenesis of *Mycobacterium tuberculosis*: dawn of a discipline. *Cell, 104*(4), 477-485. doi:10.1016/s0092-8674(01)00236-7

Glynn, J. R., Whiteley, J., Bifani, P. J., Kremer, K., & van Soolingen, D. (2002). Worldwide occurrence of Beijing/W strains of *Mycobacterium tuberculosis*: a systematic review. *Emerg Infect Dis, 8*(8), 843-849. doi:10.3201/eid0805.020002

Gomez, J. E., & McKinney, J. D. (2004). *M. tuberculosis* persistence, latency, and drug tolerance. *Tuberculosis (Edinb), 84*(1-2), 29-44.

Gupta, S., & Kakkar, V. (2018). Recent technological advancements in tuberculosis diagnostics - A review. *Biosens Bioelectron, 115*, 14-29. doi:10.1016/j.bios.2018.05.017

Hanekom, M., Mata, D., van Pittius, N. G., van Helden, P., Warren, R., & Hernandez-Pando, R. (2010). *Mycobacterium tuberculosis* strains with the Beijing genotype demonstrate variability in virulence associated with transmission. *Tuberculosis, 90*(5), 319-325.

Hanekom, M., Van Pittius, N. G., McEvoy, C., Victor, T., Van Helden, P., & Warren, R. (2011). *Mycobacterium tuberculosis* Beijing genotype: a template for success. *Tuberculosis, 91*(6), 510-523.

Harris, J., Hope, J. C., & Lavelle, E. C. (2009). Autophagy and the Immune Response to TB. *Transboundary and Emerging Diseases, 56*(6-7), 248-254. doi:10.1111/j.1865-1682.2009.01069.x

Herranz, M., Pole, I., Ozere, I., Chiner-Oms, Á., Martínez-Lirola, M., Pérez-García, F., . . . García-de-Viedma, D. (2018). *Mycobacterium tuberculosis* Acquires Limited Genetic Diversity in Prolonged Infections, Reactivations and Transmissions Involving Multiple Hosts. *Frontiers in Microbiology, 8*, 2661-2661. doi:10.3389/fmicb.2017.02661

Higgins, D., & Dworkin, J. (2012). Recent progress in Bacillus subtilis sporulation. *FEMS Microbiol Rev, 36*(1), 131-148. doi:10.1111/j.1574-6976.2011.00310.x

Hobby, G. L., Holman, A. P., Iseman, M. D., & Jones, J. M. (1973). Enumeration of tubercle bacilli in sputum of patients with pulmonary tuberculosis. *Antimicrobial Agents and Chemotherapy, 4*(2), 94-104. doi:10.1128/aac.4.2.94

Honeyborne, I., McHugh, T. D., Kuittinen, I., Cichonska, A., Evangelopoulos, D., Ronacher, K., . . . Waddell, S. J. (2016). Profiling persistent tubercule bacilli from patient sputa during therapy predicts early drug efficacy. *BMC medicine, 14*(1), 68. doi:10.1186/s12916-016-0609-3

Ioerger, T. R., Feng, Y., Ganesula, K., Chen, X., Dobos, K. M., Fortune, S., . . . Sacchettini, J. C. (2010). Variation among Genome Sequences of H37Rv Strains of *Mycobacterium tuberculosis* from Multiple Laboratories. *J Bacteriol, 192*(14), 3645-3653. doi:10.1128/jb.00166-10

Iskandar, A., Nursiloningrum, E., Arthamin, M. Z., Olivianto, E., & Chandrakusuma, M. S. (2017). The Diagnostic Value of Urine Lipoarabinomannan (LAM) Antigen in Childhood Tuberculosis. *Journal of clinical and diagnostic research : JCDR, 11*(3), EC32-EC35. doi:10.7860/JCDR/2017/20909.9542

Jones, J. (2000). Risk of vCJD lower than expected. *BMJ (Clinical research ed.), 321*(7259), 469B-469B.

Kana, B. D., Gordhan, B. G., Downing, K. J., Sung, N., Vostroktunova, G., Machowski, E. E., . . . Mizrahi, V. (2008). The resuscitation-promoting factors of *Mycobacterium tuberculosis* are required for virulence and resuscitation from dormancy but are collectively dispensable for growth in vitro. *Mol Microbiol, 67*(3), 672-684. doi:10.1111/j.1365-2958.2007.06078.x

Kato, S., Haruta, S., Cui, Z. J., Ishii, M., & Igarashi, Y. (2008). Network relationships of bacteria in a stable mixed culture. *Microb Ecol, 56*(3), 403-411. doi:10.1007/s00248-007-9357-4

Keane, J., Remold, H. G., & Kornfeld, H. (2000). Virulent *Mycobacterium tuberculosis* strains evade apoptosis of infected alveolar macrophages. *J Immunol, 164*(4), 2016-2020. doi:10.4049/jimmunol.164.4.2016

Kim, J. S., Chowdhury, N., Yamasaki, R., & Wood, T. K. (2018). Viable but non-culturable and persistence describe the same bacterial stress state. *Environ Microbiol, 20*(6), 2038-2048. doi:10.1111/1462-2920.14075

Kong, Y., Cave, M. D., Zhang, L., Foxman, B., Marrs, C. F., Bates, J. H., & Yang, Z. H. (2007). Association between *Mycobacterium tuberculosis* Beijing/W lineage strain infection and extrathoracic tuberculosis: Insights from epidemiologic and clinical characterization of the three principal genetic groups of M. tuberculosis clinical isolates. *J Clin Microbiol, 45*(2), 409-414. doi:10.1128/jcm.01459-06

Kulka, K., Hatfull, G., & Ojha, A. K. (2012). Growth of *Mycobacterium tuberculosis* biofilms. *J Vis Exp*(60). doi:10.3791/3820

Kumar, G., Shankar, H., Sharma, D., Sharma, P., Bisht, D., Katoch, V. M., & Joshi, B. (2017). Proteomics of Culture Filtrate of Prevalent *Mycobacterium tuberculosis* Strains: 2D-PAGE Map and MALDI-TOF/MS Analysis. *SLAS DISCOVERY: Advancing Life Sciences R&D, 22*(9), 1142-1149. doi:10.1177/2472555217717639

Kumar, R., Singh, P., Kolloli, A., Shi, L., Bushkin, Y., Tyagi, S., & Subbian, S. (2019). Immunometabolism of Phagocytes During *Mycobacterium tuberculosis* Infection. *Front Mol Biosci, 6*, 105. doi:10.3389/fmolb.2019.00105

Kuru, E., Hughes, H. V., Brown, P. J., Hall, E., Tekkam, S., Cava, F., . . . VanNieuwenhze, M. S. (2012). In Situ probing of newly synthesized peptidoglycan in live bacteria with fluorescent D-amino acids. *Angewandte Chemie (International ed. in English), 51*(50), 12519-12523. doi:10.1002/anie.201206749

Kyu, H. H., Maddison, E. R., Henry, N. J., Mumford, J. E., Barber, R., Shields, C., . . . Murray, C. J. L. (2018). The global burden of tuberculosis: results from the Global Burden of Disease Study 2015. *The Lancet infectious diseases, 18*(3), 261-284. doi:10.1016/S1473-3099(17)30703-X

Leung, C. C., Lange, C., & Zhang, Y. (2013). Tuberculosis: current state of knowledge: an epilogue. *Respirology, 18*(7), 1047-1055. doi:10.1111/resp.12156

Lin, P. L., & Flynn, J. L. (2010). Understanding latent tuberculosis: a moving target. *J Immunol, 185*(1), 15-22. doi:10.4049/jimmunol.0903856

Lipworth, S., Hammond, R. J., Baron, V. O., Hu, Y., Coates, A., & Gillespie, S. H. (2016). Defining dormancy in mycobacterial disease. *Tuberculosis (Edinb), 99*, 131-142. doi:10.1016/j.tube.2016.05.006

Liu, X., Wang, C., Yan, B., Lyu, L., Takiff, H. E., & Gao, Q. (2020). The potassium transporter KdpA affects persister formation by regulating ATP levels in *Mycobacterium marinum*. *Emerging Microbes & Infections, 9*(1), 129-139. doi:10.1080/22221751.2019.1710090

Liu, Y., Jiang, X., Li, W., Zhang, X., Wang, W., & Li, C. (2017). The study on the association between Beijing genotype family and drug susceptibility phenotypes of *Mycobacterium tuberculosis* in Beijing. *Scientific Reports, 7*(1), 15076. doi:10.1038/s41598-017-14119-z

Lockhart, E., Green, A. M., & Flynn, J. L. (2006). IL-17 production is dominated by gammadelta T cells rather than CD4 T cells during *Mycobacterium tuberculosis* infection. *J Immunol, 177*(7), 4662-4669. doi:10.4049/jimmunol.177.7.4662

Loebel, R. O., Shorr, E., & Richardson, H. B. (1933). The Influence of Adverse Conditions upon the Respiratory Metabolism and Growth of Human Tubercle Bacilli. *J Bacteriol, 26*(2), 167-200.

Mathabire Rucker, S. C., Cossa, L., Harrison, R. E., Mpunga, J., Lobo, S., Kisaka Kimupelenge, P., . . . Huerga, H. (2019). Feasibility of using Determine TB-LAM to diagnose tuberculosis in HIV-positive patients in programmatic conditions: a multisite study. *Global Health Action, 12*(1), 1672366. doi:10.1080/16549716.2019.1672366

Mayosi, B. M., Flisher, A. J., Lalloo, U. G., Sitas, F., Tollman, S. M., & Bradshaw, D. (2009). The burden of non-communicable diseases in South Africa. *Lancet, 374*(9693), 934-947. doi:10.1016/s0140-6736(09)61087-4

McDonough, K. A., Kress, Y., & Bloom, B. R. (1993). Pathogenesis of tuberculosis: interaction of *Mycobacterium tuberculosis* with macrophages. *Infect Immun, 61*(7), 2763-2773.

Meneghini, M. D. (2015). Spore No More: Quality Control during Bacterial Development. *Dev Cell, 34*(6), 611-612. doi:10.1016/j.devcel.2015.09.011

Mukamolova, G. V., Turapov, O., Malkin, J., Woltmann, G., & Barer, M. R. (2010). Resuscitation-promoting factors reveal an occult population of tubercle Bacilli in Sputum. *Am J Respir Crit Care Med, 181*(2), 174-180. doi:10.1164/rccm.200905-0661OC

Munoz, L., Stagg, H. R., & Abubakar, I. (2015). Diagnosis and Management of Latent Tuberculosis Infection. *Cold Spring Harb Perspect Med, 5*(11). doi:10.1101/cshperspect.a017830

Murase, Y. (2011). Recent findings on tuberculosis caused by different lineages of Mycobacterium tuberculosis. *Nihon Rinsho, 69*(8), 1475-1481.

Muttucumaru, N., Roberts, G., Hinds, J., Stabler, R., & Parish, T. (2004). Gene expression profile of *Mycobacterium tuberculosis* in a non-replicating state (Vol. 84).

Muture, B. N., Keraka, M. N., Kimuu, P. K., Kabiru, E. W., Ombeka, V. O., & Oguya, F. (2011). Factors associated with default from treatment among tuberculosis patients in Nairobi province, Kenya: a case control study. *BMC Public Health, 11*, 696. doi:10.1186/1471-2458-11-696

Nathavitharana, R. R., Cudahy, P. G. T., Schumacher, S. G., Steingart, K. R., Pai, M., & Denkinger, C. M. (2017). Accuracy of line probe assays for the diagnosis of pulmonary and multidrug-resistant tuberculosis: a systematic review and meta-analysis. *European Respiratory Journal, 49*(1), 1601075. doi:10.1183/13993003.01075-2016

Nguyen, T. N. A., Anton-Le Berre, V., Bañuls, A.-L., & Nguyen, T. V. A. (2019). Molecular Diagnosis of Drug-Resistant Tuberculosis; A Literature Review. *Frontiers in Microbiology, 10*(794). doi:10.3389/fmicb.2019.00794

North, R. J., & Jung, Y. J. (2004). Immunity to tuberculosis. *Annu Rev Immunol, 22*, 599-623. doi:10.1146/annurev.immunol.22.012703.104635

Nuwaha, F. (1998). Contemporary treatment of tuberculosis in HIV prevalent countries in sub-Saharan Africa. *East Afr Med J, 75*(6), 358-363.

Nyka, W. (1974). Studies on the effect of starvation on mycobacteria. *Infect Immun, 9*(5), 843-850.

Ojha, A. K., Baughn, A. D., Sambandan, D., Hsu, T., Trivelli, X., Guerardel, Y., . . . Hatfull, G. F. (2008). Growth of *Mycobacterium tuberculosis* biofilms containing free mycolic acids and harbouring drug-tolerant bacteria. *Mol Microbiol, 69*(1), 164-174. doi:10.1111/j.1365-2958.2008.06274.x

Okada, M., & Shirakawa, T. (2005). [Frontier of mycobacterium research--host vs. mycobacterium]. *Kekkaku, 80*(9), 613-629.

Parwati, I., van Crevel, R., & van Soolingen, D. (2010). Possible underlying mechanisms for successful emergence of the *Mycobacterium tuberculosis* Beijing genotype strains. *The Lancet infectious diseases, 10*(2), 103-111.

Pheiffer, C., Betts, J. C., Flynn, H. R., Lukey, P. T., & van Helden, P. (2005). Protein expression by a Beijing strain differs from that of another clinical isolate and *Mycobacterium tuberculosis* H37Rv. *Microbiology, 151*(4), 1139-1150. doi:https://doi.org/10.1099/mic.0.27518-0

Polikanov, Y. S., Aleksashin, N. A., Beckert, B., & Wilson, D. N. (2018). The Mechanisms of Action of Ribosome-Targeting Peptide Antibiotics. *Front Mol Biosci, 5*, 48-48. doi:10.3389/fmolb.2018.00048

Reed, M. B., Gagneux, S., Deriemer, K., Small, P. M., & Barry, C. E., 3rd. (2007). The W-Beijing lineage of *Mycobacterium tuberculosis* overproduces triglycerides and has the DosR dormancy regulon constitutively upregulated. *J Bacteriol, 189*(7), 2583-2589. doi:10.1128/jb.01670-06

Rindi, L., Lari, N., Cuccu, B., & Garzelli, C. (2009). Evolutionary pathway of the Beijing lineage of *Mycobacterium tuberculosis* based on genomic deletions and mutT genes polymorphisms. *Infect Genet Evol, 9*(1), 48-53. doi:10.1016/j.meegid.2008.09.006

Rodriguez, D. C., Ocampo, M., Salazar, L. M., & Patarroyo, M. A. (2018). Quantifying intracellular *Mycobacterium tuberculosis*: An essential issue for *in vitro* assays. *Microbiologyopen, 7*(2), e00588. doi:10.1002/mbo3.588

Rosser, A., Stover, C., Pareek, M., & Mukamolova, G. V. (2017). Resuscitation-promoting factors are important determinants of the pathophysiology in *Mycobacterium tuberculosis* infection. *Critical Reviews in Microbiology, 43*(5), 621-630. doi:10.1080/1040841X.2017.1283485

Rubin, E. J. (2018). TB diagnosis from the Dark Ages to fluorescence. *Nature Microbiology, 3*(3), 268-269. doi:10.1038/s41564-018-0118-6

Rufai, S. B., Kumar, P., Singh, A., Prajapati, S., Balooni, V., & Singh, S. (2014). Comparison of Xpert MTB/RIF with line probe assay for detection of rifampin-monoresistant Mycobacterium tuberculosis. *J Clin Microbiol, 52*(6), 1846-1852. doi:10.1128/JCM.03005-13

Shanley CA, Henao-Tamayo MI, Bipin C, et al. Biology of clinical strains of Mycobacterium tuberculosis with varying levels of transmission. *Tuberculosis (Edinb)*. 2018;109:123-133. doi:10.1016/j.tube.2018.02.003

Saito, K., Warrier, T., Somersan-Karakaya, S., Kaminski, L., Mi, J., Jiang, X., . . . Nathan, C. F. (2017). Rifamycin action on RNA polymerase in antibiotic-tolerant *Mycobacterium*

tuberculosis results in differentially detectable populations. *Proceedings of the National Academy of Sciences, 114*(24), E4832. doi:10.1073/pnas.1705385114

Salina, E. G., Grigorov, A. S., Bychenko, O. S., Skvortsova, Y. V., Mamedov, I. Z., Azhikina, T. L., & Kaprelyants, A. S. (2019). Resuscitation of Dormant "Non-culturable" *Mycobacterium tuberculosis* Is Characterized by Immediate Transcriptional Burst. *Frontiers in Cellular and Infection Microbiology, 9*(272). doi:10.3389/fcimb.2019.00272

Salina, E. G., Waddell, S. J., Hoffmann, N., Rosenkrands, I., Butcher, P. D., & Kaprelyants, A. S. (2014). Potassium availability triggers *Mycobacterium tuberculosis* transition to, and resuscitation from, non-culturable (dormant) states. *Open biology, 4*(10), 140106. doi:10.1098/rsob.140106

Samanich, K. M., Keen, M. A., Vissa, V. D., Harder, J. D., Spencer, J. S., Belisle, J. T., . . . Laal, S. (2000). Serodiagnostic potential of culture filtrate antigens of Mycobacterium tuberculosis. *Clin Diagn Lab Immunol, 7*(4), 662-668. doi:10.1128/cdli.7.4.662-668.2000

Sasindran, S. J., & Torrelles, J. B. (2011). *Mycobacterium Tuberculosis* Infection and Inflammation: what is Beneficial for the Host and for the Bacterium? *Frontiers in Microbiology, 2*, 2. Retrieved from http://europepmc.org/abstract/MED/21687401doi:10.3389/fmicb.2011.00002

Scanga, C. A., Mohan, V. P., Joseph, H., Yu, K., Chan, J., & Flynn, J. L. (1999). Reactivation of latent tuberculosis: variations on the Cornell murine model. *Infect Immun, 67*(9), 4531-4538.

Schluger, N. W., Condos, R., Lewis, S., & Rom, W. N. (1994). Amplification of DNA of *Mycobacterium tuberculosis* from peripheral blood of patients with pulmonary tuberculosis. *Lancet, 344*(8917), 232-233. doi:10.1016/s0140-6736(94)92999-8

Schuger , N. W., & Rom, W. N. (1997). The host immune response to tubeculosis *American journal of Respiratory and Critical care Medicine 157*(http://dx.doi.org/10.1164/ajrccm.157.3.9708002), 680-691.

Sebastian, J., Swaminath, S., Nair, R. R., Jakkala, K., Pradhan, A., & Ajitkumar, P. (2017). De Novo Emergence of Genetically Resistant Mutants of *Mycobacterium tuberculosis* from the Persistence Phase Cells Formed against Antituberculosis Drugs *in Vitro*. *Antimicrobial Agents and Chemotherapy, 61*(2), e01343-01316. doi:10.1128/aac.01343-16

Shabbeer, A., Cowan, L., Ozcaglar, C., Rastogi, N., Vandenberg, S., Yener, B., & Bennett, K. (2012). TB-Lineage: An online tool for classification and analysis of strains of *Mycobacterium tuberculosis* complex. *Infection, genetics and evolution : journal of molecular epidemiology and evolutionary genetics in infectious diseases, 12*, 789-797. doi:10.1016/j.meegid.2012.02.010

Snapper, S., Melton, R., Mustafa, S., Kieser, T., & WR Jr, J. (1990). Isolation and characterization of efficient plasmid transformation mutants of *Mycobacterium smegmatis*. *Molecular microbiology, 4*(11), 1911-1919.

Solokhina, A., Brückner, D., Bonkat, G., & Braissant, O. (2017). Metabolic activity of mature biofilms of *Mycobacterium tuberculosis* and other non-tuberculous mycobacteria. *Scientific Reports, 7*(1), 9225. doi:10.1038/s41598-017-10019-4

Stewart, G. R., Robertson, B. D., & Young, D. B. (2003). Tuberculosis: a problem with persistence. *Nature Reviews Microbiology, 1*(2), 97-105. doi:10.1038/nrmicro749

Sulis, G., Centis, R., Sotgiu, G., D'Ambrosio, L., Pontali, E., Spanevello, A., . . . Migliori, G. B. (2016). Recent developments in the diagnosis and management of tuberculosis. *npj Primary Care Respiratory Medicine, 26*(1), 16078. doi:10.1038/npjpcrm.2016.78

Treuner-Lange, A., Kuhn, A., & Dürre, P. (1997). The kdp system of Clostridium acetobutylicum: cloning, sequencing, and transcriptional regulation in response to potassium concentration. *J Bacteriol, 179*, 4501-4512. doi:10.1128/jb.179.14.4501-4512.1997

Van der Spoel van Dijk, A., Makhoahle, P. M., Rigouts, L., & Baba, K. (2016). Diverse molecular genotypes of *Mycobacterium tuberculosis* complex isolates circulating in the Free State, South Africa. *International journal of microbiology, 2016*.

Van Rie, A., Fitzgerald, D., Kabuya, G., Van Deun, A., Tabala, M., Jarret, N., . . . Bahati, E. (2008). Sputum Smear Microscopy: Evaluation of Impact of Training, Microscope Distribution, and Use of External Quality Assessment Guidelines for Resource-Poor Settings. *J Clin Microbiol, 46*(3), 897-901. doi:10.1128/jcm.01553-07

Wayne, L. G., & Hayes, L. G. (1996). An *in vitro* model for sequential study of shiftdown of *Mycobacterium tuberculosis* through two stages of nonreplicating persistence. *Infect Immun, 64*(6), 2062-2069.
WHO. (2017). Gobal TB report. In W. H. Organisation (Ed.), (pp. 256).
WHO. (2019). Gobal TB report 2019 In W. H. Organisation (Ed.), (pp. 297). World Health Organisation indicince report
Wood, R. (2007). The case for integrating tuberculosis and HIV treatment services in South Africa. *J Infect Dis, 196 Suppl 3*, S497-499. doi:10.1086/521118
Wu, M.-L., Gengenbacher, M., & Dick, T. (2016). Mild Nutrient Starvation Triggers the Development of a Small-Cell Survival Morphotype in Mycobacteria. *Frontiers in Microbiology, 7*(947). doi:10.3389/fmicb.2016.00947
Yu, M.-C., Chen, H.-Y., Wu, M.-H., Huang, W.-L., Kuo, Y.-M., Yu, F.-L., & Jou, R. (2011). Evaluation of the Rapid MGIT TBc Identification Test for Culture Confirmation of <span *Mycobacterium tuberculosis* Complex Strain Detection. *J Clin Microbiol, 49*(3), 802-807. doi:10.1128/jcm.02243-10